University of Naples
Federico II

PhD Course in Industrial Engineering - XXXV cycle

Excessive acceleration failure mode within the Second Generation Intact Stability Criteria

Doctoral Thesis in Aerospace and Naval Engineering

PhD candidate
Gennaro Rosano

Supervisors
Prof. Ermina Begovic
Prof. Guido Boccadamo

Naples, Italy
2023

This page was intentionally left blank.

Abstract

The development of the performance-based Second Generation Intact Stability Criteria (SGISC) was on the top of the IMO's agenda for almost 20 years, involving experts from research institutions, industry, classification societies and ship operators. Accidents occurred in the last decades showed that some ships experienced dynamical stability failures in waves, leading to important economic losses or even fatal injuries for people on-board. The accidents clearly demonstrated that the current intact stability regulations cannot always guarantee ship safety against the phenomena covered by the SGISC.

The SGISC assess five stability failure in waves: Parametric roll, Pure loss of stability, Surf-riding/broaching, Dead ship condition and Excessive acceleration. The main novelties of the criteria are the physics-based foundation and the multi-layered approach, consisting of vulnerability criteria (Level 1 and Level 2), Direct Stability Assessment (Level 3) and Operational Measures (Operational Limitations and Operational Guidance). The criteria, finalized in February 2020, are currently at their trial stage, and feedback is expected from stakeholders based on the gained experience.

The Thesis focuses on the Excessive acceleration, the less studied and the latest introduced. A short description, a state of the art and a review of the main accidents that led to its introduction in the regulatory context are provided. An overview of the process of development of the SGISC and the structure of the criteria is given with particular focus on the Excessive acceleration. The validation of a numerical code for the verification of the vulnerability criteria is shown.

In the current version of the criterion, the external excitation is modelled by the Froude-Krylov component only which is calculated by a simplified formulation specific for the beam seas case. The formulation is generalized to any wave heading to provide simple but sufficiently accurate formulas for the estimation of the wave excitation, to be implemented in the rules for the development of ship-specific Operational Guidance. The adoption of such a formulation would offer the advantage of univocal and uniform application of the rules, with no need of numerical software validation by the Administration.

A Decision Support System designed to monitor the actual condition of the vessel and to predict the lateral acceleration that could be experienced in the short-term is proposed. The system supports the crew in real operational conditions and integrate Operational Measures developed at the design stage. Two case studies are presented, referring to a bulk carrier and a fishing vessel, respectively.

The bulk carrier, engaged on long routes from Europe to Africa, is found vulnerable to Level 1 and Level 2. Operational Limitations are developed for the

bulk carrier, with particular attention to the definition of the equivalent scatter table that should be used in the verification when the ship sails on long routes. Operational Guidance are also applied, based on the generalization to any wave heading and ship speed of Level 2, in order to identify safe and unsafe sailing conditions in relevant sea states. The adopted procedure implements the proposed formulation of the Froude-Krylov exciting roll moment and shows results that are comparable to the ones obtained calculating the excitation with a 3D potential theory software.

A 34-5 meters long fishing vessel, typical of the Spanish fleet, already studied in the literature, has been object of an experimental campaign conducted at the University of A Coruña (Spain) towing tank. Results from roll decay tests are used for the assessment of Level 2, which is not satisfied. Operational Limitations are derived for the vessel referring to the specific operational area in which she operates and to the maximum significant wave height. A Direct Stability Assessment is conducted confirming the vulnerability of the vessel. By noticing that dangerous situations could by experienced also for wave heights lower than the identified maximum one, the monitoring system is applied. For its application simulated and experimental data in irregular beam waves are used.

Final remarks and issues to be addressed in future studies are summarized at the end of the Thesis.

To my family

This page was intentionally left blank.

Acknowledgements

My supervisors Professor Ermina Begovic and Professor Guido Boccadamo deserve a huge thanks, I have been really lucky to have them as mentors. They instilled in me the passion and interest regarding ship dynamics in waves. I would not have been able to afford the PhD without the background they provided me. I sincerely acknowledge them for the guide, support and encouragement, making my PhD a joyful learning experience. Many opportunities, both at national and international levels, came from their faith in me.

I would like to thank the coordinator of the PhD course in Industrial Engineering, Professor Michele Grassi for the kindness and availability, since the first days of my PhD.

Immediately after, I would like to thank Dr Barbara Rinauro, which was not only a colleague but above all a friend, always finding the time to help me even when she had literally no time. I will not forget the late night discussions regarding codes, papers to write, and presentations to complete.

Part of my research was conducted at the University of A Coruña (Spain), under the supervision of Professor Marcos Míguez González. He gave me the opportunity to collaborate with people from Grupo Integrado de Ingeniería of the Ferrol Industrial Campus. I would also like to thank Professor Lucía Santiago Caamaño, Professor Anne Gosset and Professor Marcos Lema Rodríguez for their support during my research stay.

I sincerely thank Professor Igor Bačkalov from Development Centre for Ship Technology and Transport Systems (Germany). During these years he was a source of inspiration, strengthening what I learned from Professor Begovic, i.e. the importance of international collaboration, since “the results of our efforts multiply when we work together”.

A special thank to Professor Przemyslaw Krata from the University of Gdansk (Poland), for the valuable comments and suggestions. They made me reflect on many aspects of my research and represent an inspiration for future studies.

A big thanks to Dr Stefan Rudaković from the University of Belgrade, for his help during these years, especially in cross-checking numerical codes.

Coming back to Naples, thanks to Professor Carlo Bertorello for the nice learning opportunities and the professional advice he gave me.

I sincerely thank Professor Riccardo Martino not only for the nice discussion about flooding processes, but above all for the extremely enjoyable Hydrodynamics course that encouraged me to go deeper in the studies.

Thanks to Professor Maria Acanfora with whom I participated to the EU-funded project FLARE. It was hard and challenging but we successfully achieved the result.

I have to acknowledge Professor Paola Gualeni from the University of Genoa, who invited me to join the Italian delegation at IMO, Dr Nicola Petacco from the same institution and Professor Gabriele Bulian from the University of Trieste, for sharing his knowledge and for actively involving me in the discussions.

Many thanks to the students of the first intake of the Erasmus Mundus Joint Master Degree “Sustainable Ship and Shipping 4.0 (SEAS 4.0)”, that helped me to open my mind. Many of them became my friends and I know all of them will feel mentioned in here.

People I met during my stay at the Grupo Integrado de Ingeniería must be also acknowledged, I could not expect to find so nice and supportive people. Alejandro, Alma, David, Javier, Jose, Julio, Lucía, Mar, Martin, Milica, Sara and Sergio helped me in many occasions and we had a lot of fun together.

I have received from a great support my sister Imma during my studies, especially in the last months of my PhD. She helped me in the writing process of the first draft of the Thesis. Thanks for the extreme patience, kindness and for always being there.

My parents, Mariarosaria and Carmine, and my sister deserve special thanks for the support in my decisions and for the great understanding. You have been always there to encourage, support and take care of me. Thank you for your love. Finally, my grandmother Vincenza, she has always been proud of my achievements and has a special place in my heart.

Contents

List of Figures

This page was intentionally left blank.

List of Tables

Acronyms

BSU Federal Bureau of Maritime Casualty Investigation (Bundesstelle für Seeunfalluntersuchung).

DSA Direct Stability Assessment.

DSS Decision Support Systems.

IMCO Inter-Governmental Maritime Consultative Organization.

IMO International Maritime Organization.

IMU Inertial Motion Unit.

LFE Lateral Force Estimator.

MIF Motion Induced Fatigue.

MII Motion Induced Interruptions.

MSC Maritime Safety Commitee.

MSI Motion Sickness Incidence.

OG Operational Guidance.

OL Operational Limitations.

OM Operational Measures.

RMS Root mean square.

SDC Sub-commitee on Ship Design and Construction.

SLF Sub-commitee on Stability and Load Lines and on Fishing Vessels Safety.

SOLAS International Convention for the Safety Of Life At Sea.

This page was intentionally left blank.

Nomenclature

Roman symbols

a	Real part of the Froude-Krylov roll moment	Nm
A_{44}	Added mass in roll	tm^2
A_{BK}	Total overall area of the bilge keels	m^2
a_y	Lateral acceleration per unit wave amplitude	$(\mathrm{m/s}^2)/\mathrm{m}$
$a_{y,3h}$	Mean 3-hour maximum lateral acceleration	$\mathrm{m/s}^2$
$\overline{a}_{y,T}$	Most probable extreme acceleration in the time period T	$\mathrm{m/s}^2$
$\hat{a}_{y,T}$	Extreme acceleration exceeded with probability α in the time period T	$\mathrm{m/s}^2$
b	Imaginary part of the Froude-Krylov roll moment	Nm
B	Ship breadth	m
B_e	Equivalent linear roll damping factor	Nms
BM_T	Transverse metacentric radius	m
C	Long-term excessive acceleration failure index	–
C_{44}	Restoring coefficient	Nm
C_B	Block coefficient	–
C_m	Midship section coefficient	–
$C_{m,full}$	Midship section coefficient of the fully loaded departure condition	–
$C_{s,i}$	Short-term excessive acceleration failure index	–
d	Mean draught	m
F_{ex-4}	Magnitude of the exciting roll moment	Nm
F_{FK-4}	Magnitude of the Froude-Krylov roll moment	Nm
$\hat{f}_{FK-4}$	Complex form of the sectional Froude-Krylov roll moment per unit length	Nm/m

$\hat{F}_{FK-4}$	Complex form of the Froude-Krylov roll moment	Nm
F_n	Froude number	–
f_s	Probability of the sea states per unit range of significant wave heights and mean zero-crossing period	1/ms
g	Gravity acceleration, 9.81	m/s^2
GM	Transverse metacentric height in calm water not corrected for free surface effects	m
GZ	Righting arm	m
h	Height above the roll axis of the calculation point of lateral acceleration	m
H	Height above the keel line of the calculation point of lateral acceleration	m
H_s	Significant wave height	m
I_{44}	Mass moment of inertia around x-axis	tm^2
k	Wave number, $\frac{2\pi}{\lambda}$	rad m^{-1}
KG	Height of the centre of gravity above the keel line	m
k_L	Factor that accounts for the simultaneous action of roll, yaw and pitch motions	–
L	Ship length as defined in the 2008 IS Code	m
LCG	Longitudinal position of the center of gravity	m
L_{PP}	Length between perpendiculars	m
L_{WL}	Waterline length	m
M_D	Non-linear roll damping moment	Nm
n_2	Normal vector in the y-direction	–
n_3	Normal vector in the z-direction	–
n_4	Normal vector of roll	–
p_I	Dynamic pressure of the incident wave	N/m^2
$\hat{p}_I$	Complex form of the dynamic pressure of the incident wave	N/m^2
r	Effective wave slope function	–
r	Stability failure rate	–
RAO_φ	Response Amplitude Operator	–
$S_{\alpha\alpha}$	Spectrum of the wave slope	rad^2/rad/s

$S_{\alpha\alpha,e}$	Spectrum of the effective wave slope	$\mathrm{rad}^2/\mathrm{rad/s}$
S_{φ}	Spectrum of roll motion	$\mathrm{rad}^2/\mathrm{rad/s}$
S_{a_y}	Spectrum of lateral acceleration	$(\mathrm{m}^2/\mathrm{s}^4)/\mathrm{rad/s}$
S_{ZZ}	Wave energy spectrum	$\mathrm{m}^2\mathrm{s/rad}$
T_r	Natural roll period	s
T_z	Mean zero up-crossing period	s
V_s	Ship speed	$\mathrm{m\,s^{-1}}$
W_i	Weighting factor for the short term environmental conditions	–
x_{AP}	Longitudinal distance from aft perpendicular of the calculation point of lateral acceleration	m
x_{AE}	Longitudinal coordinate of the aft end of the ship	m
x_{FE}	Longitudinal coordinate of the forward end of the ship	m
z_G	Vertical distance between the centre of gravity and the waterplane	m

Greek symbols

β	Quadratic roll damping coefficient	rad^{-1}
Δ	Ship mass displacement	t
δ	Cubic roll damping coefficient	$\mathrm{s/rad}^2$
δ_{φ}	Non-dimensional logarithmic decrement of roll decay	–
ζ_a	Wave amplitude	m
λ	Wave length	m
μ	Angle of heading	rad
μ	Linear roll damping coefficient	s^{-1}
μ_e	Equivalent linear roll damping coefficient	s^{-1}
ξ	Phase angle	rad
ρ	Water density	$\mathrm{kg/m}^3$
σ_{a_y}	Standard deviation of lateral acceleration	$\mathrm{m/s}^2$
$\hat{\varphi}$	Complex roll amplitude	rad
φ	Roll angle	rad
$\dot{\varphi}$	Roll velocity	$\mathrm{rad\,s^{-1}}$
$\ddot{\varphi}$	Roll acceleration	$\mathrm{rad/s}^2$

φ_a Roll amplitude in regular beam waves of unit amplitude $\mathrm{rad\,m^{-1}}$

φ_i Imaginary part of the roll amplitude in regular beam waves of unit amplitude $\mathrm{rad\,m^{-1}}$

φ_r Real part of the roll amplitude in regular beam waves of unit amplitude $\mathrm{rad\,m^{-1}}$

$\varphi_{unprotected}$ Angle of submergence of unprotected openings in calm water deg

φ_v Angle of vanishing stability in calm water deg

ω Wave circular frequency $\mathrm{rad\,s^{-1}}$

ω_e Encounter wave frequency $\mathrm{rad\,s^{-1}}$

ω_r Natural roll frequency $\mathrm{rad\,s^{-1}}$

Chapter 1

Introduction

The Thesis focuses on the Excessive acceleration phenomenon, one of the Second Generation Intact Stability Criteria, finalized by the Correspondence Group on Intact Stability of the International Maritime Organization (IMO), in 2020. The development process of the criteria lasted almost 20 years, involving experts from research institutions, classification societies, regulatory bodies, ship operators and industry.

The criteria cover five dangerous dynamic phenomena in waves, namely Parametric roll, Pure loss of stability, Surf-riding/broaching, Dead ship conditions and Excessive acceleration. The verification of the ship behaviour against each phenomenon is performed by means of three different levels of assessment, with increasing complexity and accuracy from the lowest to the highest level. The SGISC structure consists of two vulnerability criteria, named Level 1 and Level 2, whose aim is to identify if the ship could be susceptible to experience such phenomena, and Direct Stability Assessment (DSA) aiming to confirm or reject the vulnerability of the vessel.

Excessive acceleration criterion was introduced later in the SGISC framework, as response to accidents related to "excessive stability", where lateral accelerations greater than the gravity acceleration were experienced on board. The phenomenon is particularly felt in loading conditions characterized by high initial stability, which leads to a low roll period and, consequently, large roll accelerations.

The effect of high initial stability on lateral accelerations experienced onboard is well recognized since many decades. In the first edition of the *Principle of Naval Architecture* (1939) book series, it was suggested to avoid excessive metacentric heights to prevent violent and dangerous rolling in waves, and subsequently accelerations. The same recommendation can be found in the 2008 IS Code (IMO Res. MSC.267(85)), where, in Part B, Chapter 5, subsection 5.1.6, is written:

The stability criteria contained in part A chapter 2 set minimum values, but no maximum values are recommended. It is advisable to avoid excessive values of metacentric height, since these might lead to acceleration forces which could be prejudicial to the ship, its complement, its equipment and to safe carriage of the cargo.

From the above text, it can be recognized the concern of regulations about dangerous lateral accelerations in rolling, caused by large initial stability. Nevertheless, no prescriptive rules are defined except for the recommendation to avoid loading conditions having large metacentric heights. However, it is worth mentioning that an "acceleration criterion" exists in the rules of the Russian classification societies concerning ships of mixed navigation (sea-river, river-sea), Bačkalov (2019). In the case of the Russian River Register, the criterion must be applied for dry bulk cargo river-sea ships. In the criterion, the acceleration associated to roll motion is estimated by simple formulas and compared with the limit value $0.3g$. Wave height limitations more severe than the default ones can be imposed if the limit value is exceeded.

Lateral accelerations are typically addressed in Seakeeping studies regarding the influence of acceleration on comfort and on the ability to work on board, quantified through the Motion Induced Interruptions (MII), Motion Induced Fatigue (MIF) and Motion Sickness Incidence (MSI) indexes. In particular, the Lateral Force Estimator (LFE) is introduced and it is defined as the apparent acceleration normal to the symmetry plan perceived by an object or a person, accounting for the events that force the crewman to interrupt the current task and to hold on some anchorage to prevent loss of balance. LFE is related to the MII to account for the ability of the crew to work effectively and for the possibility to have objects sliding across the deck or toppling over, Lloyd (1989). According to the number of MII per minute, different risk level may be defined, from *Possible* to *Extreme*, with an important degradation of operations if the number of interruptions is more than one per minute.

The occurrence of accidents associated to large lateral accelerations, during the development process of the Second Generation Intact Stability Criteria, made stronger the need for quantitative rules able to prevent the ship against excessive accelerations. In 2009, the German delegation at IMO submitted a document, IMO SLF 52/3/5, proposing the introduction of an additional criterion, initially referred as Excessive stability, in the SGISC framework, to address lateral accelerations due to synchronous roll. The delegation pointed out that some ship types, as container ships and ro-ro ships, are becoming vulnerable to harmonic resonance in beam seas due to their low roll period, determined by excessive stability, especially when they are operated in part deck load conditions. The minor accident on board of containership JRS Canis (2007) and the serious accidents on board of containerships Chicago Express (2008), CCNI Guayas (2009) and Frisia Lissabon (2009), where lateral accelerations greater than $1.0g$ were experienced at the wheelhouse, were mentioned to demonstrate that the phenomenon was not sufficiently addressed by the regulations. Therefore, the working group agreed to include the phenomenon in the process of development of the dynamic phenomena under consideration by the inter-sessional working group. The structure of the vulnerability criteria and the corresponding explanatory notes were finalized at the third session of the Ship Design and Construction (SDC) Sub-Committee in 2015, although, at that time, there was still a discussion on the limit values of the vulnerability criteria, IMO SDC 3/INF.10.

In the following subsections the physical description of the phenomenon, a state of the art, the main goals of the thesis and a review of the accidents are provided.

1.1 Physical background

Excessive acceleration criterion focuses on lateral accelerations generated by waves close to beam seas, which may excite the ship close to her natural roll frequency. Lateral accelerations experienced on board magnify with the distance from the roll axis, whose trace is indicated as R in Figure 1.1, since it is larger the distance to be covered in the given roll period. For a given roll amplitude, a reduction of the roll period causes an increase in the lateral accelerations since the same distance has to be covered in a shorter time. Roll period is strictly related to the transversal metacentric height, leading to short values when the metacentric height is large. Therefore, loading conditions characterized by high initial stability, as ballast condition or ship partly loaded, are the ones particularly prone to experience dangerous lateral accelerations which are responsible of transverse inertial forces, that could be a source of risk for people and cargo.

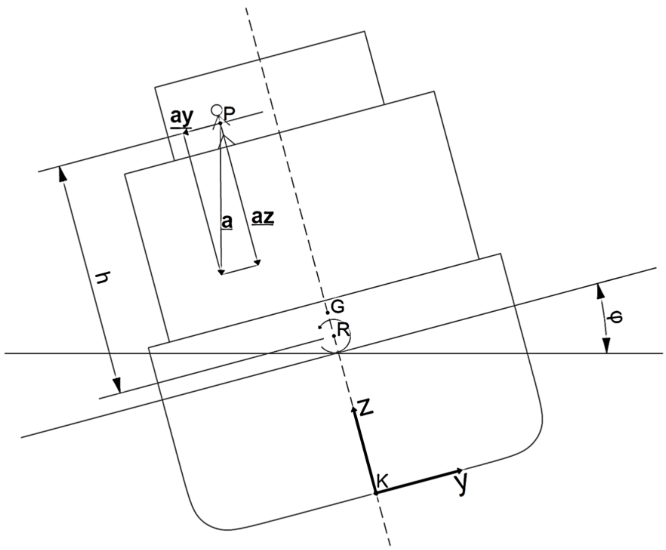

Figure 1.1: Lateral acceleration.

Let us consider a ship experiencing harmonic roll $\varphi = \varphi_0 \cdot sin\omega t$, being φ_0 the amplitude and ω the frequency of the motion. The point P, located at a height equal to h above the roll axis, experiences an acceleration $\underline{a}$ which is the result of various components: the gravity acceleration $\underline{g}$, the linear and normal accelerations associated with the roll oscillation, respectively equal to $\underline{h} \cdot \omega^2 \varphi$ and $\underline{h} \cdot \omega^2$, the vertical $\underline{a}_v$ and horizontal $\underline{a}_h$ accelerations due to ship motions different from roll, which depends on the longitudinal location of point P along the ship.

In a reference frame Kyz fixed to the ship, the so-called lateral acceleration $\underline{a}_y$ is perpendicular to the ship symmetry plan and is defined as the projection of $\underline{a}$ on the y-axis.

Synchronous roll resonance can cause large lateral accelerations, due to the amplification of the motion when the natural frequency of the ship is close to the frequency of the exciting waves. A good design of anti-rolling devices can mitigate roll motion under synchronous conditions.

1.2 State of the Art

Even if the magnification of lateral accelerations in beam or nearly beam waves under synchronous resonance is well recognized since many decades, the occurrence of the above mentioned accidents reinforced the scientific interest on the phenomenon. Research was conducted, theoretically and experimentally, not only at IMO level but also by industry and research institutions. A significant effort has been made to better understand the physics behind the nonlinear behaviour of the ship in irregular waves. Different approaches can be identified in literature, from the simplest 1-DOF roll model to multi-DOF motion models.

Fundamental works are the investigations conducted by the German Federal Bureau of Maritime Casualty Investigation concerning the dynamics of the accidents mentioned before, that clearly identified the high initial stability, the low roll damping and the influence of hull geometry as main parameters that can generate large accelerations, together with encounter frequency close to the roll natural frequency. The main findings are summarized in Section 1.4 based on the reports, BSU (2008), BSU (2009), BSU (2011) and IMO SLF 54/INF.6 (2011).

Synchronous rolling was considered in Shigunov et al. (2011) for the development of vulnerability criteria for lateral accelerations with respect to crew and cargo safety. The criteria were used as a preliminary assessment able to justify the development of ship-specific operational guidance, that should identify safe sailing conditions in relevant sea states. The Authors pointed out that the feasibility of their application should be also verified, accounting for speed loss in waves and course keeping ability in waves. Most of the adopted structure of Level 1 criterion can be recognized in the paper. The root mean square (RMS) of lateral acceleration was considered as possible criterion for the judgement of the ship behaviour, proposing $0.2g$ as possible standard, corresponding to less than one sliding event per hour on a dry deck, to be subject to verification and subsequent calibration based on a large sample of vessels. The RMS was calculated as solution of a simplified 1-DOF roll motion model, tested on a sample of six different vessels, considering loading conditions with large GM. Shigunov et al. (2013) discussed the possible application of operational guidance addressing ship motions and accelerations in heavy seas to limit cargo losses. The paper summarized the research activities of Germanischer Lloyd regarding the phenomenon, mentioning the relevance of cargo losses due to ship motions in intact conditions. Appearance of new ship typologies and not sufficient training of the crew on how to handle them increased the number of losses. Thus the control of ship operations through specific operational guidance was identified as a reasonable approach to limit cargo losses due to excessive motions and accelerations. OG were based on calculation of ship-specific design accelerations through hydrodynamic analysis of the ship behaviour in waves, replacing the empiric rule-based values. The Authors adopted a short-term criterion given by the probability of exceeding a prescribed limit, weighted through the probability of occurrence of the considered sea state, as possible measure to address long-term operational performance.

During the development of the criteria, a series of works explored the applicability of the different levels of assessment conceived in the SGISC and the potential issues. A set of 17 vessels was considered in Schrøter et al. (2017) using the full matrix of operational draughts, trims and GM values to analyze the robustness and consistency of the vulnerability criteria. The limiting GM curves for the full range of operational draughts were obtained. Sample calculations of vulnerability criteria of Excessive acceleration failure mode are reported in Belenky (2020), for a set of six vessels (one container ship, one ro-pax ferry, two cruise ships, one bulk carrier and one LNG carrier) considering several loading conditions for each of them, for a total of 31 cases. Level 2 assessment was performed considering three different techniques to the linearize roll damping term concluding that the linearization technique has not a great influence in the calculation of the long-term stability failure index, although a unique method to be implemented in the rule would be more practical and univocal. Moreover, a description of the derivation of Operational Guidance from Direct Stability Assessment or vulnerability criteria is given.

Petacco (2019) investigated the applicability of the Excessive acceleration vulnerability criteria and the related consistency referring to a mega-yach unit, a Ro-pax ferry and a set of naval vessels, providing the results through limiting KG curves and matrix calculations. The application of Operational limitations to the Ro-Ro pax ferry, assumed to operate in the Mediterranean Sea, is provided in Petacco and Gualeni (2020). The results were reported in terms of minimum height of the centre of gravity to ensure the ship against lateral accelerations, for different draughts. It was shown that the introduction of restrictions on the geographical area increased the design domain. Petacco et al. (2020) provided an example of application of Operational Guidance developed according to IMO's procedure, for a megayacht unit.

Begovic et al. (2021) developed OL related to maximum significant wave height and route for a bulk carrier vulnerable to the Excessive acceleration failure mode. Different strategies were considered to define the scatter table to be used in the assessment when the route crosses several areas, each of which characterized by its own scatter table. It was shown that too conservative results may be obtained when only the most dangerous area in the route which is considered. In some cases, more severe than the ones obtained using the standard scatter table used in Level 2 assessment. A comparison between the assessment conducted weighting according to the route length or performing a simple arithmetic mean of the scatter tables associated to the crossed area along the route was performed, showing that the simple arithmetic mean could be a reasonable strategy only on short routes. The same bulk carrier was considered in Begovic et al. (2022) to develop Operational Guidance for the Excessive acceleration according to a procedure obtained as a generalization of Level 2 to any ship speed and heading, by developing the expressions of the Froude-Krylov exciting roll moment as a function of the heading angle. The procedure was validated comparing the results with the ones obtained calculating the the 3-D potential code HydroStar®, showing comparable results.

A first attempt toward the Direct Stability Assessment for the EA failure mode was made by Kuroda et al. (2019). A model of containership reproducing Chicago Express was considered to conduct experimental tests in irregular beam waves, with the aim to evaluate whether two numerical codes (one based on frequency domain calculations and the other one on time-domain simulations) were able to predict ship roll motion in short-crested irregular waves. It was shown that both prediction methods are consistent with lower levels of assessment and have a sufficient accuracy, returning long-term probability indexes close to each other and in agreement with the results of the experiments.

Yu et al. (2022) provided a comprehensive assessment for a fishing vessel with respect to Excessive acceleration, considering the vulnerability of the vessel with and without a suspended load, which causes dynamic and periodically changing forces. Experimental and numerical investigations were performed to assess the behaviour of the vessel with respect to lateral accelerations. Results showed that the presence of the suspended load caused a non-linear magnification of lateral acceleration with wave height in beam waves.

In Duan et al. (2022) a containership in ballast condition was considered as test case for the comparison of five different approaches for the verification of the DSA with experimental tests. The first one was based on a simple 1-DOF roll model while the other four approaches were derived from a non-linear 5-DOF model based on strip theory (surge motion was ignored). For the latter, modifications in the calculation of the diffraction force and hydrodynamic coefficients were implemented. The restoring force was calculated considering the instantaneous wetted surface. The Authors confirmed that non-linear approximate time domain methods are fast and accurate methods to estimate lateral accelerations in waves.

An alternative method to evaluate the probability of exceeding a certain lateral acceleration was provided in Maki et al. (2021). The Authors proposed a method named "PDF line integral method" for the calculation of the pdf of roll angular acceleration by the knowledge of the joint pdf of roll and roll rate, demonstrating its capability to account for the non-linearities in the damping and restoring terms but keeping limited its computational costs. The method allows the evaluation the probability of exceeding a dangerous threshold of roll acceleration and it was validated through the comparison with the results obtained via Montecarlo simulations, showing a relatively good agreement. The method was further developed in Maki et al. (2022) where an explicit expression for the pdf of roll acceleration was obtained by the linearization of the restoring term with the main advantage of avoiding complex numerical integration.

Even if some other ship typologies were considered, the above mentioned works, were mainly focused on containerships, identified as the main typology affected by excessive lateral accelerations. This point of view is in the first proposals of the vulnerability criteria which were thought to be mandatory only for containerships and ships carrying deck cargoes. However, it was later recognized that other ship typologies could be affected by the phenomenon in some loading conditions, for which the application of the criteria could be worthwhile. Indeed, the SGISC are, in principle, applicable to any ship typology thanks to the physics-based foundation, independently from the particular regulation framework. Naval vessels were considered by some authors, since they have to face extreme weather conditions resulting particularly exposed to stability failures in waves. Petacco et al. (2017) considered the Naval Ship Code as a modern and innovative set of regulations that could incorporate the phenomena covered by the SGISC. A helicopter carrier, a destroyer and a patrol vessel, were considered to perform a comparison between the limiting height of the ship centre of gravity above the keel line KG curves obtained applying the navy regulations and the first vulnerability levels of the SGISC. The considered navy regulations are based on the righting arm curves characteristics but with more stringent requirements compared to the ones adopted in the 2008 IS Code, in line with the more severe operational profile. The Authors showed that the results from the application of Level 1 of Excessive acceleration criterion, which defines minimum values of the height of the centre of gravity, were too severe and in contrast with the maximum values obtained from the application of other criteria, with the results that for some displacements a range of allowable KG could not exist, or if it exists it could be too small. The vessels were further investigated in Petacco (2019) where Level 2 assessment was performed for all five SGISC, and the "design space" was defined taking into account also maximum allowable KG curves associated with the Naval Ship Code. Results showed that: for the heli-carrier, the design space exists for all the operational draughts; for the destroyer, it does not exist for the highest draught; for the offshore patrol vessel, the design space does not exist at all. The investigation continued in Petacco and Gualeni (2022) where OG were developed for a destroyer unit, an amphibious transport dock and an offshore patrol vessel considering the sea states defined by NATO regulations, showing that it could be important to provide some guidance to the crew on how to handle the vessel in heavy seas to avoid the occurrence of dangerous lateral accelerations, especially in beam and head waves.

Four ships, already studied and found vulnerable to some of the SGISC in Begovic et al. (2018) and Begovic et al. (2019), were analyzed in Boccadamo and Rosano (2019), to test the applicability of the acceleration criterion to hull forms representative of naval vessels, considering five displacements for each of them. The four ships were the models D1 and D5 of the systematic D-Series scaled to 90-meters length (Kracht and Jacobsen (1992)), a frigate and the ONR (The US Office of Naval Research) Topside Series hull form. Low roll periods and the great variations of hull geometry in vertical direction were identified as parameters that make the considered ships potentially vulnerable to the EA phenomenon. The limiting KG curves associated to Level 2 assessment were computed for each of them and compared with the curves of the maximum KG complying with intact stability criteria specified in RINA (Registro Italiano Navale) classification rules for naval ships. In the paper, it was pointed out that during the process of development of the criteria the refinement of the standards for Level 1 and 2 aimed at avoiding inconsistencies among different levels, with the drawback that the conservativeness of the adopted standards influences the limiting KG curves associated to EA. The curves can conflict with the ones associated with the remaining intact stability criteria, as demonstrated for the four considered naval vessels. Finally, the paper emphasized the importance of the proper investigation of roll damping, since navy ships, due to their typical geometrical and mechanical parameters, could have some parameters outside the range of applicability of the Simplified Ikeda's Method, which is the standard method introduced in the regulations for the roll damping estimation. Two models of the Systematic Series D and the notional ONR Tumblehome ship, were object of additional investigations in Rosano and Rinauro (2020) and Rosano et al. (2020) referring to the second level of assessment of Dead ship condition and Excessive acceleration criteria. The limiting KG curves associated with level 2 of both criteria were obtained showing that fitting the vessel with anti-rolling devices, as bilge keels, is a solution that allows to obtain safe ranges of allowable KG.

River-sea ships are not covered by the SGISC but are typically under national regulations consisting of deterministic semi-empirical procedures based on design practice and operational experience. These ships could suffer lateral accelerations and were object of an extensive research. Methods and procedures within the SGISC were investigated and eventually modified for a proper application to river-sea ships. Research works were mainly focused on the aspects affecting Excessive acceleration and Dead ship condition criteria as the adjustment of roll damping estimation method (Rudaković and Bačkalov (2017)), the modification of environmental conditions (Rudaković and Bačkalov (2019)), the calculation methods for effective wave slope coefficient (Rudaković et al. (2019)) and natural roll period calculations (Rudaković et al. (2021)).

From the above state of the art, the main works that led to the incorporation of the criterion in the stability regulations are identified. The works by the Federal Bureau of Maritime Casualty Investigation put in evidence the main parameters that can trigger the inception of dangerous lateral accelerations. It can be observed that most of the works explored the application of the different levels of assessment of the Excessive acceleration criterion. Some of the works were focused on the integration of the Excessive acceleration limits with the ones associated to the current intact stability rules and the other four SGISC. Another group of works explored the vulnerability to the phenomenon of ships not covered by the SGISC, as navy ships, inland vessels and one fishing vessel. Part of the above mentioned lines of research have been further investigated in the present Thesis, as reported in the following section.

1.3 Objectives and Outline of the Thesis

The Thesis collocates in the trial period of the SGISC during which feedback is expected based on the experience gained through the application of the different levels of assessment. The Thesis focuses on the Excessive acceleration failure mode.

The main objectives have been:

- review of the theoretical background of the Excessive acceleration and of structure adopted in the SGISC framework;
- analyze the feasibility of Operational Measures;
- identify critical points or source of potential improvements in the implemented methodologies;
- verify the proposed methodologies on test cases.

An overview of the process of development of the Second Generation Intact Stability Criteria and of the corresponding structure is given in Chapter 2. The Excessive acceleration criterion is presented in Chapter 3. The validation of the developed numerical code for the verification of the vulnerability criteria is given in Chapter 4.

The simplified formulation implemented in the rules for calculation of the Froude-Krylov excitation, specific for the beam seas case, is extended to any wave heading angle and validated in Chapter 5. The formulation has been shown to be simple but sufficiently accurate for its implementation in the rules in view of the development of ship-specific Operational Guidance.

Chapter 6 discusses an on-board Decision Support System, designed to monitor the actual condition of the vessel and to predict the lateral acceleration that could be experienced in the short-term. The system is intended to support the crew in real operational conditions and integrate Operational Measures developed at the design stage.

Finally, a bulk carrier and a fishing vessel are presented as test cases in Chapter 7 and Chapter 8, respectively.

The bulk carrier is found vulnerable to Level 1 and Level 2. Operational Limitations are developed for the bulk carrier, which is supposed to sail on long routes from Europe to Africa. The definition of the equivalent scatter table that should be used in the verification when the ship sails on long routes is discussed. Operational Guidance is developed based on the generalization to any wave heading and ship speed of Level 2. Safe and unsafe sailing conditions are identified, in relevant sea states, showing that the proposed generalization of the Froude-Krylov roll moment procedure returns results similar to the ones obtained calculating it with a 3D potential theory software.

A 34-5 meters long fishing vessel, typical of the Spanish fleet has been object of an experimental campaign at the University of A Coruña (Spain) towing tank. Level 1 and Level 2 are not satisfied and Operational Limitations related to area and to the maximum significant wave height are developed. A discussion on the feasibility of the Direct Stability Assessment using deterministic criteria is been conducted confirming the vulnerability of the vessel. Finally, the monitoring system is applied using simulated and experimental data in irregular beam waves.

In Chapter 9 the main findings of the Thesis are summarized and potential issues to be further investigated in future research are suggested.

1.4 Summary of the main accidents

A summary of the accidents that pushed to start the development of the Excessive acceleration criterion is provided in the following subsections, according to the investigation analysis conducted by the German Federal Bureau of Marine Casualty Investigation (BSU) as reported in BSU (2008), (2009), (2011) and IMO SLF 54/INF.6 (2011). The outcomes of the investigations showed some similarities among the accidents in terms of sailing conditions, loading conditions and hull geometry. The ships were sailing in ballast condition or in loading conditions close to the ballast one, characterized by large values of the initial stability. An insufficient roll damping played a fundamental role in the accidents' dynamics. The investigations showed that no simple rules exist to identify the environmental and operational conditions that may cause these kind of accidents.

A summary of the main characteristics of the ships involved in the accidents is provided in Table 1.1. The natural roll period was calculated for all ships, except for JRS Canis (her period is from the accident's report), according to the following formula from the 2008 IS Code:

$$T_r = \frac{2 \cdot C \cdot B}{\sqrt{GM}} \tag{1.1}$$

where:

$$C = 0.373 + 0.023\frac{B}{d} - 0.043\frac{L_{WL}}{100} \tag{1.2}$$

being B the ship breadth, d the mean draught, L_{WL} the length at the waterline and GM the transverse metacentric height.

Ship	$L_{OA}(m)$	$B_{OA}(m)$	$d_{mean}(m)$	$GM(m)$	$T_r(s)$	**Loading condition**
JRS Canis	129.20	20.60	7.29	1.336	13.37	Not uniformly loaded
Chicago Express	336.19	42.80	8.08	7.72	10.8	Partly loaded
CCNI Guayas	208.16	30.04	5.72	5.63	10.2	Ballast
Frisia Lissabon	207.40	29.80	5.59	4.56	11.3	Ballast
Pacific Adventurer	184.90	27.60	8.197	4.4(solid) 2.7(fluid)	9.8(solid) 12.5(fluid)	Partly loaded

Table 1.1: Summary of the ship main parameters at the time of the accidents.

1.4.1 JRS Canis

The containership JRS Canis left Bremerhaven (Germany) on 11 January 2007 evening, during the development of a storm. In the course of the night, the ship, that was sailing at about $15.5kn$ in waves up to $5m$ and wind at force 9 Bft, started to roll up to 20° to each side, losing ten containers into the sea and leaning the container stack on the port side inwards and the ones on starboard side outwards. The investigation coordinated by the German Federal Bureau of Maritime Casualty consisted of numerical simulations of accelerations on the layers in the red rectangle in Figure 1.2. According to the obtained results, lateral accelerations of about 3 to $4m/s^2$ were experienced by the layers of containers involved in the accident. A non-uniform distribution of the containers was identified as one of the possible causes of the breaking of the lashing system. Indeed, the heavier containers were located on the top layers making possible the breaking of the lashing system for lateral accelerations lower than the design value of $0.5g$.

The investigation emphasized the necessity to develop on-board systems that would enable the crew to properly handle the ship under these conditions and to avoid dangerous sea conditions based on the monitoring of ship motions.

1.4.2 Chicago Express, CCNI Guayas and Frisia Lissabon

Lateral accelerations greater than the gravity acceleration were experienced at the wheelhouse of containerships Chicago Express, CCNI Guayas and Frisia Lissabon, resulting in fatal injuries in the first two casualties and a serious injury in the last one.

The 8749 TEU container vessel Chicago Express left the port of Hong Kong on 23 September 2008, partly loaded with a limited number of containers because

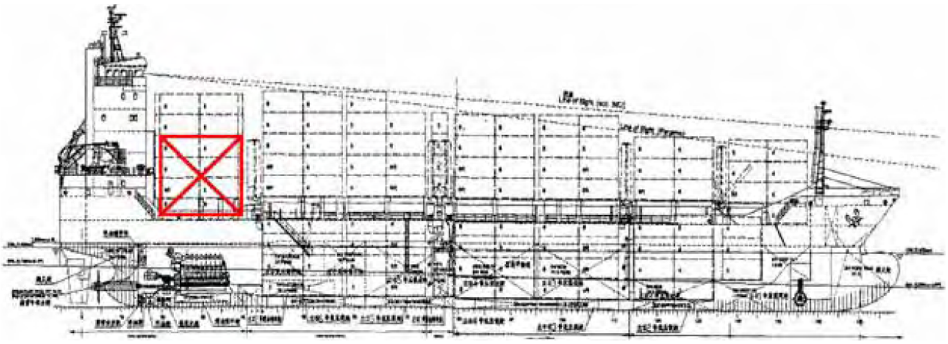

Figure 1.2: Container layers object of the investigation, BSU (2008).

of the approaching typhoon Hagupit. The vessel sailed in heavy weather with significant wave height around $7.5m$, and additional swell having a significant wave height of $3.0m$. The wave heading was between 110° and 120°, while the vessel speed oscillated in the range from 3 to $5kn$ at the time of the accident. The ship was rolling up to $20°$ when she was suddenly hit from starboard by a violent wave that amplified the vessel roll motion to more than $30°$, for an estimated period of $10s$. Due to the violent rolling, large lateral accelerations were experienced at the wheelhouse, causing the death of the Lookout due to head injuries, a serious injury of the Master and minor injuries of other four crew members. An impressive image is the one reported in Figure 1.3, where the estimated trajectories covered by the Master and the Lookout in a sequence of rolling is reported, clearly showing that they were literally launched across the entire width of the bridge, causing the serious injuries they suffered.

The large roll angles were caused by the absorption of a large amount of energy by the ship due her high initial stability (the ship left the port with a transverse metacentric height equal to $7.72m$) and by the small dissipation of energy due to low roll damping, caused by the low ship speed, allowing sequences of large waves to strongly increase roll motion. Even if a high initial stability was identified, investigations showed that a moderate reduction in stability, that was practically feasible, would not have prevented the accident. Only a marked, but unpractical, reduction in stability would have mitigated the phenomenon. A moderate increase in speed would have noticeably limited the accelerations, because of the increase in roll damping, but at the same time a parametric resonance could have encountered.

Similar extreme weather conditions were experienced by CCNI Guayas and Frisia Lissabon, which were sailing in ballast condition. On September 2009, a fatal accident occurred onboard of CCNI Guayas while she was sailing off the coast of Hong Kong, during typhoon Koppu. The storm was characterized by wind speed of 10 Bft and wave heights of $7-8m$ making the vessel rolling heavily, reaching an angle of about 35° and large accelerations at the bridge. Due to the violent rolling the third officer fell and was thrown across the bridge several time, losing his life some hours later. The ship herself reported serious damages and lost some of her equipment into the sea. A photo of the wheelhouse condition after the accident is reported in Figure 1.4.

Time domain simulations were performed, BSU (2011), to estimate accelera-

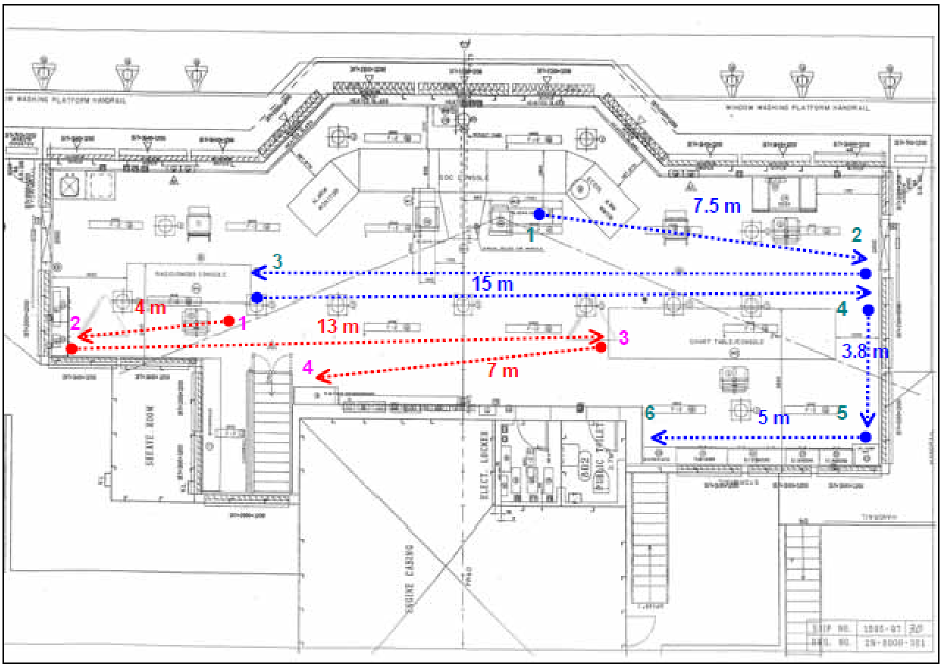

Figure 1.3: Top view of the Chicago Express wheelhouse. Estimated trajectories covered by the Master (blue) and the Lookout (red), BSU (2009).

tions on the bridge in the ballast condition, for an exposure time of $10000s$ and simulating the accident conditions. The ship speed of $2kn$, wave heading of $150°$ and three significant wave periods, 8.5, $9.0s$ and $9.5s$, were considered, obtaining accelerations up to $1.3g$ in the worst condition and greater than $1.0g$ in the most favourable one. Additional simulations were performed keeping the same wave periods, ship speed and wave heading but considering a loading condition without ballast water. A significant reduction to an acceptable level of roll angle and lateral accelerations on the bridge was obtained. Indeed, the two loading conditions were characterized by nearly the same metacentric height, but different draught and trim, as summarized in Table 1.2. It was concluded that, despite the similar initial stability, the behaviour in waves was significantly different because, in the case without ballast water, the hull is no longer immersed in the forward region, leading to a significant reduction of the exciting moment transmitted to the vessel.

The investigation recognized that the stability framework mainly focused on minimum requirements to avoid capsizing, while the same attention should be paid to define the corresponding upper bound, that otherwise could be detrimental for cargo and crew safety.

The knowledge gained from the accident was further confirmed by the investigation on the accident occurred on the containership Frisia Lissabon, a vessel almost identical to CCNI Guayas. The ship was sailing in ballast condition at very low speed in heavy weather and close to beam seas (the actual heading was around 60°) when she started to experience violent rolling due to the a series of two large waves, and subsequent lateral accelerations at bridge comparable to the

Figure 1.4: CCNI Guayas. Wheelhouse condition after the accident, BSU (2009).

	Without ballast water	**Ballast**
Draught aft (m)	7.35	7.45
Draught midships (m)	3.86	5.70
Draught fore (m)	0.37	3.95
GM (m)	5.75	5.63

Table 1.2: Comparison of relevant parameters used in the numerical simulations on the CCNI Guayas, BSU (2011).

gravity acceleration that seriously injured the pilot, thrown away by his seat.

The investigations of the accidents involving Chicago Express, CCNI Guayas and Frisia Lissabon showed some parallelism. First, the three vessels were characterized by a high initial stability, since two of them were sailing in ballast condition while the third one in a partly loaded condition. However, the accidents cannot be explained only referring to the initial stability. Low roll damping was one of the major factors of the dramatic events, due to low ship speed. An increase of the ship speed should have significantly reduced the accelerations but it would have been in contrast with the principles of good seamanship due to the possibility of experiencing other dangerous phenomena. It was noticed that different floating conditions can be characterized by different roll and accelerations responses even if the initial stability is the similar. These considerations show the inherent complexity of the on-board decision making process and demonstrate the necessity to accurately analyze the dynamic behaviour of the ship in waves at the design stage.

As a final conclusion of the investigations, it was emphasized the importance of a proper design of the navigation bridge, as indicated by international standards, which should be covered by non-slip rubber, should not have sharp edges and corners and should be equipped with hand and grab rails.

Figure 1.5: Pacific Adventurer damage, Australian Transport Safety Bureau (2009).

1.4.3 Pacific Adventurer

The accident of the Australian container vessel Pacific Adventurer on 11 March 2009, during the process of development of the Excessive acceleration criterion, gave the opportunity to further investigate the vulnerability of ships sailing with large initial stability in heavy seas. The loading condition of the vessel was characterized by the presence of large free surfaces in partly filled tanks located in the double bottom, that generated an important reduction of the metacentric height. The solid metacentric height was equal to $4.441m$ while the corrected one was equal to $2.685m$. The effect of large free surface in partly filled tanks as a device to increase roll damping was deeply analyzed, as reported in IMO SLF 54/INF.6 (2011) based on the investigation Australian Transport Safety Bureau (2009). It was pointed out in BSU (2011) that the design of tanks for partially filling could be beneficial to reduce ship stability in ballast condition and to increase roll damping, with the final aim to reduce lateral acceleration. On the other hand, it was pointed out the need to train the crew to assess the effect of free surfaces and to take appropriate decisions.

The container ship lost 31 containers overboard and damaged the ship fuel tanks causing the spill of about $270t$ of oil. The ship was sailing in beam seas at a speed of $9kn$ due to the encountered heavy seas, having significant wave height of about $4.7m$ and period of about $9 - 10s$. The ship was sailing in a partly loaded condition, characterized by a high value of the metacentric height, that lead the ship to roll heavily resulting in breaking the lashing and subsequent loss of the containers, Figure 1.5.

The analysis conducted by Germany recognized synchronous rolling in beam waves as the main cause of the accident, mentioning the large absorption of wave moments and the insufficient damping as additional issues that worsened the phenomenon. The identification of synchronous resonance in beam waves led the German delegation to reconsider some of the findings reported in the previous investigations, where only bow waves were considered as potentially dangerous in terms or large rolling and accelerations, identifying the increased roll damping due to drift motion in beam conditions as a source of reduction of roll motion. The investigation showed that partly filled double bottom tanks size have no or only marginal effect on the roll period of partly loaded container vessels in heavy weather. Additionally, roll period calculated accounting for the free surface correction on the metacentric height could lead to misleading results if the partly filled tank is not specifically designed as anti-roll device.

This page was intentionally left blank.

Chapter 2

Second Generation Intact Stability Criteria

2.1 Historical background

The IMO Maritime Safety Committee (MSC) adopted the International Code on Intact Stability (2008 IS Code), IMO Res. MSC.267(85) and the corresponding Explanatory Notes, IMO MSC.1/Circ.1281 in 2008, which entered into force as a set of mandatory rules in 2010, presenting stability criteria for ensuring the safe operation of ships. The code is the result of the revision of the 1993 Intact Stability Code, IMO Res. A749(18), as amended, IMO Res. MSC.75(69) (1998), which represent the IMO's attempt to unify all existing intact stability regulations into one document endorsed at international level.

The origin of the IS Code can be recognized in the 1960 SOLAS Conference, that provided to IMCO a recommendation to develop intact stability standards for passenger ships, cargo ships and fishing vessels. Two recommendations were given in 1968, IMCO Res. A.167 (ES.IV) and IMCO Res. A.168 (ES.IV), inspired by Rahola's PhD thesis (Rahola 1939). The recommended criteria adopted a statistical approach based on data of ships operating in the 60's, having length of 100 meters or less, linking the righting arm characteristics for still water condition to ship stability safety, based on the analysis of casualty records. Stability parameters of capsized ships were compared to the corresponding ones of ship considered to be safe in order to tune the criteria (L. Kobylinski 1975).

In 1978, a Working Group on Intact Stability was re-established, which developed the Weather Criterion, intended to prevent extreme roll motion and capsizing in beam waves and wind. The criterion, obtained merging the Japanese and USSR versions, is the first intact stability criterion based on a physical model although with some empirical assumptions that rely on casualties by the 50's, (Umeda and Francescutto 2016). The Weather Criterion for cargo and passenger ships was adopted as a recommendation in 1985, IMO Res. A.562(14) by IMO, that replaced IMCO in 1982.

A detailed description of the development process of national and international standards is reported in Kobylinski and Kastner (2003). A summary of main IMO documents, at the basis of the current intact stability rules and of the second

Document	**Year**	**Content**
IMCO Res. A.167 (ES.IV)	1968	Recommendation on intact stability for passenger and cargo ships under 100 metres in lenght
IMCO Res. A.168 (ES.IV)	1968	Recommendation on intact stability of fishing vessels
IMO Res. A.562(14)	1985	Recommendation on a severe wind and rolling criterion
IMO Res. A749(18)	1993	1993 Intact Stability Code
IMO Res. MSC.75(69)	1998	Amendements 1993 Intact Stability Code
IMO SLF 44/INF.6	2001	Study on the applicability of the Weather criterion for large passenger ships
IMO Res. MSC.267(85)	2008	2008 Intact Stability Code
IMO MSC.1/Circ.1281	2008	Explanatory Notes to the 2008 Intact Stability Code
IMO SLF 53/5/5	2010	Proposal to name the criteria "Second Generation Intact Stability Criteria"
IMO MSC.1/Circ.1627	2020	Interim guidelines on Second Generation Intact Stability Criteria
IMO MSC 105/20	2022	Approval of the Explanatory Notes on the Second Generation Intact Stability Criteria
IMO MSC.1/Circ.1652	2022	Explanatory Notes to the Interim guidelines on Second Generation Intact Stability Criteria

Table 2.1: Summary of main IMO documents at the basis of the current intact stability rules and of the second generation intact stability criteria.

generation intact stability criteria, mentioned in this chapter are summarized in Table 2.1.

The mandatory criteria in the 2008 IS Code consist of the deterministic criteria defined in the same way as was done by Rahola and the Weather Criterion. The critera are intended to be applied to all cargo and passenger ships of 24 m in length and over. The criteria can be considered as the first generation of intact stability criteria and the code itself can be seen as a part of a long-term process of rules development to guarantee ship safety in intact condition. In this respect, the preamble of the 2008 IS Code recognizes the complexity of the non-linear dynamic behaviour of the ship in a seaway, pointing the need for continuous research and investigation, which is further emphasized in Section 1.2 of Part A, dedicated to dynamic stability phenomena in waves, that mentions the need for development of performance oriented criteria. The preamble explicitly mentions the need to further revise and re-evaluate the code in the future, due to the evolution of ship design, hull form, ship size and type of operations. Indeed, new hull forms and ship typologies appeared in the last decades, as containership, Ro-Ro, and car-carriers, in response to an increasing request of cargo capacity and speed. Their geometrical and inertial characteristics are different from the ones that constituted the main data set for the development of the empirical stability criteria in force. These new ships are the ones mainly affected by the occurrence of intact stability related accidents, since current stability rules are based on a statistic analysis made on a small population of vessels which is not always representative of the actual world fleet in terms of types, size and hull form.

It is worth mentioning that despite the development of stability criteria based on motion characteristics started only in recent years, it was well recognized since the development of the first generation criteria at IMCO, in the 60's, the need for rational stability criteria able to account for the dynamical behaviour of ships in waves, Kobylinski and Kastner (1975). The statistical criteria developed at that time were agreed to be a temporary set of rules to be replaced, in the long term, by physics-based criteria once the knowledge and the tools related to the complex dynamic of ships in waves were sufficiently mature. In 1978, the re-established Working Group on Intact Stability started to consider the possibility to introduce the probabilistic approach in order to develop performance based criteria intended to replace the prescriptive ones. Due to the complexity of the task for the technology available at that time, the research on the subject continued but the rules were postponed, Kobylinski and Kastner (2003).

The IMO decision to revise the Code on Intact Stability is a consequence of significant changes in ship design. In 2001, the Italian delegation at IMO submitted to the SLF Sub-committee a document, IMO SLF 44/INF.6 (2001), questioning the applicability of the Weather Criterion to large passenger ships, whose parameters are often outside the ranges used at time of the development of the criterion and resulting in too stringent requirements for metacentric height values. Main conclusion of the document was that some of the parameters (dimensional ratios and the height of center of gravity) of the Weather Criterion are not adequate for some ship typologies, specifically large modern ships, inviting the SLF Sub-committee to review the Code on Intact Stability.

The working group on intact stability was re-established in 2002 at the 45-th session of the SLF Sub-committee, asked to deal with the review of the Intact Stability Code. In parallel to the revision of the Code, the working group started to discuss and develop a new set of rational intact stability criteria based on the physics of the addressed phenomena. The aim was to prevent the ship against total (capsizing) or partial (large heel angles or lateral accelerations) stability failures that could be dangerous to crew, passengers, cargo or ship equipment, recognizing that the actual stability regulations were not able to properly assess the intact dynamic behaviour of modern ships. This new set of criteria was initially referred as "New Generation of Intact Stability Criteria" and renamed "Second Generation Intact Stability Criteria", following a Polish proposal that emphasized the different approaches at the basis of the new criteria and the ones at the basis of the 2008 IS Code, to be considered as first generation criteria, IMO SLF 53/5/5 (2010).

The actual development of the SGISC started in 2005, at the 48-th session of the SLF Sub-committee and it was finalized in 2020 with the approval of the Interim Guidelines by the MSC at the end of 2020, IMO MSC.1/Circ.1627. The Explanatory Notes were approved at 105-th session in April 2022, IMO MSC 105/20, to be disseminated as IMO MSC.1/Circ.1652.

Currently, the criteria are on their trial period in order to check their robustness and to gain experience based on their use, to eventually refine them in next years.

A detailed summary of the SGISC development activity by the working group on intact stability is reported in Belenky et al. (2011) and Belenky (2020).

2.2 Structure of the SGISC

The SGISC are intended to be included in Part A of the 2008 Intact Stability Code in next years, after an extensive testing phase. Aim of the criteria is ensuring a sufficient level of safety regarding five phenomena in waves:

- Parametric roll;
- Pure loss of stability;
- Surf-riding/broaching;
- Dead ship condition;
- Excessive acceleration.

Parametric roll and Pure loss of stability are usually referred as restoring variation problems since they are related to the variation of the GZ curve in waves caused by changes in the underwater part of the hull. Such changes are particularly important under certain circumstances: the hull has great geometrical variations in the vertical direction at bow and stern while is nearly wall-sided in the middle part; the wave length is comparable to the the ship length; the direction of propagation of the waves is longitudinal. In such conditions the ship can experience a resonance condition, called parametric roll resonance, caused by periodic stability changes, when the encounter frequency is twice the natural roll frequency. Parametric roll can be source of large roll angles and/or accelerations that can damage the ship and cargo. Pure loss of stability typically happens when the waves are approaching from the stern, with a celerity close to the ship speed. The ship stability can be significantly reduced when the wave crest is located amidship since the waterplane area becomes minimal. If this situation is prolonged, and a sufficiently large heeling moment occurs, then large heel angles or even capsizing can occur.

Surf-riding/broaching is a manoeuvring related problem that may occur when the ship is sailing in following or quartering waves with ship speed slightly lower than the wave celerity and ship length comparable to the wave length. A sufficiently steep wave having length between one to three times longer than the ship accelerates the ship to wave celerity, making her directionally unstable. An uncontrollable turn to beam waves, called broaching, may occur despite the maximum steering effort which can produce a large heeling angle and eventually capsizing.

In the Dead ship condition the ship has lost her power, losing her ability to steer and manoeuvre. This scenario is already included in the 2008 IS Code, as Weather Criterion (Severe wind and rolling criterion). It is assumed that the ship turns into beam seas, rolling under the action of wind and waves; a steady wind acting on the lateral exposed area combined with the hydrodynamic reaction caused by the transverse motion of the ship force the ship to heel on one side. Then, a sudden and long gust occurs when the ship is rolled at the maximum windward roll angle resulting in an increase of the maximum leeward roll angle. If the resulting heeling angle is too large the ship could capsize.

Further details of the physics governing the addressed phenomena can be found in IMO SDC 8/WP.4/Add.2 (2022).

It has to be mentioned that other dynamic phenomena could be addressed by regulations in future. The Polish delegation noticed that one of the limits of the SGISC is that the phenomena are modelled as separated from each other with no mutual interference, IMO SLF 52/3/2 (2009). The delegation underlined that the most dangerous situations for intact stability arise in steep quartering waves, where multiple phenomena can occur simultaneously or in sequence, as wave impacts, water on deck, stability reduction on wave crests etc. The working group on intact stability, recognized the importance of the phenomena identified by the Polish delegation, and decided to postpone the inclusion of the phenomena in a later stage of development of the criteria, due to the limited available time and resources, IMO SLF 52/WP.1 (2010).

The main novelties of the criteria, with respect to the first generation criteria developed for calm water and zero-speed conditions, are the probabilistic approach to model the stability failure, which is a stochastic event, and the physics-based foundation. For each phenomenon, a physical model is developed accounting for ships speed and non-linearities associated to large motions, which are usually neglected in Seakeeping studies. The adopted approach makes the criteria applicable to any ship, regardless of the specific typology and characteristics. Due to the complexity of the phenomena a multi-tiered structure is introduced, consisting of three different levels of assessment plus an extra level addressing the operational aspect of ship safety:

- Level 1;
- Level 2;
- Direct Stability Assessment (DSA);
- Operational Measures (OM).

The complexity of the assessment increases, while the conservatism reduces, from Level 1 to DSA, due to the greater accuracy of the associated physical model. The modularity of the criteria theoretically allows to remove or replace one of the levels, if necessary, without the need to reconsider the entire structure of the criteria. A schematic representation of the application logic of the criteria is shown in Figure 2.1.

The verification of any of the SGISC can start from any of the levels, even if the logical application is from the simplest to the most conservative one. A ship found vulnerable to a certain phenomenon should be subject to a revision of her design or the vulnerable loading conditions should be discarded. Another option is the application of the Operational Measures (OM) to loading conditions for which one of the levels fails. Their development may be considered when changes in ship design are not feasible, since they can increase the costs or can be in contrast with other requirements, as ship resistance or cargo capacity .

A brief overview of Vulnerability criteria, Direct Stability Assessment and Operational Measures is given in the following subsections.

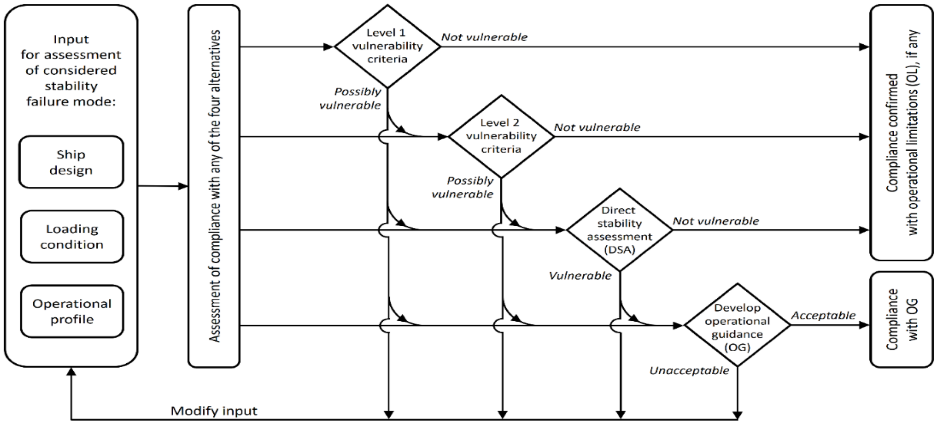

Figure 2.1: Schematic representation of the application structure of the second generation intact stability criteria (IMO MSC.1/Circ.1627 2020).

2.2.1 Vulnerability criteria

The first two levels are called Vulnerability criteria and represent simplified tools to identify potentially vulnerable loading conditions for the subject ship.

Level 1, the simplest and most conservative one, identifies loading conditions potentially vulnerable to the considered phenomenon and it is thought to be applied with very simple calculation tools, in a relatively short time. A ship that does not pass Level 1, in one or more loading conditions, is referred as "unconventional".

Level 1 criterion for Parametric roll judges a ship vulnerable if the ratio between the amplitude of the variation of the metacentric height in waves and the metacentric height in calm water, is greater than a limit value, which is a function of main ship dimensions and of the total area of the bilge keels. Ships having the Froude number at service speed greater than 0.24 should be verified against Level 1 of the Pure loss of stability, which requires that the minimum value of the metacentric height in waves is greater than $0.05m$. Ships having length greater than $200m$ and Froude number at service speed greater than 0.24 fail Level 1 of Surf-riding/broaching. Level 1 of the Dead ship condition is the Weather Criterion, already implemented in the current intact stability regulations.

If a certain loading condition fails Level 1, the verification may progress to the less conservative Level 2, that could confirm or reject the vulnerability. Level 2 relies on more sophisticate tools even if some simplifying assumptions are still kept to make its verification feasible, in terms of time, tools and computational costs. Level 2 requires the calculation of a long-term index, based on the calculation of short-term indexes calculated for the sea states reported in a standard wave scatter table.

Level 2 of parametric roll is based on the calculation of two criteria, $C1$ and $C2$. The first is a function of the metacentric height in waves, the second one is determined from the estimation of the maximum roll angles in head and following waves, for different ship speeds, obtained by the solution of a 1-DOF roll motion equation in the time domain. The Level 2 for Pure loss of stability is verified through two criteria, $CR1$ and $CR2$, based on the estimation of the minimum value of angle of vanishing stability and the maximum value of the static angle of righting arm curve in waves, respectively. For Surf-riding/broaching, Level 2 is based on the solution of surge motion equation, following Melnikov's method, to identify Surf-riding threshold. The critical ship speed corresponding to Surf-riding threshold is then combined with the probability of encountering a local regular wave that causes the instability, for a certain sea state. Level 2 of Dead ship condition requires the computation of a long-term stability failure index C and it is verified if it is lower than a limit value. The long-term index is obtained as weighted sum of short-term indexes $C_{s,i}$, calculated for each sea state for an exposure time of $3600s$, modelling the capsizing event as a Poisson process. A detailed description of Level 1 and 2 of the Excessive acceleration criterion is given in Chapter 3.

2.2.2 Direct Stability Assessment

Level 3, the so-called Direct Stability Assessment (DSA), can be applied if the ship is still recognized as potentially vulnerable from the application the Vulnerability criteria. DSA relies on the most advanced numerical simulation tools and experimental tests, to assess the likelihood of the stability failure in a seaway, accounting for the relevant number of degrees-of-freedom and for proper modelling of environmental conditions, roll damping, forces and moments.

The failure event is defined as:

1. exceedance of a certain roll angle, defined as the minimum among three values: 40°; the angle of vanishing stability in calm water, φ_v; the angle of submergence of unprotected openings in calm water $\varphi_{unprotected}$; or
2. exceedance of the lateral acceleration of $9.81m/s^2$, at the highest location along the length of the ship where passengers or crew may be present.

The outcome of DSA can be accepted by the Administration if an acceptable low probability of stability failure is demonstrated. DSA is not expected to be applied to most of the ships, due to its complexity which requires advanced simulation tools, professional figures able to conduct the assessment and large costs in terms of time and economical resources, but it could be performed when dealing with innovative or high value-added vessels.

In conducting a DSA, particular attention must be paid in replicating ship motions in waves, which can be evaluated by numerical simulations and/or experimental tests. The fulfillment of some requirements for the proper modelling of waves, roll damping, external forces and moments is necessary for the acceptance of the results by the Administration. Waves have to be statistically independent, while roll damping may be evaluated experimentally (decay or forced roll tests) or by empirical formulas. If CFD simulations are performed, the agreement with experiments has to be demonstrated. Regarding the modelling of forces and moments, specific requirements are requested for the specific failure mode under investigation, for example a body-exact formulation should be used in the evaluation of the Froude-Krylov forces and moments for Dead ship condition, Pure loss of stability and Parametric roll.

Particular attention is paid to the minimum number of degrees of freedom to be included in the numerical simulations, specified for each failure mode as follows:

- **Dead ship condition**: sway, heave, roll and pitch;
- **Excessive acceleration**: heave, roll and pitch. Particular attention has to be paid in the calculation of lateral acceleration when sway is neglected;
- **Pure loss of stability**: surge, sway, roll and yaw;
- **Parametric roll**: heave, roll and pitch;
- **Surf-riding/broaching**: surge, sway, roll and yaw.

Three equivalent alternatives are proposed to perform a DSA:

1. *Full probabilistic assessment.* The estimate of the mean long-term stability failure rate is used as criterion to identify the failure. For a specific loading condition, it is calculated as a weighted average over all relevant sea states, wave heading angle and ship forward speeds, assuming the standard wave scatter table for the North Atlantic to define the probabilities of the sea states. The assessment is satisfied if the long-term stability failure rate is lower than $2.6 \cdot 10^{-8}(1/s)$. The wave heading angles and the ship speeds are assumed uniformly distributed, except Dead ship condition for which zero speed, beam waves and wind are considered,

2. *Assessment in design situations using probabilistic criteria.* For each failure mode, specific design situations are prescribed as combination of forward speed, wave heading angle, wave height and mean zero-crossing period. It has to be verified that the maximum stability failure rate (defined in each design situation as the upper boundary of its 95% confidence interval) is lower than threshold corresponding to one stability failure every 2 hours in full scale in design sea states with probability density $10^{-5} 1/(m \cdot s)$. Sea states for which the assessment has to be performed are defined associating each mean zero-crossing period the significant wave height that define the sea state with probability density of 10^{-5}.

3. *Assessment in design situations using deterministic criteria.* Design situations are specified for each failure mode. For each situation, it has to be verified that the mean 3-hour maximum roll amplitude or lateral acceleration should not exceed half of the values in the definition of stability failure event. Then, for roll angle it has to be:

$$\varphi_{3h} < \frac{1}{2} \min\{40^\circ; \varphi_v; \varphi_{unprotected}\} \tag{2.1}$$

while for lateral acceleration:

$$a_{y,3h} < \frac{9.81}{2} \frac{m}{s^2} \tag{2.2}$$

where φ_{3h} is the mean 3-hour maximum roll angle and $a_{y,3h}$ is the mean 3-hour lateral acceleration. Sea states for which the assessment has to be

	Probabilistic criteria	**Deterministic criteria**
$T_z(s)$	$H_s(m)$	$H_s(m)$
4.5	2.8	2.0
5.5	5.5	4.4
6.5	8.2	6.9
7.5	10.6	9.1
8.5	12.5	10.9
9.5	13.8	12.1
10.5	14.6	12.8
11.5	15.1	13.1
12.5	15.1	13.0
13.5	14.8	12.5
14.5	14.1	11.3
15.5	12.9	9.0
16.5	10.9	-

Table 2.2: Design sea states for DSA conducted using probabilistic criteria and deterministic criteria - Unrestricted service.

performed are defined associating to each mean zero-crossing period the significant wave height that defines the sea state with probability density of $7 \cdot 10^{-5} 1/(m \cdot s)$.

The simulations or model tests for each design situation should comprise at least five 3 hours tests (for a total of 15 hours in full scale).

The full probabilistic assessment requires the verification of the ship behaviour in all the sea states reported in the assumed standard wave scatter table, i.e. a huge number of simulations and/or tests to be performed. The complexity of the assessment is reduced from the full probabilistic to the probabilistic criteria, since design situations are significantly. The simulation time is further reduced in the assessment with deterministic criteria, due to the simplified simpler criterion used to judge the ship vulnerability. Such a reduction is compensated by a greater conservatism.

Table 2.2 reports the design sea states to be considered in the DSA conducted using probabilistic criteria and deterministic criteria, for ships designed for unrestricted service. The table specifies design sea states based on the corresponding joint probability density f_s, defined as the probability of the sea states per unit range of significant wave heights and mean zero-crossing period. In detail, the sea states are the ones for which:

- the probability density f_s is $10^{-5}(ms)^{-1}$ for DSA with probabilistic criteria;
- the probability density f_s is $7 \cdot 10^{-5}(ms)^{-1}$ for DSA with deterministic criteria.

2.2.3 Operational Measures

If a certain loading condition is found vulnerable to one or more criteria, the development of ship-specific Operational Measures (OM) is permitted to solve the identified vulnerability. OM are provided to the Master as a support to decision-making on board. Their aim is to reduce the likelihood of the stability failure till an acceptable level by limiting operations or defining sailing conditions to be avoided. The safety level ensured by the OM should be at least equal to that provided by the vulnerability criteria or the direct stability assessment.

In the stability rules currently in force, IMO Res. MSC.267(85) (2008), OM are introduced through the circular IMO MSC.1/Circ.1228 (2007). It is recognized that specific sailing conditions, defined as combinations of wave heading and ship speed, can be a source of risk in certain sea states, for the ship complying with the 2008 IS Code, in terms of roll motions and accelerations or even capsizing. In the circular, guidelines on how to handle the ship in adverse weather and sea conditions are provided to the Master. The phenomena covered by the circular are divided in:

- surf-riding/broaching and pure loss of stability;
- synchronous rolling motion;
- parametric roll.

In the SGISC, OM are conceived as an integration to design, superseding the provisions in the circular IMO MSC.1/Circ.1228 (2007), and are divided in:

- Operational Limitations (OL) that limit ship operations to specific areas, routes and seasons or to maximum significant wave height;
- Operational Guidance (OG) that define sailing conditions to be avoided in considered sea states.

OL related to maximum significant wave height and OG require weather forecast information for possible route changes to avoid dangerous situations. OL related to maximum significant wave height and OG cannot be provided for the ship vulnerable to the Dead ship condition, due to the peculiar scenario. Indeed, the ship is not able neither to avoid the encountered environmental conditions nor to modify the sailing condition.

The Interim guidelines mention that the development of OG regarding a certain failure mode should be also complemented by the verification of the feasibility of the identified safe sailing conditions, since an increase in ship speed or a change in heading could be not possible in heavy weather, due to speed loss in waves and reduced steering capabilities. In addition, the sailing conditions judged to be safe should not be in contrast with other dangerous phenomena not covered by the SGISC, as slamming, water on deck etc.

A concept map that summarizes the structure of OM is reported in Figure 2.2. A description of OL and OG, together with few notes on the preparation stage and their acceptance by the Administration, is given in the following Subsections.

Operational Limitations

Operational Limitations define limits for the environmental conditions under which the ship can sail. They are divided in:

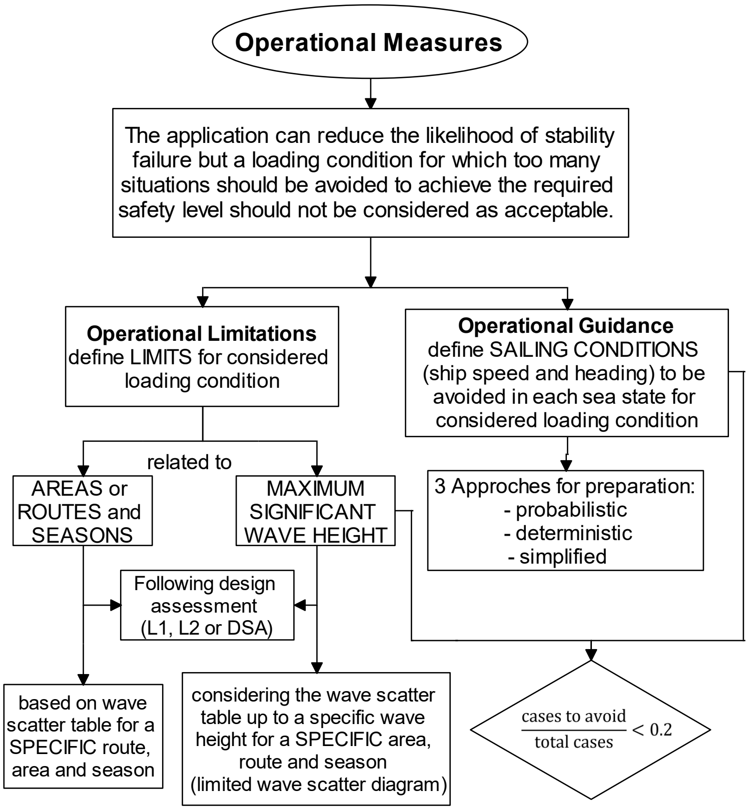

Figure 2.2: Concept map of Operational Measures application, Begović et al. (2023).

- OL related to areas or routes and season, that permit operations in specific operational areas or routes and specific season;
- OL related to maximum significant wave height that permit operation in weather conditions up to a certain significant wave height.

A combination of both types is also envisaged, for example defining the maximum allowable significant wave height for a specified area.

For a given loading condition, OL may be prepared based on vulnerability criteria or DSA procedures, replacing the North Atlantic wave scatter diagram (IACS Rec. No.34 (2001)), that represents the standard environmental conditions used in Level 2 assessment, by a different scatter table which can be derived by:

- a specific table for the area in which the ship is intended to operate;
- a combination of the tables of the areas related to a specific route;
- a specific table related to the season during which the ship is intended to operate;

- a limited wave scatter diagram obtained considering a specific scatter table up to a maximum significant wave height. In this case, a forecast is required for the prediction of the significant wave height.

As concerns the OL related to maximum significant wave height, the limited wave scatter diagram cuts off all sea states in which the ship cannot operate. The diagram can be normalized if the ship is thought to operate all the time and eventually change route to avoid the excluded sea states. The normalization considers the sum of the number of occurrences of the limited wave scatter diagram equal to the total number of occurrences. If the ship is thought to remain in port during the dangerous sea states no normalization is performed, and the probability of occurrence of the phenomenon is then reduced to zero in the sea states having significant wave height larger than the maximum identified one.

The application of Operational Limitations has been explored by some authors in recent years. Tompuri et al. (2016) proposed the limiting GM curves derived form Level 2 vulnerability criteria for three ships (a ro-ro, a passenger ship and a container vessel) as a way to develop OL in early design stage, in order to have an insight into possible severe restrictions for the vessel. Rudaković and Bačkalov (2019) examined the behaviour of an inland container vessel sailing in North Sea coastal zone referring to Excessive acceleration and Dead ship condition criteria. Wind and wave measurements in Belgian coastal zone were considered as alternative environmental conditions for OL development demonstrating that operational limitations of the vessel cannot be expanded by imposing a draught reduction to the selected sample ship when sailing in coastal zones. Unconventional vertical distributions of containers can significantly reduce the imposed limitations. Petacco and Gualeni (2020) considered a Ro-Ro pax ferry operating in the Mediterranean Sea and applied OL in the form of minimum height of the centre of gravity to ensure the ship against lateral accelerations, for different draughts. An increase of the design domain, defined as the area between the maximum and minimum KG limiting curves where the design centre of gravity may be placed safely, was shown by the introduction of restrictions on the geographical area. Rinauro et al. (2020) developed OL for Surf-riding/broaching for a 90 meter length ship considering a hypothetical route in Western Mediterranean Sea, showing that an improvement in the allowed ship speed can be obtained applying limitations to the geographical area and maximum significant wave height. Bulian and Orlandi (2022) investigated the effect of modified environmental conditions on the outcomes of OL development. The Authors pointed out that the MetOcean data for a specific geographical area may be obtained from multiple sources based on different approaches of data collection and elaboration, that may affect the results and lead to a non-uniform, and eventually opportunistic, application of the rules. Five different sources of data were used to quantify the effect on the the verification against the Parametric roll Level 1 and the criterion C1 of Level 2. A RoPax and the publicly available CEHIPAR2792 ship were considered, assuming the Mediterranean Sea as operational area showing a large variability depending on the source of data, for both Level 1 and criterion C1.

Operational Guidance

Operational Guidance identify sailing conditions, defined as combinations of ship speed and wave heading, that may be a source of risk for the ship, people on board and cargo, developed for the sea states reported in the assumed scatter table.

OG are intended to support ship operations, and integrate the “prudent seamanship” assumption implied by regulations, that works well for conventional ships but could be source of an increased risk for innovative and unconventional hull forms, where the crew experience is not consolidated (Shigunov et al. (2013), Bačkalov et al. (2016)). After removing the dangerous sailing conditions from the whole set of sailing conditions under the considered environmental conditions, the ship should be able to sail with a safety level at least equal to the one prescribed in the vulnerability criteria or DSA.

OG may be presented as polar diagrams reporting ship speed and wave heading for a certain sea state or they may be presented in a different form that must clearly indicate acceptable and unacceptable sailing conditions. In any case, the adopted representation must be clear, informative and easily understood by the crew. Detailed forecast information are required in order to allow route changing in sufficient time before potentially dangerous environmental conditions are encountered.

As concerns the development of OG three different approaches are suggested by the Interim guidelines, IMO MSC.1/Circ.1627 (2020):

- probabilistic;
- deterministic;
- simplified.

In the probabilistic OG, sailing conditions to be avoided are the ones for which:

$$r > 10^{-6} s^{-1} \tag{2.3}$$

being r the upper boundary of the 95% confidence interval of the stability failure rate. The failure rate r is calculated as the mean value over several simulations in irregular seaways. For each simulation, the failure rate is related to the time until the first stability failure occurs.

In the deterministic OG, the maximum roll angle or lateral acceleration in the exposure time is used as criterion to judge if a sailing condition has to be avoided or not. In particular, the following inequality has to be verifiedif roll angle is considered:

$$\varphi_{3h} < \frac{1}{2}\min\{40°; \varphi_v; \varphi_{unprotected}\} \tag{2.4}$$

being φ_{3h} the mean 3-hour maximum roll angle, φ_v the angle of vanishing stability in calm water and $\varphi_{unprotected}$ the angle of submergence of unprotected openings in calm water.

If lateral acceleration is considered, the following inequality has to be verified:

$$a_{y,3h} < \frac{9.81}{2}\frac{m}{s^2} \tag{2.5}$$

where $a_{y,3h}$ is the mean 3-hour maximum lateral acceleration.

For each design situation, the mean 3-hour maximum roll angle φ_{3h} and the mean 3-hour lateral acceleration $a_{y,3h}$ values are defined performing simulations or model tests that comprise at least 15 hours in full scale. At least five values of the 3-hour maximum amplitude of roll angle or lateral acceleration should be provided whose mean value is the mean 3-hour maximum amplitude.

The environmental conditions to be considered in the verification are the ones defined in the DSA based on deterministic criteria, that prescribe specific combinations of mean zero-crossing period and significant wave height.

Probabilistic and deterministic approaches require experimental tests and/or numerical simulations that share the same level of complexity as DSA making their development complex and time consuming.

Simplified OG may be developed as an alternative to the more complex probabilistic and deterministic approaches which provide accurate recommendations but require non negligible resources in terms of costs, time and expertise. Simplified OG are based on conservative procedures derived from Level 2 vulnerability assessment with appropriate changes to account for variations in ship speed and wave heading. Even if the guidelines provide simple approaches that can be used to develop the simplified OG, the adoption of different approaches is admitted.

An example of application to a megayacht of 65-meter length of OG for the excessive acceleration failure mode according to the simplified procedure is reported in Petacco et al. (2020). The results were given by polar plots for selected sea states, showing a pronounced vulnerability of the ship in beam and bow seas, with a beneficial effect of ship speed due to the increased roll damping, and noting that for certain sea states may be identified some wave headings for which no ship speed can guarantee safety against excessive accelerations. Applications of OG for phenomena different from the excessive acceleration one have been provided by some authors in recent years. Rinauro et al. (2020) provided OG for a semi-displacement hull found vulnerable to Surf-riding/broaching. The results were provided in tabular form, identifying the critical Froude number for the sea states reported in the standard wave scatter table. Belenky (2020) developed OG for Parametric roll, derived from Level 2 vulnerability assessment and from DSA. An innovative approach for Parametric roll OG was proposed in Petacco (2022) that developed a method identified as an intermediate stage between simplified and deterministic OG, providing a good compromise between accuracy and simulation time.

Preparation and acceptance of Operational Measures

The development of OM is allowed at different stages, requiring in any case accurate weather forecast in a sufficient time before encountering a storm, to allow for route change if safe operations in the storm are not possible (IMO SDC 8/WP.4/Add.5 2022):

- at design stage;
- in port before departure;
- during operation (on board or on shore) using actual weather and loading condition data and simplified numerical tools and statistical procedures.

The pre-computation at the design stage has the advantage of the possible approval by the Administration and the use of the most comprehensive numerical tools, statistical procedures, qualified staff, and dedicated hardware but has the drawback that only theoretical environmental conditions, as the standard sea and wind spectra, and predefined loading conditions, as the ones provided in the stability booklet, can be assumed in the analysis. Additionally, the OG development at design stage may become a long and expensive process since several scenarios may be considered, in terms of loading conditions, ship speeds, wave and wind characteristics. Conversely, the preparation of OG in port before departure, by qualified staff and advanced tools, or onboard, by simplified methods, allows the use of accurate weather data and more detailed information on the loading condition. Real-time monitoring tools using measures of ship responses can provide a realistic situational awareness and identify hazardous situations and alerting the crew to take corrective actions (Shigunov et al. (2021)). Such systems should be designed to minimize the crew interaction with the system and to provide the relevant information concerning the potential danger in a clear and understandable way. The system should be accurate enough to let the crew rely on it when taking decisions, since the trust of the crew in operational guidance and decision support information is related to the understanding of the theoretical and technical background of the system and very dependent on the correspondence of the provided information to their own experience (Bačkalov et al. (2016)).

The preparation of OM requires the education and training of the crew since they will be properly considered and applied only if well understood. Crews should be sufficiently informed on the complex dynamic stability phenomena that ships can experience. In particular, training should be also thought to be ship-specific, by using the simulations obtained at design stage to let understand the specific behaviour of the ship under specific situations and the counteracting measures that can be taken, as outlined by Kruger et al. (2008). Alternatively, the crew should be at least informed about the outcomes of the vulnerability criteria for their ship, in order to be conscious of the phenomena the ship could be prone to, (Bačkalov et al. (2016)).

The Administration can accept Operational Measures according to the scheme summarized in the concept map in Figure 2.3.

Different levels of acceptance are defined in Section 4.4 of IMO MSC.1/Circ.1627 (2020) referring to unrestricted operation, limited operation and operation using onboard guidance. In detail, a loading condition is:

1. *acceptable for unrestricted operation* if it is not vulnerable to any of the five stability failure modes;

2. *acceptable for limited operation* if OL are provided for one or more stability failure modes for unrestricted operation and satisfies all the other criteria;

3. *acceptable for operation using on board operational guidance*, if it is provided with OG for one or more stability failure modes for unrestricted operation and is either provided with OL for unrestricted operation or satisfies all the other criteria;

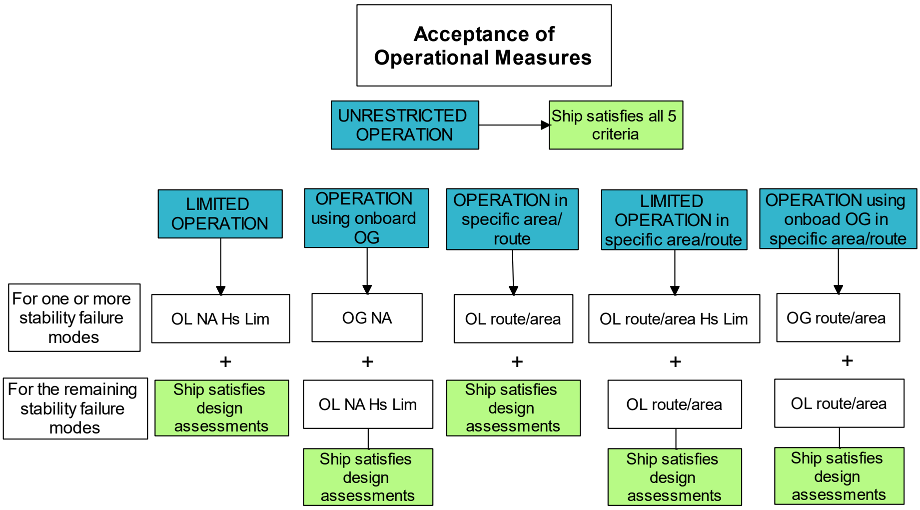

Figure 2.3: Operational Measures acceptance, Begović et al. (2023).

4. *acceptable for operation in a specified area or on a specified route during a specific season* if it is provided with OL for one or more stability failure modes for a specified area or route and season, and satisfies all the other criteria;

5. *acceptable for limited operation in a specified area or on a specified route during a specific season* if it is provided with OL for one or more stability failure modes for a given significant wave height limit for an area or route and season, and either has OL without specification of maximum operational significant wave height for this area or route and season, or satisfies all the other criteria;

6. *acceptable for operation using onboard operational guidance in a specified area or on a specified route during a specified season* if it is provided with OG for one or more stability failure modes for this area or route and season and is either provided with OL for this area or route and season or satisfies the remaining criteria.

OL related to maximum significant wave height OG allows to reduce the stability failure rate to any low level but the loading condition cannot be considered acceptable if too many situations have to be avoided. The Interim guidelines set a maximum value for the ratio between the duration of the situations to be avoided and the total operational time for the acceptance of the loading condition:

$$\frac{\text{total duration of situation to be avoided}}{\text{total operational time}} < 0.2 \tag{2.6}$$

In the calculation of the ratio, the probabilities of the sea states are taken according to the full scatter table while wave headings and ship speeds are assumed to be uniformly distributed. All the speeds between zero and the service one must be considered.

Chapter 3

Excessive acceleration within the SGISC

3.1 Vulnerability criteria

The first proposals for Level 1 and Level 2 of the Excessive acceleration criterion were submitted by the German and Chinese delegations in 2011, (IMO SLF 54/INF.12, Annexes 1 to 3), in response to the invitation of the intersessional Correspondence Group on Intact Stability to elaborate methodologies for vulnerability criteria and direct stability assessment, assuming the ship at zero speed in irregular beam waves.

The Chinese version of Level 1 adopted limit values for the accelerations depending on the ship length and calculating the angle of roll and the ship natural roll period according to the formulas implemented in the Weather Criterion, based on sample calculations for a set of containerships. As second level of assessment, a time-domain 3-DOF (roll, heave and pitch) motion model was proposed for the calculation of roll angle and acceleration, able to account for the wind action as well. The greater complexity of the model, compared to Level 1, aimed at effectively identifying ships potentially vulnerable to the phenomenon and consequently limit the workload for the direct stability assessment. Chinese point of view was to make the criterion applicable only to containerships and cargo ships carrying deck cargoes and preferably not mandatory to avoid conflicts among the maximum required GM to limit acceleration and the minimum one defined by other stability criteria.

The German proposal for Level 2 was a criterion based on a linearized 1-DOF roll motion model on a finite range of wave frequencies. Level 1 was derived from Level 2 observing that, for the considered scenario, most of the energy is concentrated around the natural roll frequency. Therefore, the main parameters of the 1-DOF model were replaced by the ones calculated at the natural roll frequency obtaining a simpler and more conservative criterion. The standard deviation of lateral acceleration was assumed to be the parameter to be used for the verification of the criterion, proposing $0.2g$ as possible standard value. The consistency among the proposed criteria and the results from direct stability assessment was demonstrated through sample calculations.

Document	Sample ships	Standard values Level 1 (m/s^2)	Level 2 (-)	Inconsistencies	Comments
SDC.3/INF.10 Annex 8 (2015)	57	8.69	$1.0 \cdot 10^{-3}$	YES	No inconsistencies if Level 2 standard was grater than $2.81 \cdot 10^{-3}$
SDC.3/INF.10 Annex 9 (2015)	10	8.69	$1.0 \cdot 10^{-3}$	YES	
SDC.4/INF.4/Add.2 Annex 4 (2016)	17	5.3	$1.1 \cdot 10^{-4}$	YES	Inconsistency for a gas tanker
SDC.4/INF.4/Add.2 Annex 7 (2016)	24	8.69	$2.8 \cdot 10^{-2}$	YES	Inconsistency for a cement carrier. Avoided if standard for Level 2 greater than $4.3 \cdot 10^{-2}$
SDC.4/INF.9 (2016)	17	5.3	$1.0 \cdot 10^{-3}$	YES	
SDC.4/5/13 (2016)	22	5.88	$3.9 \cdot 10^{-4}$	NO	

Table 3.1: Summary of sample calculations.

The structure, the main parameters and the standards of the criteria were widely discussed and tested through sample calculation by the correspondence group during the following years. A summary of the sample calculations, the number of tested ships and the assumed standard values is reported in Table 3.1.

The working group agreed to adopt a simplified 1-DOF roll motion model for both Level 1 and Level 2 to keep the verification sufficiently simple and accurate. A joint proposal by Germany and China, submitted in 2014, represents the first draft of the Excessive acceleration failure mode (IMO SDC 2/INF.10). It was proposed to exclude from the verification ships having length less than $100m$ and different limit values were proposed for ships having length less than $250m$ and for ships having length greater than $250m$. The criteria, but not the corresponding limit values, were finalized at the third session of the (SDC) Sub-Committee in 2015 (IMO SDC 3/INF.10), where the distinction among the limit values for different ship lengths and the exemption of ships less than $100m$ were removed. The application of the criteria was prescribed for all the ships having length equal or greater than $24m$ and for each loading condition, provided that:

- the distance from the waterline to the highest location along the length of the ship where passengers or crew may be present exceeds 70% of the breadth of the ship; and

- the metacentric height exceeds 8% of the breadth of the ship.

The selection of the standards for Level 1 and Level 2 was subject of discussion and the Interim guidelines mention the possibility to further revise them in future. German delegation stated that the standards chosen must be able to find vulnerable the loading condition of container vessel Chicago Express at the time of the accident with all level of assessment (IMO SDC 4/5/13 2016). The standards were obtained from backward analysis performing calculations, taking into account Chicago Express' loading condition: the attained values were $7.66m/s^2$ for Level 1 and $3.9 \cdot 10^{-4}$ for Level 2. Hence, Germany proposed to take the obtained value for Level 2 as standard, while a smaller value of $5.88m/s^2$ was proposed for Level 1 to avoid inconsistencies. This last value was evaluated through sample calculations

Document	Level 1 (m/s^2)	Level 2 ($-$)
IMO MSC.1/Circ.1627 (2020)	4.64	$3.9 \cdot 10^{-4}$

Table 3.2: Current standards.

performed on a set of five container ships, one gas carrier, thirteen cruise vessels, and three ro-pax ships. Germany also compared results obtained using this set of values with the ones obtained using standard values proposed by Chinese and Japanese delegations: these values were not able to judge the loading conditions of Chicago Express as vulnerable at the time of the accident; on the contrary, the standard values proposed by Germany were able to identify this vulnerability showing, on the other hand, a certain severity that could have a strong impact on ship design. The final standard for Level 1 was further reduced to $4.64 m/s^2$ during the 6-th session of the SDC Sub-Committee, where delegations replied to a questionnaire in which four options were presented (IMO SDC 6/INF.3 2018). Some criticism came from the French delegation that noticed that the selected option was too conservative, since it judged vulnerable to Excessive acceleration oil tankers and bulk carriers, which are quite safe regarding this phenomenon. The adopted standards are summarized in Table 3.2.

In the following subsections, a description of the current version of Level 1 and Level 2 criteria is provided, Sections 3.1.1 and 3.1.2, respectively.

3.1.1 Level 1

Level 1 criterion is based on the 1-DOF roll motion model adopted for Level 2, with the main simplification of conducting the verification at the natural roll frequency, resulting simpler and more conservative ensuring the consistency between the levels. The derivation of Level 1 model developed for the second level assessment is shown in Petacco (2019).

Only the main dimensions of the ship (length, breadth and draught), the block coefficient, the midship section coefficient (only if bilge keel are present), the area of the bilge keels (if any), the height of center of gravity above the keel and the height and the longitudinal location along the ship of the location where passengers or crew may be present are required.

Level 1 verification is performed comparing a calculated lateral acceleration to the limit value $R_{EA1} = 4.64 m/s^2$. The lateral acceleration to be calculated is a function of the natural roll period T_r, the height h of the considered location above the roll axis and the longitudinal position x_{AP} of the location with respect to the aft perpendicular through a factor k_L. Level 1 is satisfied, for the considered loading condition and location, if:

$$\varphi k_L \left(g + 4\pi^2 \frac{h}{T_r^2} \right) < R_{EA1} \tag{3.1}$$

The roll axis is assumed to be located at the midpoint between the centre of gravity and the waterline. The natural roll period is calculated through a formula, common to all the criteria and currently implemented in the 2008 IS Code, as a function of the main ship dimensions and of the transverse metacentric height not corrected for free surface effects, equation 1.1.

The factor k_L is constant and equal to 1 if the calculation point is located between $0.20L$ and $0.65L$ and linearly increases outside this range, reaching its local maxima at for and aft ends of the ship:

$$k_L = \begin{cases} 1.125 - 0.625\frac{x_{AP}}{L} & \text{if } x_{AP} < 0.2L \\ 1.0 & \text{if } 0.2L \leq x_{AP} \leq 0.65L \\ 0.527 + 0.727\frac{x_{AP}}{L} & \text{if } x_{AP} > 0.65L \end{cases} \tag{3.2}$$

The characteristic roll amplitude φ is calculated as a function of the effective wave slope coefficient r, the logarithmic decrement of roll decay δ_φ and the wave steepness s:

$$\varphi = 4.43\frac{rs}{\delta_\varphi^{0.5}} \tag{3.3}$$

The effective wave slope r is calculated through the formula:

$$r = \frac{K_1 + K_2 + OG \cdot F}{\frac{B^2}{12C_B d} - \frac{C_B d}{2} - OG} \tag{3.4}$$

being the coefficients K_1, K_2 and F functions of the following ship parameters: block coefficient, C_B; breadth, B; mean draught, d; natural roll period, T_r; height of the centre of gravity with respect to the waterline, $OG = KG - d$.

In particular, the coefficients K_1, K_2 and F are defined as follows:

$$K_1 = \frac{1}{4\pi^2}\ g\beta {T_r}^2(\tau + \tau\tilde{T} - \frac{1}{\tilde{T}}) \tag{3.5}$$

$$K_2 = \frac{1}{4\pi^2}\ g\tau {T_r}^2(\beta - \cos\tilde{B}) \tag{3.6}$$

$$F = \beta(\tau - \frac{1}{\tilde{T}}) \tag{3.7}$$

where:

$$\beta = \frac{\sin\tilde{B}}{\tilde{B}} \tag{3.8}$$

$$\tau = \frac{e^{-\tilde{T}}}{\tilde{T}} \tag{3.9}$$

$$\tilde{B} = \frac{2\pi^2 B}{g{T_r}^2} \tag{3.10}$$

$$\tilde{T} = \frac{4\pi^2 C_B d}{g{T_r}^2} \tag{3.11}$$

The wave steepness s is given in tabular form as a function of the ship natural roll period.

The non-dimensional logarithmic decrement of roll decay δ_φ is calculated as:

$$\delta_\varphi = 0.5\pi R_{PR} \tag{3.12}$$

being R_{PR} calculated according to the formulation provided in first level of parametric rolling failure mode:

$$R_{PR} = \begin{cases} 1.87 & \text{if the ship has a sharp bilge} \\ 0.17 + 0.425\left(\frac{100A_k}{LB}\right) & \text{if } C_{m,full} > 0.96 \\ 0.17 + (10.625 \cdot C_{m,full} - 9.775)\left(\frac{100A_k}{LB}\right) & \text{if } 0.94 \geq C_{m,full} \leq 0.96 \\ 0.17 + 0.2125\left(\frac{100A_k}{LB}\right) & \text{if } C_{m,full} < 0.94 \end{cases} \tag{3.13}$$

The ratio $\frac{100A_k}{LB}$ should not exceed 4.

In equation 3.13. the following parameters are defined: A_k total overall area of the bilge keels; $C_{m,full}$ midship section coefficient of the fully load departure condition in calm water.

3.1.2 Level 2

The second level of assessment is verified through the computation of a long-term stability failure index C obtained as weighted sum of short-term indexes $C_{s,i}$, calculated for assumed sea states:

$$C = \sum_{i=1}^{N} W_i C_{s,i} \tag{3.14}$$

The criterion is verified if the long-term index C is lower than the limit value $R_{EA2} = 3.9 \cdot 10^{-4}$.

The calculation of the short-term indexes is performed by solving the 1-DOF roll motion equation for the ship at zero speed in a beam seaway:

$$(I_{44} + A_{44})\,\ddot{\varphi} + M_D(\dot{\varphi}) + C_{44}\varphi = F_{ex-4}(\omega t) \tag{3.15}$$

where: φ, $\dot{\varphi}$ and $\ddot{\varphi}$ are the roll displacement, velocity and acceleration, respectively; I_{44} and A_{44} are the mass moment of inertia and the added mass in roll; $M_D(\dot{\varphi})$ is the non-linear damping moment; C_{44} is the restoring coefficient, calculated as $\Delta g GM$, being Δ the ship mass displacement; $F_{ex-4}(\omega t)$ the exciting roll moment due to the action of the waves. The exciting roll moment $F_{ex-4}(\omega t)$ is calculated by Froude-Krylov component only, neglecting diffraction. In complex form it is:

$$\hat{F}_{FK-4} \cdot e^{i\omega t} = (a + ib)\, e^{i\omega t} \tag{3.16}$$

being a and b the real and imaginary parts of the Froude-Krylov exciting roll moment. According to the explanatory notes, they can be calculated via integration of the dynamic pressure of the incident wave (IMO SDC 8/WP.4/Add.2 2022):

$$a = \rho g \zeta_a \iint_{S_{Body}} e^{kz} \cos(ky)\, n_4 dS \tag{3.17}$$

$$b = -\rho g \zeta_a \iint_{S_{Body}} e^{kz} \sin(ky)\, n_4 dS \tag{3.18}$$

In equations 3.17 and 3.18: ρ is the density of sea water; ζ_a is the wave amplitude; x, y and z are the coordinates of the points on the mean wetted hull surface of ship; S_{Body} is the mean wetted hull surface of ship; k is the wave number, $n_4 = yn_3 - zn_2$ is the normal vector of roll and n_2 and n_3 are the normal vectors in the y and z directions. In Level 2 verification, a simplified formulation is proposed for the calculation of a and b, based on the concept of effective wave slope function:

$$a = 0 \tag{3.19}$$

$$b = -\Delta gGMr\left(\omega\right)\frac{\omega^2}{g} \tag{3.20}$$

In equation 3.20 the effective wave slope function $r\left(\omega\right)$ is defined as a linear function of the Froude-Krylov roll moment:

$$r\left(\omega\right) = \left|\frac{F_{FK-4}\left(\omega\right)}{\rho g\nabla GM\ k\zeta_a}\right| \tag{3.21}$$

being ∇ the volume of displacement. The explanatory notes of the Interim guidelines allow the computation of the effective wave slope function according to different methods based either on strip-theory or on 3D panel methods. A methodology based on strip theory, hereinafter “IMO’s standard methodology”, is the recommended one due to its minimum computational effort. The methodology associates an equivalent rectangle to each transversal section of the ship, through a transformation algorithm that keeps the underwater sectional area and the breadth at waterline. The transformation algorithm and the procedure are reported in Subsection 3.2.

Equation 3.15 is linearized to be solved in the wave frequency domain. The linearization is done introducing an equivalent linear roll damping factor B_e such that the non-linear damping moment can be expressed as:

$$M_D\left(\dot{\varphi}\right) = B_e\dot{\varphi} \tag{3.22}$$

The equivalent linear damping coefficient is rewritten as:

$$B_e = 2\mu_e\left(I_{44} + A_{44}\right) \tag{3.23}$$

being μ_e the linear roll damping coefficient. The linear damping coefficient can be calculated either calculating damping at 15° roll angle or through a stochastic linearization, IMO SDC 8/WP.4/Add.2 (2022), once a set of damping coefficients, linear μ, quadratic β, and cubic δ, is known:

$$\mu_e = \mu + \sqrt{\frac{2}{\pi}}\beta\sigma_{\dot{\varphi}}\left(\mu_e\right) + \frac{3}{2}\delta\left(\sigma_{\dot{\varphi}}\left(\mu_e\right)\right)^2 \tag{3.24}$$

The equivalent linear roll damping depends on the considered sea state, being $\sigma_{\dot{\varphi}}$ the standard deviation of roll rate, which is in turn a function of the linear damping coefficient. Thus, an iterative procedure is required to calculate it.

The linear, quadratic and cubic terms can be calculated through the evaluation of roll damping for several roll amplitudes by means of the Simplified Ikeda’s

Method (Kawahara et al. (2009)), a prediction method based on the original Ikeda's method, Ikeda et al. (1978a) and Ikeda et al. (1978b). In particular, the three coefficients can be obtained fitting the quadratic parabola by means of the least square method:

$$\frac{B_e\left(\varphi_a\right)\omega_r^2}{2WGM}\rightarrow\mu+\frac{4}{3\pi}\beta\omega_r\varphi+\frac{3}{8}\delta\omega_r^2\varphi^2 \tag{3.25}$$

Alternative methods can be used, as experimental tests, when the ship parameters are outside the range of applicability of the Simplified Ikeda's Method.

Introducing the damping factor in equation 3.15 and dividing it by $(I_{44}+A_{44})$ it becomes:

$$\ddot{\varphi}+2\mu_e\dot{\varphi}+\omega_r^2\varphi=\frac{F_{FK-4}\left(\omega t\right)}{I_{44}+A_{44}} \;=\frac{(a+ib)}{I_{44}+A_{44}}\;e^{i\omega t} \tag{3.26}$$

being $\frac{F_{FK-4}(\omega t)}{I_{44}+A_{44}}$ the Froude-Krylov roll moment per unit mass moment of inertia and $\omega_r=\sqrt{\frac{\Delta gGM}{I_{44}+A44}}$ the ship natural roll frequency. The roll response, solution of equation 3.26 is harmonic and can be written as:

$$\varphi(t)=\hat{\varphi}_a\;e^{i\omega t} \tag{3.27}$$

being $\hat{\varphi}_a$ the complex roll amplitude, which contains both the magnitude and phase of the response. Therefore, the roll amplitude in complex form can be obtained:

$$\hat{\varphi}_a=\frac{a+ib}{-I_{44}+A_{44}\omega^2+\Delta gGM+i\omega B_e} \tag{3.28}$$

It can be divided into the real and imaginary parts:

$$\varphi_r=\frac{a[\Delta gGM-(I_{44}+A_{44})\omega^2]+bB_e\omega}{[\Delta gGM-(I_{44}+A_{44})\omega^2]^2+\left(B_e\omega\right)^2} \tag{3.29}$$

and

$$\varphi_i=\frac{b[\Delta gGM-(I_{44}+A_{44})\omega^2]-aB_e\omega}{[\Delta gGM-(I_{44}+A_{44})\omega^2]^2+\left(B_e\omega\right)^2} \tag{3.30}$$

Thus the roll amplitude in regular beam waves of unit amplitude is derived:

$$\varphi_a\left(\omega\right)=\sqrt{\varphi_r\left(\omega\right)^2+\varphi_i\left(\omega\right)^2} \tag{3.31}$$

The transfer function of lateral acceleration may be derived from the roll response per unit wave amplitude (Shigunov et al. (2011)):

$$a_y\left(\omega\right)=k_L\left(g+h\omega^2\right)\varphi_a\left(\omega\right) \tag{3.32}$$

being k_L and h defined as in Section 3.1.1. Once the wave energy spectrum $S_{zz}\left(\omega\right)$ is defined, the spectrum of lateral acceleration can be expressed as:

$$S_{a_y}\left(\omega\right)=\left(a_y\left(\omega\right)\right)^2S_{zz}\left(\omega\right) \tag{3.33}$$

The area under the spectrum of lateral acceleration gives the variance of lateral acceleration:

$$\sigma_{a_y}^2(\omega) = 0.75 \int_0^{+\infty} (a_y(\omega))^2 S_{zz}(\omega)\, d\omega \tag{3.34}$$

where a reduction factor, equal to 0.75, is introduced to account for the wave spreading (IMO SDC 8/WP.4/Add.1 (2022)).

Lateral accelerations is assumed to follow a Rayleigh distribution, then the short-term excessive acceleration failure index $C_{s,i}$ describes the probability of exceeding a lateral acceleration equal to the gravity acceleration, at the considered location on the ship, at least once in the considered sea state:

$$C_{s,i} = \exp\left(-\frac{R_2^2}{2\sigma_{a_y}^2}\right) \tag{3.35}$$

being $R_2 = 9.81\frac{m}{s^2}$.

The short-term failure index must be calculated for all combinations of significant wave height H_s and average zero-crossing period T_z reported in the standard scatter table and multiplied by the statistical frequency of occurrence of the corresponding sea state, W_i. The adopted standard wave scatter table, Table 3.3, describes the wave data of the North Atlantic.

Number of occurrences: 100 000 / T_z (s) = average zero-crossing wave period / H_s (m) = significant wave height

Tz (s) ► / Hs (m) ▼	3.5	4.5	5.5	6.5	7.5	8.5	9.5	10.5	11.5	12.5	13.5	14.5	15.5	16.5	17.5	18.5
0.5	1.3	133.7	865.6	1186.0	634.2	186.3	36.9	5.6	0.7	0.1	0.0	0.0	0.0	0.0	0.0	0.0
1.5	0.0	29.3	986.0	4976.0	7738.0	5569.7	2375.7	703.5	160.7	30.5	5.1	0.8	0.1	0.0	0.0	0.0
2.5	0.0	2.2	197.5	2158.8	6230.0	7449.5	4860.4	2066.0	644.5	160.2	33.7	6.3	1.1	0.2	0.0	0.0
3.5	0.0	0.2	34.9	695.5	3226.5	5675.0	5099.1	2838.0	1114.1	337.7	84.3	18.2	3.5	0.6	0.1	0.0
4.5	0.0	0.0	6.0	196.1	1354.3	3288.5	3857.5	2685.5	1275.2	455.1	130.9	31.9	6.9	1.3	0.2	0.0
5.5	0.0	0.0	1.0	51.0	498.4	1602.9	2372.7	2008.3	1126.0	463.6	150.9	41.0	9.7	2.1	0.4	0.1
6.5	0.0	0.0	0.2	12.6	167.0	690.3	1257.9	1268.6	825.9	386.8	140.8	42.2	10.9	2.5	0.5	0.1
7.5	0.0	0.0	0.0	3.0	52.1	270.1	594.4	703.2	524.9	276.7	111.7	36.7	10.2	2.5	0.6	0.1
8.5	0.0	0.0	0.0	0.7	15.4	97.9	255.9	350.6	296.9	174.6	77.6	27.7	8.4	2.2	0.5	0.1
9.5	0.0	0.0	0.0	0.2	4.3	33.2	101.9	159.9	152.2	99.2	48.3	18.7	6.1	1.7	0.4	0.1
10.5	0.0	0.0	0.0	0.0	1.2	10.7	37.9	67.5	71.7	51.5	27.3	11.4	4.0	1.2	0.3	0.1
11.5	0.0	0.0	0.0	0.0	0.3	3.3	13.3	26.6	31.4	24.7	14.2	6.4	2.4	0.7	0.2	0.1
12.5	0.0	0.0	0.0	0.0	0.1	1.0	4.4	9.9	12.8	11.0	6.8	3.3	1.3	0.4	0.1	0.0
13.5	0.0	0.0	0.0	0.0	0.0	0.3	1.4	3.5	5.0	4.6	3.1	1.6	0.7	0.2	0.1	0.0
14.5	0.0	0.0	0.0	0.0	0.0	0.1	0.4	1.2	1.8	1.8	1.3	0.7	0.3	0.1	0.0	0.0
15.5	0.0	0.0	0.0	0.0	0.0	0.0	0.1	0.4	0.6	0.7	0.5	0.3	0.1	0.1	0.0	0.0
16.5	0.0	0.0	0.0	0.0	0.0	0.0	0.0	0.1	0.2	0.2	0.2	0.1	0.1	0.0	0.0	0.0

Table 3.3: Standard wave scatter table, IMO MSC.1/Circ.1627 (2020).

The range of wave frequencies to be considered in the assessment is the interval $[\omega_1, \omega_2]$, being $\omega_1 = \min(0.5/T_r, 0.2)$ and $\omega_2 = \max(25/T_r, 2.0)$, to be divided in $N = 100$ intervals at least.

The algorithm for Level 2 procedure is given in Figure 3.1.

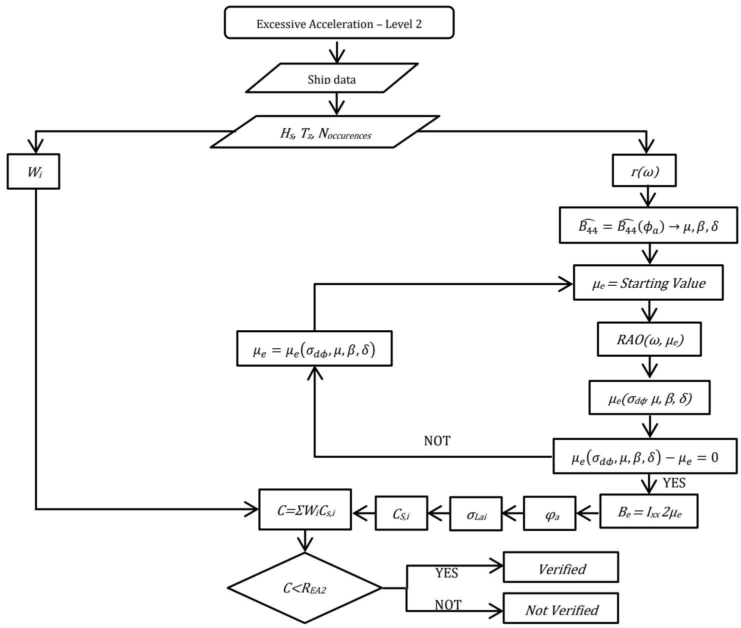

Figure 3.1: Algorithm for Level 2 procedure.

3.2 Standard methodology for the estimation of the effective wave slope function

The standard methodology developed in Level 2, for the estimation of the effective wave slope function, is $2D$ procedure, IMO SDC 8/WP.4/Add.2 (2022).

Each transversal section of the ship is transformed into a rectangular one having the same breadth at waterline and the same underwater area of the original section. The transformation algorithm, that neglects sections having zero breadth at waterline, as the ones in the bulb region, is reported here for the reader's convenience:

$$\begin{cases} \text{if } A(x) > 0 \text{ and } B(x) > 0 & \begin{cases} \text{if } \frac{A(x)}{B(x)} \leq d(x): & \begin{cases} A_{eq}(x) = A(x) \\ B_{eq}(x) = B(x) \\ d_{eq}(x) = \frac{A(x)}{B(x)} \end{cases} \\ \text{if } \frac{A(x)}{B(x)} > d(x): & \begin{cases} d_{eq}(x) = d(x) \\ B_{eq}(x) = B(x) \\ A_{eq}(x) = \frac{A_{eq}(x)}{B_{eq}(x)} \end{cases} \end{cases} \\ \text{otherwise:} \begin{cases} A_{eq}(x) = 0 \\ B_{eq}(x) = 0 \\ d_{eq}(x) = 0 \end{cases} \end{cases} \tag{3.36}$$

The main properties of the "equivalent vessel" are calculated as follows. The underwater volume, ∇_{eq} (m^3):

$$\nabla_{eq} = \int_{xAE}^{xFE} A_{eq}(x)dx \tag{3.37}$$

the transverse metacentric radius, $BM_{T,eq}$ (m):

$$BM_{T,eq} = \frac{1}{\nabla_{eq}} \int_{xAE}^{xFE} \frac{1}{12} {B_{eq}}^3(x)dx \tag{3.38}$$

the height of the centre of buoyancy above the base line, KB_{eq} (m):

$$KB_{eq} = T - \frac{1}{\nabla_{eq}} \int_{xAE}^{xFE} \frac{d_{eq}(x)}{2} A_{eq}(x)dx \tag{3.39}$$

the height of the centre of gravity above the base line, KG_{eq} (m):

$$KG_{eq} = KB_{eq} + BM_{T,eq} - GM \tag{3.40}$$

where x_{AE} x_{FE} are the longitudinal coordinates of the aft and forward ends of the ship, respectively.

Therefore, the Froude-Krylov roll moment for in beam waves is obtained by means of formulas, which are exact for rectangles.

The effective wave slope function is defined as:

$$r(\omega) = \left| \frac{\int_L C(x)\, dx}{\nabla_{eq}\, GM} \right| \tag{3.41}$$

where:

$$C(x) = \begin{cases} 0 \text{ if } A_{eq}(x) = 0 \text{ and } B_{eq}(x) = 0 \\ A_{eq}(x) \left[K_1(x) + K_2(x) + F_1(x)\, OG_{eq} \right] \end{cases} \tag{3.42}$$

and:

$$K_1(x) = \frac{\sin\left(k\frac{B_{eq}(x)}{2}\right)}{\left(k\frac{B_{eq}(x)}{2}\right)} \frac{\left(1 + kd_{eq}(x)\right) e^{-kd_{eq}(x)} - 1}{k^2\; d_{eq}(x)} \tag{3.43}$$

$$K_2(x) = -\frac{e^{-kd_{eq}(x)}}{k^2\; d_{eq}(x)} \left[\cos\left(k\frac{B_{eq}(x)}{2}\right) - \frac{\sin\left(k\frac{B_{eq}(x)}{2}\right)}{\left(k\frac{B_{eq}(x)}{2}\right)} \right] \tag{3.44}$$

$$F_1(x) = -\frac{1 - e^{-kd_{eq}(x)}}{k\; d_{eq}(x)} \frac{\sin\left(k\frac{B_{eq}(x)}{2}\right)}{\left(k\frac{B_{eq}(x)}{2}\right)} \tag{3.45}$$

being $B_{eq}(x)$, $d_{eq}(x)$, $A_{eq}(x)$ the equivalent breadth at waterline, draught, and underwater area of each transversal sections, according to the transformation procedure. OG_{eq} is the height of the centre of gravity above the waterline.

3.3 Direct Stability Assessment and Operational Guidance

Direct Stability Assessment and Operational Guidance for the Excessive acceleration failure mode share some minimum requirements. One of these is the minimum number of degrees of freedom for the DSA and for probabilistic and deterministic OG: at least heave, roll and pitch should be modelled to assess the ship behaviour in waves. In the assessment, the Froude-Krylov forces do not require a body-exact formulation.

Both DSA performed using deterministic criteria and deterministic Operational Guidance need the calculation of the mean 3-hours acceleration $a_{y,3h}$, for each considered situations. For its calculation at least 15 hours (full scale) of simulations must be conducted, to be divided in five 3 hours tests. For each test the greatest acceleration is taken. The mean 3-hours acceleration $a_{y,3h}$ is the average value of the greatest accelerations associated to the tests. The maximum value of the mean 3-hours acceleration $a_{y,3h}$ calculated in all situations must be lower than half of the gravity acceleration to identify the considered situation as safe.

In the DSA performed using probabilistic or deterministic criteria, the mean zero-crossing periods to be considered are defined as a fraction of the natural roll period T_r, specifically the interval from $0.7T_r$ to $1.3T_r$. The same environmental conditions must be considered in the probabilistic and deterministic OG.

Simplified OG for the Excessive acceleration failure mode should be developed for all the combinations of wave heading (from following to head seas) and ship speed (from zero to the service speed) for all the sea states reported in the assumed wave scatter table. Sailing conditions to be avoided are the ones for which:

$$C_{s,i} > 10^{-6} \tag{3.46}$$

being $C_{s,i}$ the short-term stability failure index as defined in equation (3.35), that quantifies the probability of exceeding the lateral acceleration of $9.81\frac{m}{s^2}$ in the considered sea state.

This page was intentionally left blank.

Chapter 4

Validation of the numerical code for vulnerability criteria verification

4.1 Introduction and description of the ship

A numerical code has been written in Matlab® programming language to perform the verification of the vulnerability criteria.

The stochastic linearization has been implemented to deal with the linearization of the damping term. The Simplified Ikeda's Method has been assumed as default method for the calculation of the linear, quadratic and cubic damping coefficients, to be used in the calculation of the linear roll damping coefficient, equation 3.24. The IMO' standard methodology has been adopted for the evaluation of the effective wave slope function, Subsection 3.2.

The code has been designed to perform the following tasks:

1. Level 1 criterion assessment;
2. Level 2 criterion assessment:
    (a) effective wave slope function calculation;
    (b) estimation of the roll damping coefficients on the basis of the Simplified Ikeda's Method;
    (c) evaluation of transfer function of roll motion and lateral acceleration;
    (d) calculation of the short-term stability failure indexes;
    (e) calculation of the long-term stability failure index.

The validation of the code has been performed at the beginning of the PhD research activity according to the version of the Explanatory Notes available at that time, IMO SDC 4/5/1/Add.4 (2016). The validation has been performed again once the most recent version of the Explanatory Notes of the Interim guidelines was published at the beginning of 2022, where an example of assessment of Level

2 of the Excessive acceleration failure mode is provided, IMO SDC 8/WP.4/Add.2 (2022).

The example refers to the containership APL China, which belong to the C11 class. The ship suffered parametric rolling in head seas, in 1998, while she was sailing in the North Pacific Ocean, losing one-third of her deck containers and damaging another one-third, (France et al. 2001). The cost of the accident was estimated to more than 50 million dollars. Due to the huge economical loss, the accident has been widely studied by the research community, both numerically and experimentally. The C11 containership has been used by the SDC Sub-Committee as reference ships to provide examples of application of Level 1 and 2 for all criteria, except surf-riding/broaching failure mode.

The results of the application of Level 2 procedure for the C11 containership are given in the following. Her main dimensions are listed in Table 4.1 and the body plan is shown in Figure 4.1.

In the spectral analysis, the wave frequency range from 0.2 to 2.0 rad/s has been divided into 200 intervals.

Principal characteristics	**Units**	
Length between perpendiculars, L_{pp}	*(m)*	262
Breadth, B	*(m)*	40.0
Draught, d	*(m)*	11.5
Trim, θ	$\circ$	0
Block coefficient, C_B	-	0.56
Midship section coefficient, C_m	-	0.959
Bilge keel length over ship length, l_{BK}/L_{pp}	-	0.292
Bilge keel breadth over ship breadth, b_{BK}/B	-	0.010
Height of the centre of gravity, KG	*(m)*	12.75
Metacentric height, GM	*(m)*	8.00
Natural roll period, T_r	*(s)*	9.6
Longitudinal distance of the bridge deck from AP, x_{AP}	*(m)*	177.41
Height of the bridge deck from BL, H_{BL}	*(m)*	48.72

Table 4.1: C11 main parameters.

4.2 Effective wave slope function and roll damping

Thu hull has been divided into 21 transversal sections, from the aft to the forward perpendicular. The relative location with respect to the aft perpendicular, the breadth at the waterline, the local draught and the area of the underwater part of each transversal section are given in Table 4.2. These are input values used to obtain the corresponding “equivalent underwater sections” according to the transformation algorithm reported Section 3.2.

The following quantities have been calculated for the “equivalent vessel”, performing an integration along the length of the ship by the Simpson’s first rule.
The underwater volume, ∇_{eq}:

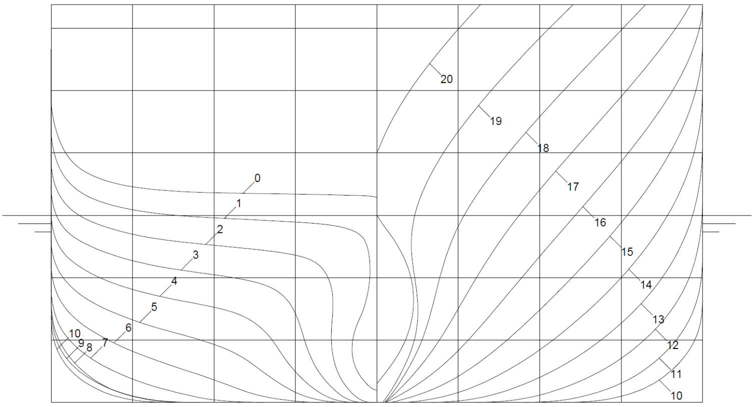

Figure 4.1: Body plan of the C11 containership.

Station	x/L	B(x)	d(x)	A(x)
-	-	(m)	(m)	(m^2)
0	0.00	0.0	0.0	0.0
1	0.05	22.8	10.5	23.6
2	0.10	36.3	11.5	109.8
3	0.15	39.3	11.5	191.0
4	0.20	40.0	11.5	262.5
5	0.25	40.0	11.5	326.6
6	0.30	40.0	11.5	385.0
7	0.35	40.0	11.5	421.7
8	0.40	40.0	11.5	441.5
9	0.45	40.0	11.5	446.6
10	0.50	40.0	11.5	441.2
11	0.55	40.0	11.5	424.1
12	0.60	40.0	11.5	392.5
13	0.65	38.9	11.5	345.7
14	0.70	35.9	11.5	287.6
15	0.75	31.0	11.5	225.0
16	0.80	24.7	11.5	165.4
17	0.85	17.8	11.5	114.8
18	0.90	11.0	11.5	75.5
19	0.95	4.9	11.5	47.8
20	1.00	0.0	0.0	0.0

Table 4.2: Relative location, breadth at waterline, local draught and area of the underwater part of the C11 transversal sections.

$$\nabla_{eq} = 6.72 \cdot 10^4 m^3 \tag{4.1}$$

The transversal metacentric radius, $BM_{T,eq}$:

$$BM_{T,eq} = 13.82\ m \tag{4.2}$$

The vertical position of the centre of buoyancy with respect to the keel line, KB_{eq}:

$$KB_{eq} = 6.94\ m \tag{4.3}$$

The vertical position of the centre of gravity with respect to the keel line, KB_{eq}:

$$KG_{eq} = 12.76\ m \tag{4.4}$$

Hence, the height of the centre of gravity OG_{eq} on the waterline is:

$$OG_{eq} = 1.26\ m \tag{4.5}$$

The obtained effective wave slope function as a function of the wave length to ship breadth ration is reported in Figure 4.2a.

Roll damping calculated by the Simplified Ikeda's Method for the amplitudes from 0° to 20° is given in Figure 4.2b.

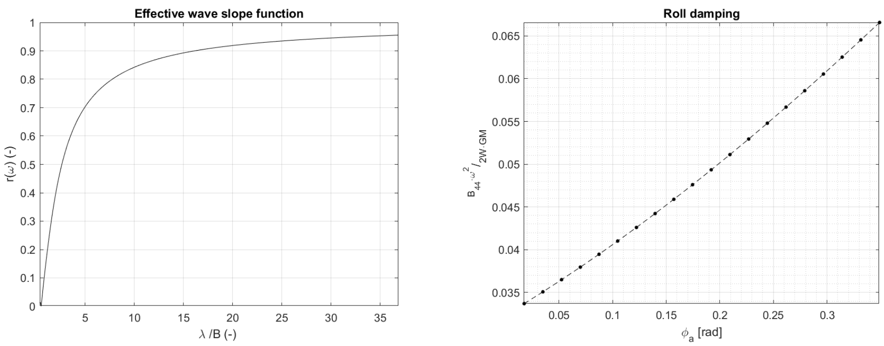

(a) IMO' standard method (b) Simplified Ikeda's Method

Figure 4.2: C11 - Effective wave slope function and roll damping.

4.3 Standard deviation of lateral acceleration and long-term stability failure index

The standard deviation of lateral acceleration for each combination of significant wave height H_s and mean zero up-crossing period is given in Table 4.3.

The obtained long-term stability failure index is:

$$C = 5.44 \cdot 10^{-4}$$

while the one reported in the Explanatory notes is equal to $4.7 \cdot 10^{-4}$. The results are satisfactory if compared with the ones in the Explanatory notes. The differences are mainly attributed to the different linearization techniques, which are the stochastic linearization in the present code and the damping at 15° angle of roll in the example in the Explanatory notes. The results are coherent with the ones shown in Belenky (2020) where similar differences are shown when comparing the

Standard deviation of lateral acceleration σ_{LAi}																	
		Tz (s)															
		3.5	**4.5**	**5.5**	**6.5**	**7.5**	**8.5**	**9.5**	**10.5**	**11.5**	**12.5**	**13.5**	**14.5**	**15.5**	**16.5**	**17.5**	**18.5**
	0.5	0.055	0.122	0.241	0.315	0.323	0.300	0.266	0.233	0.203	0.177	0.155	0.136	0.121	0.107	0.096	0.087
	1.5	0.164	0.363	0.698	0.895	0.917	0.853	0.763	0.671	0.587	0.514	0.452	0.399	0.355	0.316	0.284	0.256
	2.5	0.274	0.601	1.128	1.422	1.453	1.357	1.218	1.076	0.946	0.832	0.734	0.651	0.579	0.518	0.466	0.420
	3.5	0.383	0.837	1.533	1.908	1.945	1.820	1.641	1.456	1.285	1.134	1.003	0.891	0.795	0.713	0.642	0.580
	4.5	0.492	1.070	1.919	2.359	2.400	2.250	2.035	1.812	1.605	1.421	1.261	1.123	1.004	0.901	0.813	0.736
	5.5	0.602	1.300	2.287	2.782	2.825	2.653	2.407	2.150	1.910	1.695	1.508	1.346	1.205	1.084	0.979	0.887
	6.5	0.711	1.529	2.639	3.181	3.224	3.032	2.758	2.470	2.200	1.958	1.746	1.561	1.400	1.261	1.141	1.035
	7.5	0.820	1.754	2.977	3.558	3.601	3.391	3.091	2.776	2.479	2.211	1.975	1.769	1.590	1.434	1.298	1.180
Hs (m)	**8.5**	0.929	1.978	3.304	3.918	3.959	3.733	3.409	3.068	2.746	2.454	2.196	1.970	1.774	1.602	1.452	1.321
	9.5	1.038	2.199	3.618	4.261	4.300	4.058	3.713	3.349	3.003	2.689	2.410	2.166	1.952	1.766	1.603	1.459
	10.5	1.147	2.419	3.923	4.590	4.626	4.370	4.004	3.618	3.250	2.916	2.618	2.356	2.127	1.926	1.749	1.595
	11.5	1.257	2.636	4.219	4.906	4.939	4.668	4.285	3.878	3.490	3.136	2.820	2.541	2.296	2.082	1.893	1.727
	12.5	1.366	2.851	4.506	5.210	5.239	4.956	4.555	4.129	3.722	3.349	3.016	2.721	2.462	2.234	2.034	1.857
	13.5	1.474	3.063	4.785	5.504	5.529	5.233	4.816	4.372	3.947	3.556	3.207	2.897	2.624	2.383	2.171	1.984
	14.5	1.583	3.274	5.057	5.788	5.808	5.501	5.068	4.608	4.165	3.758	3.393	3.068	2.782	2.529	2.306	2.109
	15.5	1.692	3.484	5.321	6.063	6.078	5.760	5.313	4.836	4.377	3.954	3.574	3.236	2.937	2.672	2.439	2.232
	16.5	1.801	3.691	5.580	6.329	6.340	6.011	5.550	5.058	4.583	4.146	3.751	3.399	3.088	2.813	2.569	2.353

Table 4.3: C11 - Table of standard deviations of lateral acceleration.

long-term stability failure indexes calculated with different linearization methods. Furthermore, differences in the input data, in the number of interval for the wave frequencies range and in the number of transversal sections used in the calculation of the effective wave slope function can be an additional cause of such small differences, since many data are not specified in the example provided in Explanatory notes, IMO SDC 8/WP.4/Add.2 (2022).

This page was intentionally left blank.

Chapter 5

Froude-Krylov roll moment for any wave heading angle

The proper estimation of the external forces and moments is of paramount importance for the assessment of the ship behaviour in waves.

As described in Section 3.3, the simplified Operational Guidance for the Excessive acceleration are based on the estimation of the probability of exceeding a lateral acceleration equal to the gravity one, equation 3.35, for all the combinations of wave heading and ship speeds and for all the sea states reported in the standard wave scatter table. For each sea state, wave heading from following to head sea and ship speeds from zero to the service speed must be considered to discriminate between safe and unsafe sailing conditions.

Such verification requires the modelling of the external excitation and the question that arises is how to model it for a practical application in the rules. Although it could be calculated by a commercial software, it must be noted that the simplified OG are thought to share the methods and the same level of complexity of the corresponding vulnerability criteria. In Level 2, the standard methodology for the estimation of the effective wave slope function, Section 3.2, is recommended to model the external excitation. Indeed, the Explanatory notes (IMO SDC 8/WP.4/Add.2 2022), recommend it "since the vulnerability criteria is required to be applied with minimal computational efforts".

For this reason, an extension of the standard methodology is developed in this Chapter, providing an expression for the calculation of the Froude-Krylov roll moment for any wave heading angle, to be applied in the development of the simplified OG. The procedure is 2D and based on the standard methodology for the evaluation of the effective wave slope function which associates to each ship transversal section an equivalent rectangular one.

The expression that will be presented is in line with the philosophy at the basis of the regulations, that should provide simple but sufficiently accurate expressions for the calculation of the quantities of interest. The additional computational effort is minimal allowing the development of simplified OG through a procedure that has a complexity similar to Level 2 vulnerability criteria. The implementation in the rules of such formulation would ensure a uniform and univocal application of the simplified OG, avoiding the necessity of commercial software validation by the Administration.

5.1 Froude-Krylov exciting roll moment

The derivation of the expression for the calculation of the Froude-Krylov roll moment for any wave heading angle is based on the geometrical transformation of the IMO's standard methodology (IMO SDC 8/WP.4/Add.2 (2022)) which transforms each transversal section of the ship into a rectangular one having the same breadth at waterline and the same underwater area of the original section. The transformation algorithm, that neglects sections having zero breadth at waterline, is reported in Section 3.2. Therefore, the Froude-Krylov roll moment for any wave heading angle is obtained by means of formulas, which are exact for rectangles.

A right-handed coordinate system Oxyz moving with the forward speed of the ship V_s, assumed to be constant, is considered. The plane xy coincides with the mean water level, with x-axis pointing in the direction of ship's speed, and z-axis pointing upwards. At the instant t=0 the origin O is on the vertical through the centre of mass G. A regular wave propagates in the x' direction, inclined at an angle μ to the x-axis, Figure 5.1.

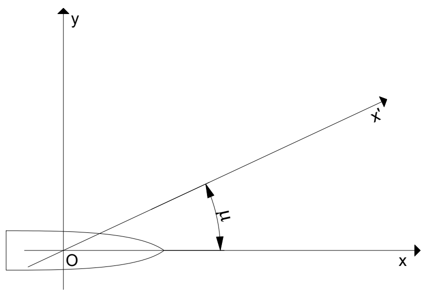

Figure 5.1: Frames of references.

The incident wave potential in the moving reference frame Oxyz is:

$$\phi_I = \frac{g\zeta_a}{\omega} e^{kz} \cos(\omega_e t - kxcos\mu - kysin\mu) \tag{5.1}$$

The dynamic pressure of the incident wave, disregarding the non-linear term in Bernoulli's equation, can be expressed in the moving reference frame as, Newman (1977):

$$p_I = -\rho \left(\frac{\partial \phi_I}{\partial t} - V_s \frac{\partial \phi_I}{\partial x} \right) = \rho g \zeta_a \; e^{kz} \;\; \sin(\omega_e t - kxcos\mu - kysin\mu) \tag{5.2}$$

In complex form:

$$\widehat{p}_I = \rho g \zeta_a e^{kz} e^{i\omega_e t} e^{i(-kxcos\mu - kysin\mu)} \tag{5.3}$$

The Froude-Krylov exciting roll moment is obtained via integration of the dynamic pressure p_I of the incident wave over the calm water wetted surface of the body:

$$F_{FK-4} = \iint_{S_{Body}} p_I \left(yn_3 - zn_2\right) dS \tag{5.4}$$

where n_2 and n_3 are the normal vectors in the y and z directions. Following strip theory assumptions and referring to the centre of gravity of the vessel, the integral can be rewritten as follows:

$$F_{FK-4} = \int_0^L \int_{C(x)} p_I \left[yn_3 - (z - z_G)\, n_2\right] dC dx \tag{5.5}$$

where $z_G = OG = KG - d$ is the vertical distance between the centre of gravity and waterplane area; KG is the height of the centre of gravity above the keel line; $C(x)$ is the contour of the wetted surface at rest, at station x. According to the geometrical transformation, $C(x)$ reduces to the wetted contour of the equivalent rectangular section, having local draught $d(x)$ and breadth at waterline $B(x)$.

It can be expressed in complex form by means of equation 5.3:

$$\hat{F}_{FK-4} = \rho g \zeta_a e^{i\omega_e t} \int_0^L e^{-ikxcos\mu} \int_{C(x)} e^{kz} e^{-ikysin\mu} \left[yn_3 - (z - z_G)\, n_2\right] dC dx \tag{5.6}$$

being $\hat{F}_{FK-4}$ the complex form of the Froude-Krylov exciting roll moment. In beam seas, the real and imaginary parts reduce to equations 3.17 and 3.18, respectively. The complex form of the sectional Froude-Krylov roll moment per unit length is defined by the line integral over $C(x)$.

$$\hat{f}_{FK-4} = \rho g \zeta_a \int_{C(x)} e^{kz} e^{-ikysin\mu} \left[yn_3 - (z - z_G)\, n_2\right] dC \tag{5.7}$$

The line integral can be expressed, for a rectangular section having local draught d and breadth at waterline B, as a sum of three integrals:

$$\begin{aligned} &\int_{C(x)} e^{kz} e^{-ikysin\mu} \left[yn_3 - (z - z_G)\, n_2\right] dC = \\ &= -\int_{-d}^{0} e^{kz} e^{-ik\left(-\frac{B}{2}\right)sin\mu} (z - z_G)(-1)\, dz + \int_{-\frac{B}{2}}^{\frac{B}{2}} e^{-kd} e^{-ikysin\mu} y\,(-1)\, dy + \\ &\qquad - \int_{-d}^{0} e^{kz} e^{-ik\frac{B}{2}sin\mu} (z - z_G)(1)\, dz \end{aligned} \tag{5.8}$$

Therefore:

$$\int_{C(x)} e^{kz} e^{-ikysin\mu} \left[yn_3 - (z - z_G)\, n_2\right] dC =$$

$$= \left(e^{ik\frac{B}{2}sin\mu} - e^{-ik\frac{B}{2}sin\mu}\right) \int_{-d}^{0} e^{kz}\,(z - z_G)\, dz - e^{-kd} \int_{-\frac{B}{2}}^{\frac{B}{2}} e^{-ikysin\mu} y dy \quad (5.9)$$

The sectional Froude-Krylov roll moment divided by $\rho g \zeta_a$ becomes:

$$\frac{\hat{f}_{FK-4}}{\rho g \zeta_a} = \left(e^{ik\frac{B}{2}sin\mu} - e^{-ik\frac{B}{2}sin\mu}\right) \cdot$$
$$\cdot \left[\left(\frac{d}{k} + \frac{1}{k^2 sin^2\mu}\right) e^{-kd} - \left(\frac{1}{k^2} + \frac{z_G}{k}\right)\left(1 - e^{-kd}\right)\right] +$$
$$- \frac{Bi}{2ksin\mu} e^{-kd} \left(e^{-ik\frac{B}{2}sin\mu} + e^{ik\frac{B}{2}sin\mu}\right) \quad (5.10)$$

Euler's formula, $e^{i\alpha} = cos\alpha + isin\alpha$, allows to rewrite equation 5.10 as follows:

$$\frac{\hat{f}_{FK-4}}{\rho g \zeta_a} = \Bigg\{ 2\left[\left(\frac{d}{k} + \frac{1}{k^2 sin^2\mu}\right) e^{-kd} - \left(\frac{1}{k^2} + \frac{z_G}{k}\right)\left(1 - e^{-kd}\right)\right] \cdot$$
$$\cdot\, sin\left(k\frac{B}{2}sin\mu\right) - \frac{B}{ksin\mu} e^{-kd} cos\left(k\frac{B}{2}sin\mu\right) \Bigg\} i \quad (5.11)$$

Equation 5.11 is in complex form and its magnitude represents the sectional Froude-Krylov roll moment amplitude, divided by $\rho g \zeta_a$, for a generic heading angle μ:

$$\frac{f_{FK-4}}{\rho g \zeta_a} = 2\left[\left(\frac{d}{k} + \frac{1}{k^2 sin^2\mu}\right) e^{-kd} - \left(\frac{1}{k^2} + \frac{z_G}{k}\right)\left(1 - e^{-kd}\right)\right] \cdot$$
$$\cdot\, sin\left(k\frac{B}{2}sin\mu\right) - \frac{B}{ksin\mu} e^{-kd} cos\left(k\frac{B}{2}sin\mu\right) \quad (5.12)$$

Equation 5.12 is not defined for heading angles equal to 0° or 180°. However, the sectional Froude-Krylov roll moment in following and head seas is equal to zero since equation 5.9 goes to zero.

The quantity $A(x)$ is introduced to represent the term in curly brackets in equation 5.11 and to emphasize the x-dependence of its terms, since breadth at waterline and local draught change along x. Then:

$$A\,(x) = 2\Bigg[\left(\frac{d(x)}{k} + \frac{1}{k^2 sin^2\mu}\right) e^{-kd(x)} +$$
$$-\left(\frac{1}{k^2} + \frac{z_G}{k}\right)\left(1 - e^{-kd(x)}\right)\Bigg] sin\left(k\frac{B(x)}{2}sin\mu\right) - \frac{B(x)}{ksin\mu} e^{-kd(x)} cos\left(k\frac{B(x)}{2}sin\mu\right)$$
$$(5.13)$$

The total Froude-Krylov roll moment can be obtained introducing the complex form of the sectional Froude-Krylov roll moment amplitude, equation 5.11, in equation 5.6.

$$\hat{F}_{FK-4} = \rho g \zeta_a e^{i\omega_e t} \int_0^L e^{-ikxcos\mu} A(x) i dx \tag{5.14}$$

The Froude-Krylov roll moment can be expressed as a sum of two integrals, separating the real and imaginary parts:

$$\hat{F}_{FK-4} = \rho\, g \zeta_a e^{i\omega_e t} \left(i \int_0^L \cos\left(kxcos\mu\right) A\left(x\right) dx + \int_0^L \sin\left(kxcos\mu\right) A\left(x\right) dx \right) \tag{5.15}$$

Each integral can be calculated separately with a suitable integration method. Therefore, the Froude-Krylov roll moment amplitude can be expressed as:

$$F_{FK-4} = \rho g \zeta_a \sqrt{\left[\int_0^L \cos\left(kxcos\mu\right) A\left(x\right) dx \right]^2 + \left[\int_0^L \sin\left(kxcos\mu\right) A\left(x\right) dx \right]^2} \tag{5.16}$$

Equation 5.16 allows the computation of the effective wave slope function according to equation 3.21.

An exact solution of equation 5.14 can be obtained if a barge with zero trim is considered. Indeed, all the terms in 5.13 are constant along x, and the Froude-Krylov roll moment amplitude can be written as:

$$\begin{aligned} &F_{FK-4} = \\ &= \rho g \zeta_a \Bigg\{ 2 \left[\left(\frac{d}{k} + \frac{1}{k^2 sin^2 \mu} \right) e^{-kd} - \left(\frac{1}{k^2} + \frac{z_G}{k} \right) \left(1 - e^{-kd} \right) \right] sin \left(k \frac{B}{2} sin\mu \right) + \\ &- \frac{B}{ksin\mu} e^{-kd} cos \left(k \frac{B}{2} sin\mu \right) \Bigg\} \frac{1}{kcos\mu} \sqrt{\left[1 - cos\left(kLcos\mu\right)\right]^2 + \left[sin\left(kLcos\mu\right)\right]^2} \end{aligned} \tag{5.17}$$

5.2 Validation of the proposed formulation for the Froude-Krylov exciting roll moment

The formulas presented in Section 5.1 for the calculation of the Froude-Krylov roll moment have been validated in three steps:

1. showing that the formula for the sectional Froude-Krylov roll moment, 5.12, reduces to the ones reported in the IMO's standard methodology if the beam seas case is considered;
2. the amplitude of the Froude-Krylov roll moment for a barge is calculated for different headings and compared with the one obtained by the 3-D potential software HydroStar® developed by Bureau Veritas;

3. the same comparison is performed for a sample ship, considering four wave headings.

5.2.1 Beam seas case - IMO's standard methodology

IMO's formulas for the effective wave slope function may be obtained from the sectional Froude-Krylov roll moment amplitude, equation 5.12, considering the beam seas case, $\mu = 90°$. It results:

$$\frac{f_{FK-4}}{\rho g \zeta_a} = 2\left[\left(\frac{d}{k}+\frac{1}{k^2}\right)e^{-kd}-\left(\frac{1}{k^2}+\frac{z_G}{k}\right)\left(1-e^{-kd}\right)\right]\cdot \\ \cdot\, sin\left(k\frac{B}{2}\right)-\frac{B}{k}e^{-kd}cos\left(k\frac{B}{2}\right) \quad (5.18)$$

Equation 5.18 can be rearranged as follows:

$$\frac{f_{FK-4}}{\rho g \zeta_a} = Bd\Bigg[\frac{2}{B}\frac{e^{-kd}}{k}sin\left(k\frac{B}{2}\right)+\frac{2}{Bd}\frac{e^{-kd}}{k^2}sin\left(k\frac{B}{2}\right)-\frac{2}{Bdk^2}sin\left(k\frac{B}{2}\right)+ \\ +\frac{2}{Bd}\frac{e^{-kd}}{k^2}sin\left(k\frac{B}{2}\right)-\frac{2}{Bd}\frac{z_G}{k}sin\left(k\frac{B}{2}\right)+\frac{2}{Bd}\frac{z_G}{k}e^{-kd}sin\left(k\frac{B}{2}\right)-\frac{e^{-kd}}{kd}cos\left(k\frac{B}{2}\right)\Bigg] \quad (5.19)$$

Dividing both parts of the equation for the wave number the following expression is obtained:

$$\frac{f_{FK-4}}{\rho g k \zeta_a} = Bd\Bigg[\frac{2}{B}\frac{e^{-kd}}{k^2}sin\left(k\frac{B}{2}\right)+\frac{2}{Bd}\frac{e^{-kd}}{k^3}sin\left(k\frac{B}{2}\right)-\frac{2}{Bdk^3}sin\left(k\frac{B}{2}\right)+ \\ +\frac{2}{Bd}\frac{e^{-kd}}{k^3}sin\left(k\frac{B}{2}\right)-\frac{2}{Bd}\frac{z_G}{k^2}sin\left(k\frac{B}{2}\right)+\frac{2}{Bd}\frac{z_G}{k^2}e^{-kd}sin\left(k\frac{B}{2}\right)-\frac{e^{-kd}}{k^2 d}cos\left(k\frac{B}{2}\right)\Bigg] \quad (5.20)$$

The sum of first, third and fourth elements in the square brackets returns the term $K_1(x)$ of the IMO' standard methodology, equation 3.43:

$$\frac{2}{B}\frac{e^{-kd}}{k^2}sin\left(k\frac{B}{2}\right)-\frac{2}{Bdk^3}sin\left(k\frac{B}{2}\right)+\frac{2}{Bd}\frac{e^{-kd}}{k^3}sin\left(k\frac{B}{2}\right)= \\ =\frac{sin\left(k\frac{B}{2}\right)}{k\frac{B}{2}}\left[\frac{(1+kd)\,e^{-kd}-1}{k^2 d}\right]=K_1(x) \quad (5.21)$$

The sum of seventh and second elements returns the term $K_2(x)$, equation 3.44:

$$
-\frac{e^{-kd}}{k^2d}cos\left(k\frac{B}{2}\right)+\frac{2}{Bd}\frac{e^{-kd}}{k^3}sin\left(k\frac{B}{2}\right)=
$$

$$
=-\frac{e^{-kd}}{k^2d}\left[cos\left(k\frac{B}{2}\right)-\frac{sin\left(k\frac{B}{2}\right)}{k\frac{B}{2}}\right]=K_2\left(x\right) \quad (5.22)
$$

The sum of fifth and sixth elements returns the term which depends on the loading condition, i.e. the product between $F_1\left(x\right)$, equation 3.45, and OG, being $z_G=OG=KG-d$:

$$
-\frac{2}{Bd}\frac{z_G}{k^2}sin\left(k\frac{B}{2}\right)+\frac{2}{Bd}\frac{z_G}{k^2}e^{-kd}sin\left(k\frac{B}{2}\right)=
$$

$$
=-\left[\left(\frac{1-e^{-kd}}{kd}\right)\right]\frac{sin\left(k\frac{B}{2}\right)}{k\frac{B}{2}}z_G=F_1\left(x\right)OG \quad (5.23)
$$

Therefore, the sectional term $C\left(x\right)$, equation 3.42, is obtained:

$$
\frac{f_{FK-4}}{\rho gk\zeta_a}=Bd\left[K_1\left(x\right)+K_2\left(x\right)+F_1\left(x\right)OG\right]=C(x) \quad (5.24)
$$

Finally, the effective wave slope function according to IMO's standard methodology, is obtained:

$$
r\left(\omega\right)\ =\left|\frac{F_{FK-4}\left(\omega\right)}{\rho g\nabla G\ M\ k\zeta_a}\right|=\left|\frac{\int_L f_{FK-4}(x)dx}{\rho gk\zeta_a\nabla\ GM}\right|=\left|\frac{\int_L\ C\left(x\right)dx}{\nabla\ GM}\right| \quad (5.25)
$$

5.2.2 Barge

The IMO's standard methodology and the formulation derived in the present Chapter are based on the geometrical transformation that associates to each ship transversal section an equivalent rectangle. Therefore, the formulation should be exact for a barge, whose sections are rectangles. The exact solution of the Froude-Krylov roll moment acting on a barge with zero trim and for any heading angle is equation 5.17.

A 20-m long barge has been considered to validate equation 5.17. The main particulars are reported in Table 5.1.

Four heading angles have been considered: 90°, 120°, 150°, 179°. According to the assumed convention, 0° corresponds to following waves while 180° to head waves. The results of the comparison are shown in Figure 5.2 showing a good agreement between the results obtained with the proposed formulation, referred as "Modified IMO's procedure" and the ones obtained by HydroStar®.

Main characteristics	Units	
Length, L	(m)	20.0
Breadth, B	(m)	10.0
Draught, d	(m)	5.0
Displacement, Δ	(t)	1025.0
Block coefficient, C_B	-	1.00
Height of the centre of gravity, KG	(m)	2.5
Metacentric height, GM	(m)	1.67

Table 5.1: Barge main parameters.

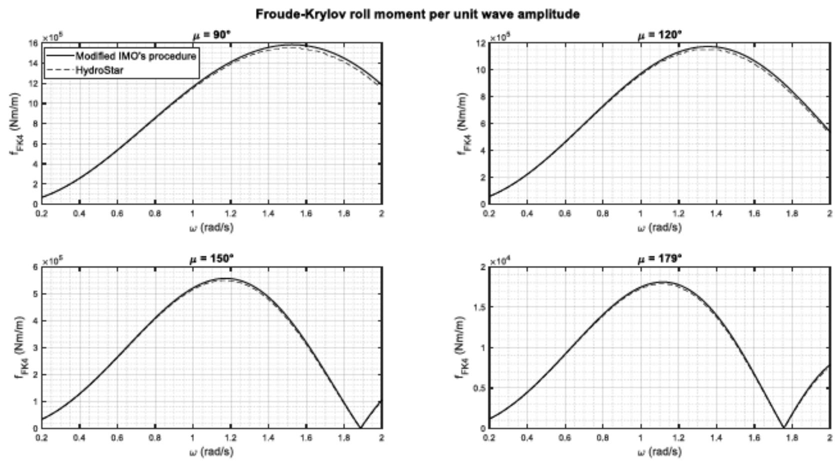

Figure 5.2: Froude-Krylov roll moment acting on the barge for different wave headings.

5.2.3 Bulk

A bulk carrier, whose main dimension are reported in Table 5.2 and the cross sections are reported in Chapter 7, is considered for the validation of expression of the Froude-Krylov roll moment calculated by the simplified procedure presented in this Chapter with the one calculated by a more sophisticated tool, able to account for the 3-D geometry of the ship. Its geometrical representation in HydroStar® software is given in Figure 5.3.

The comparison between the Froude-Krylov roll moment calculated with the two methodologies is given in Figure 5.4 as a function of the wave frequency in the range from 0.2 to $2.0rad/s$, showing a good agreement up to $1.0rad/s$, for all headings. The differences tend to increase for higher frequencies, i.e. for waves with period lower than $6s$, since the the wavelength and the ship breadth become comparable, as shown in Figure 5.5. However, the amplitudes match well at the ship natural roll frequency, drawn as dot-slash line in Figure 5.4, around which most of the energy under synchronous resonance is concentrated.

Main characteristics	**Units**	
Length between perpendiculars, L_{pp}	*(m)*	112.8
Breadth, B	*(m)*	16.8
Draught, d	*(m)*	6.7
Displacement, Δ	*(t)*	10562
Height of the centre of gravity, KG	*(m)*	5.38
Metacentric height, GM	*(m)*	1.71

Table 5.2: Bulk carrier main parameters.

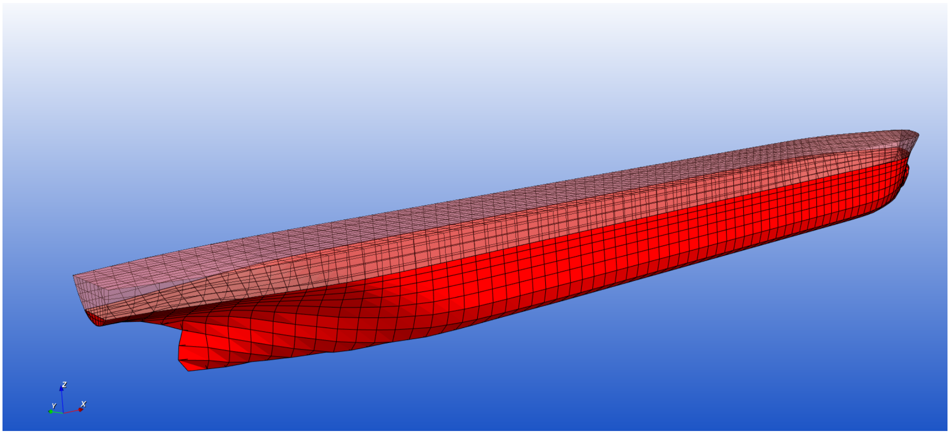

Figure 5.3: Bulk carrier representation in HydroStar®.

5.3 Conclusions

In the present Chapter a formulation for the estimation of the Froude-Krylov exciting roll moment has been developed based on the IMO's standard methodology for the estimation of the effective wave slope function. The standard methodology consists of two parts: the geometrical transformation that associates to each ship transversal sections an equivalent rectangle and a 2D strip theory algorithm that uses formulas which are exact for rectangular sections and specific for the beam seas case. In the proposed formulation, the geometrical transformation has been kept and the 2D algorithm has been extended to any wave heading angle.

The proposed formulation is intended to be used in the development of the simplified OG, that requires the verification of the behaviour of the vessel in many sailing conditions, requiring the proper description of the external excitation. The procedure shows a good agreement with results obtained by a commercial software, making suitable its implementation in the rules due to the good compromise between accuracy and very limited computational cost.

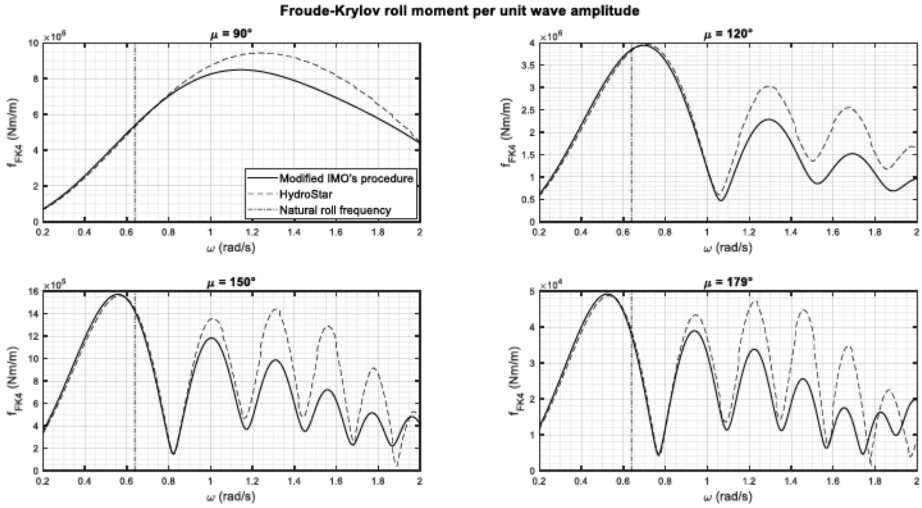

Figure 5.4: Froude-Krylov roll moment acting on the bulk carrier for different wave headings as a function of the wave frequency.

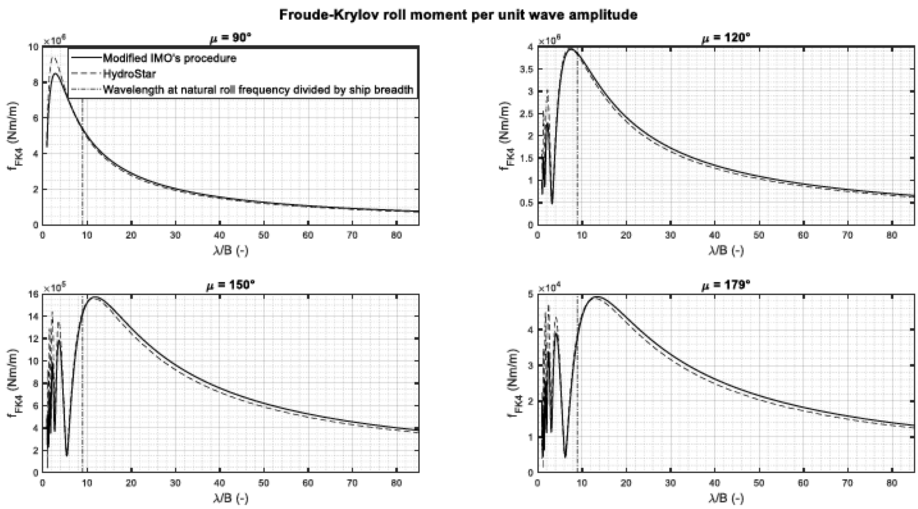

Figure 5.5: Froude-Krylov roll moment acting on the bulk carrier for different wave headings as a function of the ratio λ/B.

Chapter 6

On-board decision support system

The SGISC allow the development of ship-specific Operational Measures to permit safe ship operation under certain conditions. OM consist of Limitations to the environmental conditions under which the ship can sail or Guidance on how to handle the ship if certain conditions are met.

In the SGISC framework the possibility to develop OM based on computations during operations is envisaged, IMO SDC 8/WP.4/Add.5 (2022). The advantage is that most actual weather and loading condition data may be used. In this Chapter, the possibility to equip the vessel with systems that, based on real-time measurements of ship responses, may warn the crew if dangerous situations are identified is investigated.

The importance of monitoring ship motions, to avoid dangerous situations that could be a source of risk for people on board and cargo, is well recognized as a good practice on-board of seagoing ships since many years, Papanikolau et al. (2014). As an example, the investigation report on the accident involving JRS Canis in 2008, linked to lateral accelerations, can be mentioned, BSU (2008). One of the main conclusion of the report was a recommendation to further develop systems that, based on the monitoring of the vessel's motions, can effectively assist the vessel's command. Information collected during the navigation can be used to statistically characterize and predict ship responses to allow route planning or changes in sailing conditions in a sufficient time before experiencing dangerous conditions.

Monitoring systems and real-time Operational Guidance, defined as Decision Support Systems (DSS), allow to overcome the intrinsic limitation of the guidance developed at the design stage, which are based on a set of theoretical sea states and loading conditions. Indeed, due to the stochastic nature of the marine environment and the fact that the actual loading condition may not match any of the assumed conditions, the choice of the most representative guidance among those developed at the design stage can be challenging.

A monitoring system for lateral accelerations is presented in the following. Accelerations measured on-board are used to evaluate the actual operational condition of the vessel by comparison with two thresholds. Acceleration magnitude changes can be a source of risk for people and cargo and can be caused by variations in the sea state and/or in the loading conditions over time. In addition to the monitoring task, measurements are also used to predict the extreme lateral accelerations that could be experienced in the short-term. Timely identification of dangerous situations allow the crew or automatic systems to take corrective actions, as the change of ship speed or of the heading angle.

In recent years, the monitoring of the actual state of a vessel has been made by statistical tests developed by the application of the detection theory on measured ship motions. In Galeazzi et al. (2013), two complementary detection schemes were presented to alert the crew when the vessel is close to or already in parametric roll: one in the frequency domain that evaluates whether pitch and roll are close to a 2:1 ratio in frequency; the other in the time domain that tests the phase alignment between pitch and roll. If the values returned by the two detectors are both above their thresholds, a resonant event is identified, and the monitoring system raises an alarm. The performance of the system was further investigated in Galeazzi et al. (2015) proving the detection robustness and the low false warning rates through a bivariate statistical analysis, by considering long-term voyage data and full-scale resonance events.

In Santiago Caamaño et al. (2019), the fishing vessel considered in the present Thesis was used to validate a stability monitoring system that estimates the actual metacentric height. Two stages can be identified in the proposed system: an estimation stage of the roll natural frequency obtained and a detection stage that models the natural roll frequency as realizations of a Weibull distributed random process. The Generalized Likelihood Ratio Test was applied in the detection stage to discriminate if the current estimates belong or not to a safe condition, raising an alarm if the risky condition is met. The monitoring system was tested against simulated roll motion times series and validated through an experimental campaign in Santiago Caamaño et al.(2019), confirming the ability of the system to trail variations in transverse stability parameters.

In Santiago Caamaño et al. (2019) an onboard stability monitoring system was proposed. This system estimates in real-time the natural roll frequency of the vessel and triggers an alarm when this parameter cross the safe limit. The estimation is done using signal processing techniques in time domain while the detection is performed applying the Generalized Likelihood Ratio Test. The monitoring system was tested against simulated roll motion times series in Santiago Caamaño et al. (2019) and validated through an experimental campaign in Santiago Caamaño et al. (2019), confirming the ability of the system to trail variations in the natural roll frequency.

In addition to decision support system based on detection theory, other examples were proposed in the literature to monitor ship responses. Nielsen et al. (2009) accounted for uncertainties associated to random variables involved in the development of on-board Decision Support Systems. Wave induced accelerations on-board of a containership were calculated by parallel system analysis and compared with results from Monte Carlo simulations, showing a good agreement and a faster computational time but still not-sufficiently fast for real-time on board decision support systems. Míguez González et al. (2011) developed a system, based on Artificial Neural Networks, able to predict the inception of parametric resonance. Two fishing vessels were considered to train and test the system showing good performance in predicting roll motion up to 40 s ahead in the case of the shortest model, allowing the crew to take corrective actions. The performance decreased when testing the longer model, where a good prediction was obtained up to 10 s ahead, which could allow the immediate action of an automatic prevention system but not a manual one from the crew. Terada et al. (2018) proposed an estimation method of the ship natural roll frequency, using Bayesian modelling procedure and the measured roll motion, whose knowledge can help to avoid dangerous situations, as harmonic roll resonance and parametric roll. The method was tested by data recorded onboard of a fisheries research vessel.

6.1 Monitoring of lateral accelerations and prediction of extreme values

Ship responses under wind and waves excitation are random processes. Due to the stochastic nature of lateral accelerations, several observations are needed to statistically describe the phenomenon.

The proposed system is designed to perform two main tasks, based on real-time measurements of accelerations at a given location along the ship:

- monitoring of the actual operational condition of the vessel by calculating the root mean square (RMS) of the lateral acceleration time series in a certain time window;
- estimation of the extreme accelerations that could be experienced in the short-term based on the measurement of the lateral acceleration in the last time window.

An Inertial Motion Unit (IMU) can be used to measure real-time accelerations at the wheelhouse or at any relevant location on board of the ship, keeping the cost of the system very limited.

The detailed description of the tasks is provided in the following subsections.

6.1.1 Monitoring of the actual operational condition

The root mean square associated to specific time windows can be calculated during ship operations from the recording of the lateral accelerations at a given location. The length of the time window should be sufficiently long to properly describe the phenomenon in statistical terms. In the present analysis, time windows of 20 minutes are considered to capture at least 100 waves during each recording, Journee and Massie (2001).

The knowledge of the root mean square allows the monitoring of the potential risk of the vessel by comparing it with a reference value. Two thresholds are introduced for the monitoring of the actual condition: $0.10g$ that corresponds to a probable risk (0.5 MII per minute) and $0.2g$ corresponding to an extreme risk (5 MII per minute) characterized by more than 2 sliding events each three hours on a dry deck (Graham (1990), Shigunov et al. (2011)). An alert is provided if the calculated RMS is in between the two limiting values, warning the crew about a potentially dangerous situation (orange colour). An alarm is given if the RMS exceeds the greatest value, identifying an actual dangerous situation (red colour). The limit values could be lowered for wet decks, for example the fishing deck.

6.1.2 Estimation of the extreme lateral accelerations

The extreme acceleration that could occur in the short-term can be estimated from the last recorded data by application of the extreme value theory.

The extreme value of a random process $x(t)$ is defined as the largest values that is expected to occur in a sequence of n maxima (or minima) of that process, Ochi (1989).

Given the ordered sample $(u_1, u_2, ..., u_n)$ of the maxima, defined such that $u_1 < u_2 < ... < u_n$, it is assumed that the elements of the sample are statistically independent. The largest value u_n of the ordered sample constitutes a random variable itself, characterized by its own probability distribution. This allows to consider the largest lateral acceleration values in certain exposure time as a realization of a random process.

Lateral accelerations are modeled as a zero-mean Gaussian random process, considered to be stationary in the given time window. The amplitudes of the accelerations are assumed to be statistically independent. Under these assumptions, the expected extreme acceleration (most probable extreme value) which will be exceeded in a given time period T, in seconds, is calculated according to the formulation reported in Ochi (1973):

$$\overline{a}_{y,T} = \sqrt{2\ln\left(\frac{T}{2\pi}\sqrt{\frac{m_2}{m_0}}\right)} \cdot \sqrt{m_0} = \sqrt{2\ln\frac{T}{T_z}} \cdot \sqrt{m_0} \tag{6.1}$$

where T_z is the mean zero up-crossing period of the lateral acceleration time series; m_0 and m_2 are the zero-th and second order moments of the lateral acceleration spectrum. The most probable extreme value is schematically represented in Figure 6.1, defined as the modal value of the probability distribution of the extreme values of the random process.

If a preassigned probability of exceeding α is introduced, the extreme lateral acceleration exceeded with that probability is given by the following, that holds for small values of α:

$$\hat{a}_{y,T} = \sqrt{2\ln\left(\frac{T}{2\pi\alpha}\sqrt{\frac{m_2}{m_0}}\right)} \cdot \sqrt{m_0} = \sqrt{2\ln\frac{T}{\alpha T_z}} \cdot \sqrt{m_0} \tag{6.2}$$

One of the main advantages of equations 6.1 and 6.2 is that they are valid for any bandwidth parameter ϵ. This means that the system can be applied for processes having the energy over a narrow band of frequencies and for for processes having the energy over a wide band of frequencies, since the width of the process is accounted by the mean zero-crossing period. In addition, the exposure time T to the environmental conditions can be fixed instead of a preassigned number of cycles.

The system calculates the most probable extreme value $\overline{a}_{y,T}$ and the predicted extreme value $\hat{a}_{y,T}$, associated to the exposure time T.

As concerns the limit value to be exceeded for raising an alarm, half of the gravity acceleration g is considered. This value is taken from the Interim guidelines

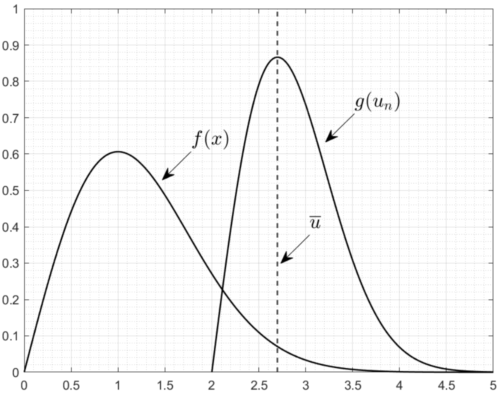

Figure 6.1: Schematic representation of the probability density function of the amplitudes and extreme values of a random process $x(t)$.

on SGISC that, in the deterministic Operational Guidance, identify as dangerous sailing conditions the ones for which:

$$a_{y,3h} > \frac{9.81}{2} \tag{6.3}$$

being $a_{y,3h}$ the maximum 3-hour lateral acceleration value, as explained in IMO MSC.1/Circ.1627 (2020). Such value is not small, and experiencing accelerations of such a magnitude could be risky for people on board. Therefore, an additional limit value has been introduced, equal to $g/3$. A safe condition is provided if the most probable acceleration $\overline{a}_{y,T}$ is lower than $g/3$, an alert is provided if it is in between $g/3$ and $g/2$, and an alarm is given if it is greater than $g/2$.

This page was intentionally left blank.

Chapter 7

Case study 1 - Bulk carrier

The bulk carrier presented in Chapter 5.2.3 is chosen as first case study of the Excessive acceleration criterion.

The application of Level 1 and Level 2 criteria has been performed to identify the vulnerability of the ship to the phenomenon. Then, Operational Measures have been considered to solve the identified vulnerability:

- Operational Limitations related to route and maximum significant wave height have been discussed with particular emphasis on the definition of the scatter table associated to long routes;
- simplified Operational Guidance have been applied considering the Froude-Krylov roll moment obtained from the formulation presented in Chapter 5.

The ship main parameters, the service speed and the location of the wheelhouse, assumed as calculation point for lateral acceleration, are reported in Table 7.1. The body plan and a 3-D view of the ship are given in Figure 7.1 and Figure 7.2, respectively. The ship has been assumed with zero initial trim and heel.

Main characteristics	**Units**	
Length between perpendiculars, L_{pp}	*(m)*	112.8
Breadth, B	*(m)*	16.8
Draught, d	*(m)*	6.7
Displacement, Δ	*(t)*	10562
Block coefficient, C_B	-	0.81
Midship section coefficient, C_m	-	0.98
Height of the centre of gravity, KG	*(m)*	5.38
Metacentric height, GM	*(m)*	1.71
Natural roll period, T_r	*(s)*	9.83
Longitudinal distance of the bridge deck from AP, x_{AP}	*(m)*	17.90
Height of the bridge deck from BL, H_{BL}	*(m)*	19.5
Ship speed, V_s	*(kn)*	14.0

Table 7.1: Bulk carrier main parameters.

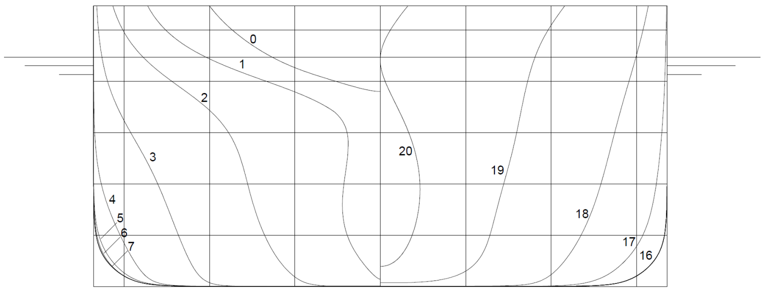

Figure 7.1: Body plan of the bulk carrier.

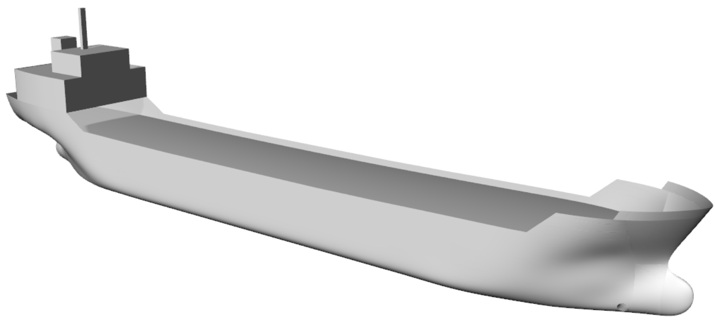

Figure 7.2: Bulk carrier 3D view.

The Excessive acceleration is the only criterion the ship has been found vulnerable to, in the considered loading condition. For the assumed service speed the verification to pure loss of stability and surf-riding broaching criteria is not required, while no vulnerability to Level 1 of parametric rolling has been identified. These are expected results due to the particular geometry and characteristics of the ship. As concern the dead ship condition criterion, the loading condition satisfies the Level 1, which is the Weather Criterion implemented in the 2008 IS Code.

In all the calculations, the roll damping has been estimated by the Simplified Ikeda's Method, introducing the lift damping component to account for the ship speed. The eddy damping component has been calculated adopting the correction proposed in Rudaković and Bačkalov (2017) due to the high value of the block coefficient C_B. Indeed, the Authors showed in their work that for $C_B > 0.84$ the Simplified Ikeda's Method provides negative values of the eddy damping component, and questioned the applicability of the formulation for $C_B > 0.74$.

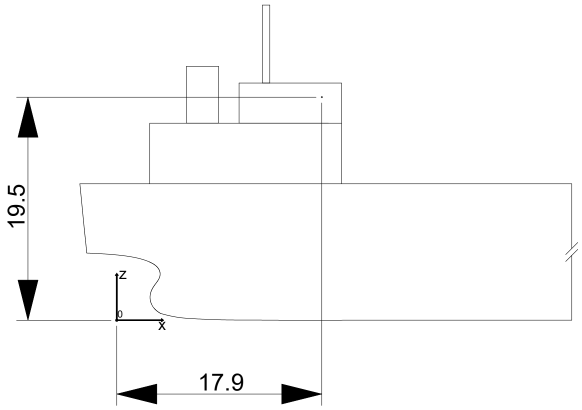

Figure 7.3: Calculation point for lateral acceleration.

7.1 Vulnerability criteria

The verification of the Excessive acceleration criterion is required in the loading condition under analysis since the metacentric height and the height of the location above the waterline exceed the 8% and 70% of the ship breadth, respectively.

The ship does not meet the vulnerability criteria for the Excessive acceleration failure mode. Level 1, equation 3.1, is not verified being the computed acceleration higher than the limit value:

$$\varphi k_L \left(g + 4\pi^2 \frac{h}{T_r^2} \right) = 8.37 m/s^2 > R_{EA1} = 4.64 m/s^2$$

where:

$$\varphi = 0.53 \ rad$$

$$k_L = 1.03$$

$$T_r = 9.83 s$$

and h is the height of the considered location above the roll axis, assumed to be located at the midpoint between the centre of gravity and the waterline:

$$h = H_{BL} - 0.5(d + KG) = 13.43 m$$

Therefore, the second level of assessment has been performed. The obtained short-term stability failure indexes, weighted according to the probability of occurrence of the sea states reported in standard wave scatter table, are given in Table 7.2.

The long-term stability failure index, equation 3.14, has been calculated confirming the vulnerability of the vessel to Level 2:

Excessive acceleration Level 2: weighted short-term indexes $W_iC_{s,i}$																	
		Tz (s)															
		3.5	4.5	5.5	6.5	7.5	8.5	9.5	10.5	11.5	12.5	13.5	14.5	15.5	16.5	17.5	18.5
Hs (m)	0.5	0.0E+00	0.0E+00	1.2E-196	2.0E-92	6.5E-82	2.8E-92	2.1E-114	4.3E-147	3.5E-191	4.4E-248	0.0E+00	0.0E+00	0.0E+00	0.0E+00	0.0E+00	0.0E+00
	1.5	0.0E+00	4.7E-218	2.8E-29	2.6E-15	1.1E-13	3.7E-15	2.2E-18	4.2E-23	2.6E-29	3.7E-37	8.1E-47	1.7E-58	1.5E-72	0.0E+00	0.0E+00	0.0E+00
	2.5	0.0E+00	5.8E-85	1.5E-14	3.3E-08	3.7E-07	1.2E-07	5.3E-09	4.4E-11	7.5E-14	2.5E-17	1.6E-21	1.5E-26	1.9E-32	2.7E-39	0.0E+00	0.0E+00
	3.5	0.0E+00	3.1E-48	1.4E-10	2.5E-06	2.5E-05	2.1E-05	4.0E-06	2.4E-07	5.0E-09	3.8E-11	1.0E-13	9.5E-17	2.7E-20	2.2E-24	4.7E-29	0.0E+00
	4.5	0.0E+00	0.0E+00	3.2E-09	8.8E-06	1.0E-04	1.5E-04	6.3E-05	9.9E-06	6.8E-07	2.2E-08	3.3E-10	2.3E-12	7.5E-15	1.0E-17	5.0E-21	0.0E+00
	5.5	0.0E+00	0.0E+00	7.8E-09	9.3E-06	1.3E-04	2.9E-04	2.1E-04	5.9E-05	8.2E-06	6.0E-07	2.4E-08	5.1E-10	6.2E-12	4.1E-14	1.4E-16	3.2E-19
	6.5	0.0E+00	0.0E+00	8.1E-09	5.5E-06	9.6E-05	3.0E-04	3.1E-04	1.4E-04	3.1E-05	3.8E-06	2.8E-07	1.2E-08	3.4E-10	5.6E-12	5.3E-14	3.3E-16
	7.5	0.0E+00	0.0E+00	0.0E+00	2.4E-06	5.1E-05	2.1E-04	2.9E-04	1.8E-04	5.7E-05	1.1E-05	1.2E-06	8.6E-08	4.1E-09	1.3E-10	2.8E-12	3.0E-14
	8.5	0.0E+00	0.0E+00	0.0E+00	8.4E-07	2.2E-05	1.2E-04	2.1E-04	1.7E-04	7.0E-05	1.7E-05	2.7E-06	2.8E-07	2.0E-08	9.8E-10	3.2E-11	7.1E-13
	9.5	0.0E+00	0.0E+00	0.0E+00	3.3E-07	8.2E-06	5.4E-05	1.2E-04	1.2E-04	6.3E-05	2.0E-05	4.1E-06	5.6E-07	5.4E-08	3.7E-09	1.8E-10	7.0E-12
	10.5	0.0E+00	0.0E+00	0.0E+00	0.0E+00	2.8E-06	2.2E-05	6.0E-05	7.2E-05	4.6E-05	1.8E-05	4.5E-06	7.7E-07	9.7E-08	8.8E-09	5.6E-10	4.0E-11
	11.5	0.0E+00	0.0E+00	0.0E+00	0.0E+00	8.4E-07	8.3E-06	2.6E-05	3.7E-05	2.8E-05	1.3E-05	3.9E-06	8.2E-07	1.3E-07	1.3E-08	1.2E-09	1.5E-10
	12.5	0.0E+00	0.0E+00	0.0E+00	0.0E+00	3.2E-07	2.9E-06	1.0E-05	1.7E-05	1.5E-05	8.1E-06	2.8E-06	7.0E-07	1.3E-07	1.6E-08	1.4E-09	0.0E+00
	13.5	0.0E+00	0.0E+00	0.0E+00	0.0E+00	0.0E+00	9.9E-07	3.8E-06	7.3E-06	7.4E-06	4.5E-06	1.8E-06	5.2E-07	1.1E-07	1.5E-08	2.9E-09	0.0E+00
	14.5	0.0E+00	0.0E+00	0.0E+00	0.0E+00	0.0E+00	3.7E-07	1.2E-06	2.9E-06	3.2E-06	2.2E-06	1.0E-06	3.2E-07	7.4E-08	1.2E-08	0.0E+00	0.0E+00
	15.5	0.0E+00	0.0E+00	0.0E+00	0.0E+00	0.0E+00	0.0E+00	3.4E-07	1.1E-06	1.3E-06	1.0E-06	4.9E-07	1.8E-07	3.5E-08	1.8E-08	0.0E+00	0.0E+00
	16.5	0.0E+00	0.0E+00	0.0E+00	0.0E+00	0.0E+00	0.0E+00	0.0E+00	3.1E-07	4.8E-07	3.5E-07	2.4E-07	7.8E-08	4.7E-08	0.0E+00	0.0E+00	0.0E+00

Table 7.2: Bulk carrier - Weighted short-term stability failure indexes.

$$C = 4.2 \cdot 10^{-3} > R_{EA2} = 3.9 \cdot 10^{-4}$$

It is worth commenting the effect of the adopted modified formulation for the eddy-making component on the long-term stability failure index. Indeed, the long-term index calculated modelling the damping by the Simplified Ikeda's Method without any modification is:

$$C = 2.4 \cdot 10^{-3} > R_{EA2} = 3.9 \cdot 10^{-4}$$

which is lower than the one calculated with the modified formulation, but still able to identify the ship vulnerability to the Excessive acceleration.

In order to explain the obtained difference, the modification introduced in the formulation of the eddy damping component by Rudaković and Bačkalov (2017) is recalled. The eddy component in non-dimensional form is:

$$\hat{B}_E = \frac{4\hat{\omega}\varphi_a}{3\pi \frac{B}{d} C_B} c_R \tag{7.1}$$

where φ_a is the roll amplitude and $\hat{\omega}$ is:

$$\hat{\omega} = \omega \sqrt{\frac{B}{2g}} \tag{7.2}$$

The coefficient c_R in equation 7.1 is in turn a linear function of a coefficient A_E and of the ship parameters $\frac{B}{d}$, c_B, c_M, $\frac{OG}{d}$:

$$c_R = f\left(A_E, \frac{B}{d}, c_B, c_M, \frac{OG}{d}\right) \tag{7.3}$$

The coefficient A_E is given by the following:

$$A_E = A_{E1} + A_{E2} \tag{7.4}$$

The introduced modification is in the coefficient A_{E2}, which was derived by regression analysis in the original method, Kawahara et al. (2009). It is not properly estimated for block coefficient higher than 0.74, which is the case of the bulk carrier under investigation, whose block coefficient is 0.81. An updated formulation was provided by Rudaković and Bačkalov (2017) and it is graphically compared as a function of the block coefficient in Figure 7.4. It can be noticed that the modified formulation provides a lower value of the coefficient A_{E2} for the block coefficient of the bulk carrier, leading to a smaller value of the eddy damping component. The latter is plotted as a function of the roll angle in the range from 0° to 20°, with a difference of the order of 30% compared to the same component calculated by the Simplified Ikeda's Method without any modification. The lower roll damping explains the more severe long-term stability failure index obtained with the modified formulation.

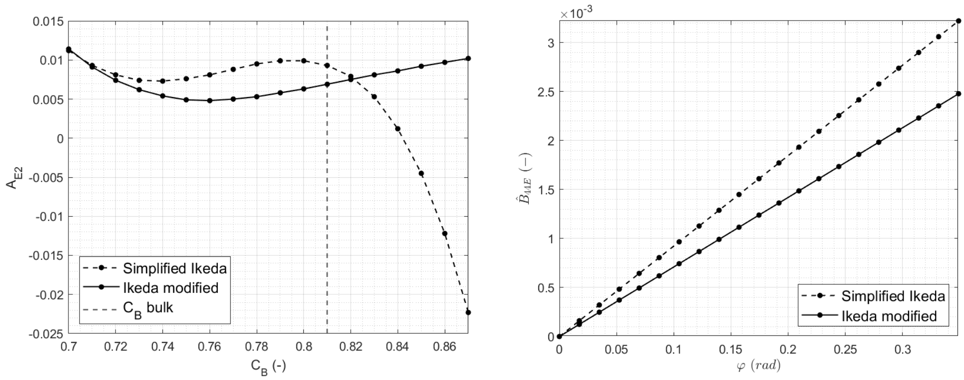

Figure 7.4: Coefficient A_{E2} and non-dimensional eddy damping component.

7.2 Operational Limitations and impact of route definition

Once the vulnerability of the bulk carrier to the Excessive acceleration has been identified, Operational Limitations have been developed to check if the loading conditions can be accepted by imposing some limitations to the environmental conditions under which the ship can sail. OL have been applied in two ways:

- identifying the maximum significant wave height associated to the North Atlantic wave scatter table;
- considering two alternative routes and determining the maximum significant wave height if the ship is vulnerable along the route.

The routes have been selected among the commercial routes of an operating shipping company. The corresponding track has been defined using MarineTraffic® Voyage Planner tool. The length of the route segments in each area has been measured on Google Earth®.

The first route, shown in Figure 7.5a, links Livorno (Italy) with Luanda (Angola), crossing areas 25, 26, 36, 58, 68, as defined in Hogben et al., (1986), and its length is about 4850 nautical miles. The second route, shown in Figure 7.5b, links Antwerp (Belgium) with Luanda (Angola), crossing areas 11, 16, 17, 25, 36, 58, 68, and its length is about 5000 nautical miles.

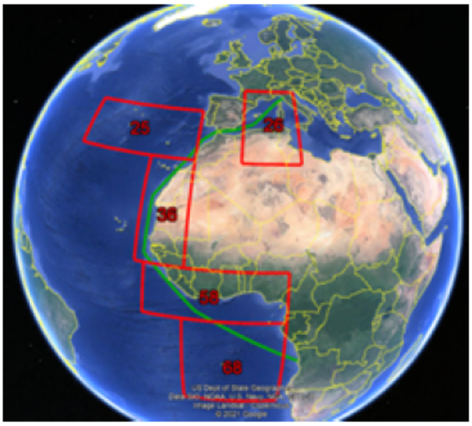

(a) Route 1: Livorno - Luanda

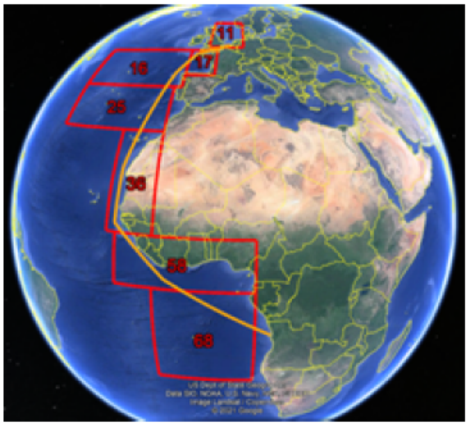

(b) Route 2: Antwerp - Luanda

Figure 7.5: Routes 1 and 2.

Preliminary, OL related to maximum significant wave height have been prepared for the standard wave scatter table. No normalization has been performed in the definition of the limited scatter table. The long-term stability failure index, C, has been plotted in Figure 7.6 as a function of the significant wave height, H_S, used to determine different limiting scatter tables for the calculation of OL. The identified H_S corresponds to the mean value of the corresponding range of heights.

The maximum significant wave height is equal to $4.5m$, representing the range of waves having height in the range from $4.0m$ to $5.0m$. The minimum value of significant wave height, H_{min}, which verifies the condition of less than 20% of total situations to be avoided, equation 2.6, is equal to $4.5m$ for the North Atlantic, therefore, the loading condition can be accepted for unrestricted operations under Operational Limitations related to maximum significant wave height, as explained in Section 2.2.3.

The verification of the criterion along the two considered routes has been performed as second step. Different wave scatter tables have been defined to represent each route according to the following cases:

Case 1: as mean values of the crossed areas by the route. Therefore, the wave occurrence of each sea state, is obtained as mean value of the corresponding ones associated to the crossed areas on the selected route.

Case 2: as weighted sum of the crossed areas by the route. Therefore, for each combination of significant wave height H_s and zero-crossing period T_z, the joint probability of the sea state is calculated as the weighted sum of the corresponding joint probabilities on the selected route, in terms of route length, as follows:

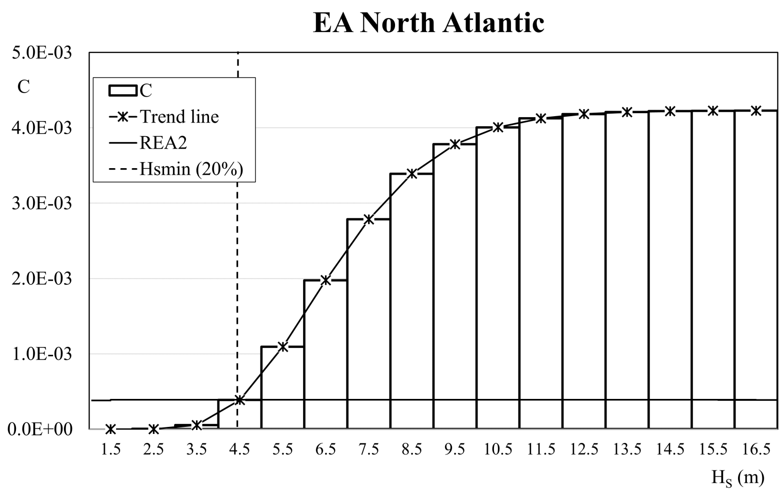

Figure 7.6: Long-term index as a function of the significant wave height for the standard wave scatter table.

$$W_{ij-Weighted} = \frac{1}{L_{Route}} \sum_{k=1}^{n} L_k W_{ij,k} \tag{7.5}$$

being:

- $L_{Route} = \sum_{k=1}^{n} L_k$ the total route length;
- n the number of crossed areas;
- L_k the length of the segment of the route in the k-th area;
- $W_{ij,k}$ the joint probability of the sea state as reported in scatter table of the k-th area;

Figures 7.7a and 7.7b represent the weighted scatter diagrams for Route 1 and Route 2, respectively.

Case 3: considering the single crossed areas and taking the table associated to the most dangerous area as representative of the route.

In order to identify the most dangerous area along each route and take the corresponding results as representative of the entire route, the assessment has been performed for all the areas that the ship crosses on the considered route. Figures 7.8a and 7.8b show that Area 25 and 16 are the most dangerous ones on Route 1 and Route 2, respectively. The curves show a maximum significant wave height equal to 3.5.m for area 25 on Route 1 and for area 16, on Route 2.

In case of Route 2, Area 16 returns results even more conservative that the ones obtained by assuming the standard wave scatter table for the North Atlantic, due to the particular harsh conditions that characterize Area 16.

Route 1

SIGNIFICATIVE WAVE HEIGHT (m)	<4	4-5	5-6	6-7	7-8	8-9	9-10	10-11	11-12	12-13	>13	
	23.5	**112.0**	**224.6**	**256.8**	**197.3**	**111.5**	**48.8**	**17.8**	**5.1**	**1.2**	**1.7**	**1000**
>14	0	0	0	0	0	0	0	0	0	0	0	**0**
13-14	0	0	0	0	0	0	0	0	0	0	0	**0**
12-13	0	0	0	0	0	0	0	0	0	0	0	**0**
11-12	0	0	0	0	0	0	0	0	0	0	0	**0**
10-11	0	0	0	0	0	0	0	0	0	0	0	**0**
9-10	0	0	0	0	0	0.0	0.10	0	0	0	0	**0.1**
8-9	0	0	0	0	0.0	0.10	0.10	0.10	0.10	0	0	**0.4**
7-8	0	0	0.19	0.19	0.29	0.20	0.20	0.20	0.10	0	0	**1.4**
6-7	0	0	0.19	0.38	0.67	0.87	0.50	0.40	0.20	0.10	0	**3.3**
5-6	0	0.19	0.56	1.23	2.05	2.70	2.00	1.32	0.30	0.10	0	**10.4**
4-5	0	0.56	2.39	5.38	7.76	8.16	5.79	2.67	1.02	0.20	0.10	**34.0**
3-4	0.19	2.16	9.81	21.81	28.69	23.45	12.85	5.38	1.87	0.44	0	**106.6**
2-3	0.76	10.71	41.35	73.80	72.24	43.71	18.12	5.80	1.15	0.34	1.65	**269.6**
1-2	4.91	44.45	112.3	123.6	76.11	30.19	9.00	1.96	0.34	0	0	**402.9**
0-1	17.61	53.93	57.79	30.43	9.47	2.16	0.1	0	0	0	0	**171.5**

ZERO CROSSING PERIOD (s)

(a) Route 1: weighted scatter table

Route 2

SIGNIFICATIVE WAVE HEIGHT (m)	<4	4-5	5-6	6-7	7-8	8-9	9-10	10-11	11-12	12-13	>13	
	9.0	**62.3**	**171.6**	**249.1**	**231.9**	**153.8**	**77.3**	**31.1**	**9.9**	**2.6**	**1.7**	**1000**
>14	0	0	0	0	0	0	0	0	0	0	0	**0**
13-14	0	0	0	0	0	0	0	0	0	0	0	**0**
12-13	0	0	0	0	0	0	0	0	0	0	0	**0**
11-12	0	0	0	0	0	0	0	0.09	0	0	0	**0.1**
10-11	0	0	0	0	0	0	0.17	0.09	0.09	0	0	**0.4**
9-10	0	0	0	0.03	0.03	0.17	0.39	0.17	0.09	0	0	**0.9**
8-9	0	0	0	0.03	0.20	0.50	0.56	0.48	0.39	0.09	0	**2.3**
7-8	0	0	0.03	0.14	0.44	0.89	1.07	0.87	0.48	0.09	0	**4.0**
6-7	0	0	0.05	0.28	1.22	2.12	2.15	1.47	0.69	0.21	0	**8.2**
5-6	0	0.03	0.11	1.09	3.50	5.63	4.99	3.15	1.08	0.39	0	**20.0**
4-5	0	0.05	1.24	5.18	10.99	13.85	10.72	5.34	1.99	0.51	0.12	**50.0**
3-4	0	0.61	6.13	20.97	35.11	33.13	19.82	8.50	2.73	0.74	0	**127.7**
2-3	0.22	4.95	30.68	71.17	82.29	55.80	24.92	8.173	1.82	0.53	1.6	**282.2**
1-2	2.10	26.85	89.55	120.2	86.29	38.47	12.11	2.79	0.53	0	0	**378.9**
0-1	6.71	29.81	43.83	30.05	11.79	3.18	0.38	0	0	0	0	**125.8**

ZERO CROSSING PERIOD (s)

(b) Route 2: weighted scatter table

Figure 7.7: Weighted scatter tables of Route 1 and Route 2.

The results obtained by assuming the most dangerous area, the weighted and the mean scatter table are compared in Figures 7.9a for Route 1 and Figure 7.9b for Route 2. Trend lines for the long-term stability failure index show that computations lead to more conservative results going from the weighted tables to the considered most dangerous area for both routes.

The minimum significant wave height H_{min}, which verifies the condition of less than 20% of situations to be avoided equals $3.5m$ for Area 25, on Route 1; it equals to $3.5m$ for the mean and weighted tables and $4.5m$ for area 16, on Route 2.

It can be noticed that the loading condition can be accepted for limited operation on the selected routes, except for the Route 2 when the most dangerous area along the route (Area 16) is selected as the representative area of the route.

The results and the corresponding levels of acceptance are summarized in Table 7.3 for all the considered cases on Route 1 and Route 2.

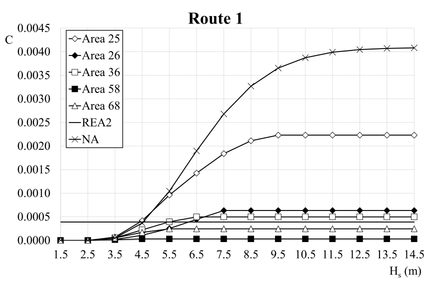

(a) Route 1: Long-term indexes

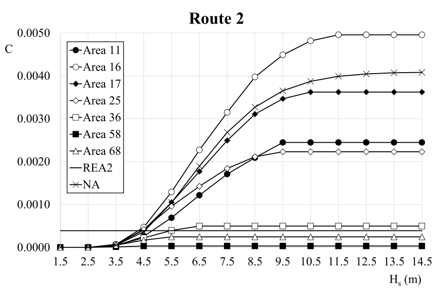

(b) Route 2: Long-term indexes

Figure 7.8: Long term index as a function of the significant wave height for the single areas crossed by Route 1 and Route 2.

Finally, to analyse the effect of roll damping and to emphasize the importance of its proper estimation, Operational Limitations have been again applied

---

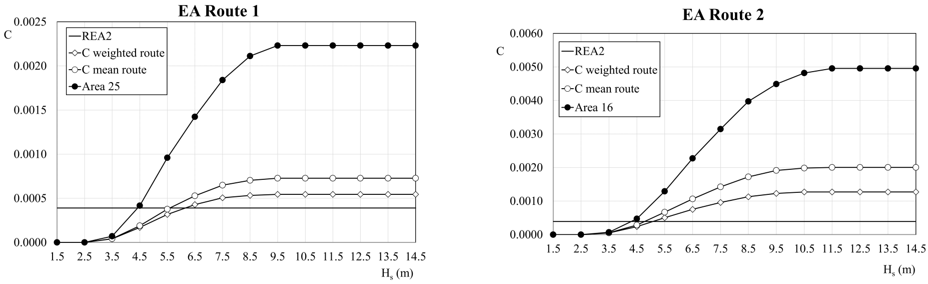

(a) Route 1: Long-term indexes

(b) Route 2: Long-term indexes

Figure 7.9: Long-term index as a function of the significant wave height.

	Route 1		**Route 2**	
Case 1	$H_{s,max} = 5.5m$	Acceptable for limited operation on the route	$H_{s,max} = 4.5m$	Acceptable for limited operation on the route
Case 2	$H_{s,max} = 5.5m$	Acceptable for limited operation on the route	$H_{s,max} = 4.5m$	Acceptable for limited operation on the route
Case 3	Area 25: $H_{s,max} = 3.5m$	Acceptable for limited operation on the route	Area 16: $H_{s,max} = 3.5m$	Not acceptable for limited operation on the route

Table 7.3: Summary of application of Operational Limitations.

to Route 1 by evaluating the roll damping by the Simplified Ikeda's Method with no modifications. The effect of the modified formulation is the identification of the ship vulnerability to the phenomenon in all cases, while the application of the Simplified Ikeda's Method without any modification would identify the loading condition as not vulnerable on Route 1 when considering the mean and weighted scatter tables. The long-term indexes are given in Figure 7.10.

7.3 Simplified Operational Guidance

Simplified Operational Guidance have been developed for the subject ship as an alternative to Operational Limitations, providing indications to the crew on how handle the vessel if certain loading conditions are met, identifying safe and unsafe sailing conditions.

OG for the Excessive acceleration have been introduced in Chapter 3 and the simplified are recalled here. Simplified OG must consider all the combinations of wave heading (from following to head seas) and ship speed (from zero to the service speed), for all the sea states reported in the assumed wave scatter table. Dangerous sailing conditions are the ones for which the long-term stability failure index is:

$$C_{s,i} > 10^{-6}$$

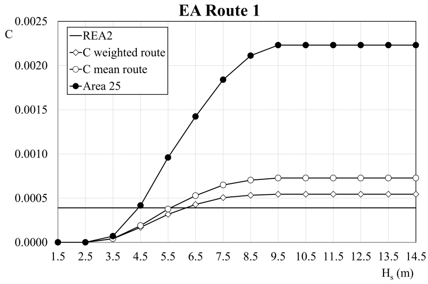

(a) Long-term indexes, Ikeda modified

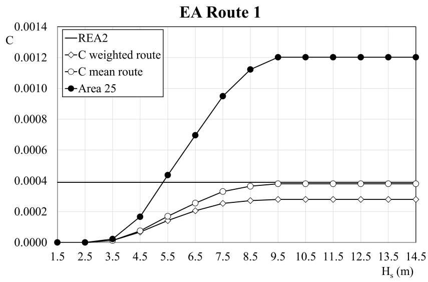

(b) Long-term indexes, Simplified Ikeda

Figure 7.10: Long-term index as a function of the significant wave height on Route 1, by the Simplified Ikeda's Method with and without modification in eddy damping component.

The short-term stability failure index $C_{s,i}$, equation 3.35, is calculated from the spectrum of lateral acceleration.

The second level of assessment was developed by the IMO for the ship at zero speed in beam waves due to the dynamic of the accidents that led to the introduction of the criterion. In this section, OG have been derived based on a generalization of Level 2 procedure to derive the short-term probability indexes $C_{s,i}$ for all combinations of wave heading and ship speed according to the formulation of the Froude-Krylov exciting roll moment presented in Chapter 5. A variance-preserving transformation is introduced to avoid discontinuities in the wave and response spectra in following and quartering waves.

7.3.1 Variance preserving transformation

In Level 2, the assessment is performed in the wave circular frequency since it is thought for the ship at zero speed in beam waves. The ship experiences the motions with the encounter frequency, $\omega_e = \omega - \frac{\omega^2}{g} V_s cos\mu$, when she advances with a constant speed V_s, different from zero, in long-crested waves with a constant direction of propagation μ, different from 90° or 270°. Under these circumstances, the spectral analysis has to be conducted in the encounter frequency domain.

In quartering or following waves the transformation from wave to encounter frequency is multi-valued and a variance-preserving transformation from the encounter to the wave frequency domain can be applied to calculate the spectral moments, Lewis (1989):

$$m_n = \int_0^{+\infty} \left| \omega - \frac{\omega^2}{g} V_s cos\mu \right|^n \left| \hat{\varphi}_a(\omega) \right|^2 S_{zz}(\omega)\, d\omega \tag{7.6}$$

where m_n is the nth-order spectral moment of roll response, $\hat{\varphi}_a$ is the transfer function of roll motion and S_{zz} the wave energy spectrum.

The transformation may be used in two parts of the simplified *OG* development process:

1. in the stochastic linearization where the variance of roll velocity is needed:

$$\sigma_{\dot{\varphi}}^2 = \int_0^{+\infty} \left| \omega - \frac{\omega^2}{g} V_s cos\mu \right|^2 \left| RAO_{\varphi}(\omega) \right|^2 S_{\alpha\alpha,e}(\omega)\, d\omega \tag{7.7}$$

where $S_{\alpha\alpha,e}(\omega)$ is the effective wave slope spectrum, calculated as $S_{\alpha\alpha,e}(\omega) = (r(\omega))^2 S_{\alpha\alpha}(\omega)$, being $r(\omega)$ the effective wave slope function and $S_{\alpha\alpha}(\omega)$ the wave slope spectrum; RAO_{φ} is the response amplitude operator of roll motion. The latter can be expressed in the wave frequency domain as follows, (St. Denis and Pierson (1953)):

$$RAO_{\varphi}(\omega, \mu_e) = \frac{\omega_r^2}{\sqrt{\left[\omega_r^2 - \left(\omega - \frac{\omega^2}{g} V_s cos\mu\right)^2\right]^2 + \left[2\mu_e\left(\omega - \frac{\omega^2}{g} V_s cos\mu\right)\right]^2}} \tag{7.8}$$

2. in the calculation of variance of lateral acceleration spectrum:

$$\sigma_{a_y}^2 = \int_0^{+\infty} (a_y(\omega))^2 S_{zz}(\omega)\, d\omega \tag{7.9}$$

where $a_y(\omega)$ is the transfer function of lateral acceleration computed for the considered sailing condition.

7.3.2 Simplified OG development

Simplified OG are developed according to the proposed generalization of Level 2 procedure. The Bretschneider wave energy spectrum has been assumed to describe the environmental conditions.

The Froude-Krylov roll moment amplitude has been calculated according to equation 5.16 and used in the calculation of the effective wave slope function according to equation 3.21. The short-term stability failure indexes have been obtained via calculation of the standard deviation of lateral accelerations by means of the variance preserving transformation, Section 7.3.1, to properly deal with any heading angle. The factor k_L, calculated according to the formulation provided in the Interim guidelines, equation 3.2, is equal to 1.03 and it has kept constant for all wave headings.

The roll axis is assumed to be located at the midpoint between the centre of gravity and the waterline, as in Level 2. The range of wave frequencies is the same assumed in Level 2 criterion, i.e. from 0.2 to $2.0 rad/s$, corresponding to the range of wavelength from 15 to $1541 m$.

The procedure of the development of OG is summarized in Figure 7.11, which has been implemented in Matlab® programming language.

The results have been presented as polar diagrams and in tabular form. In the polar plots, 0° corresponds to following waves while 180° to head waves. The calculations have been performed considering 15° angular interval around following and head seas and reduced to 5° around beam seas. Ship speeds from zero to the service speed of $14 kn$ have been reported along the radius of the graph with a

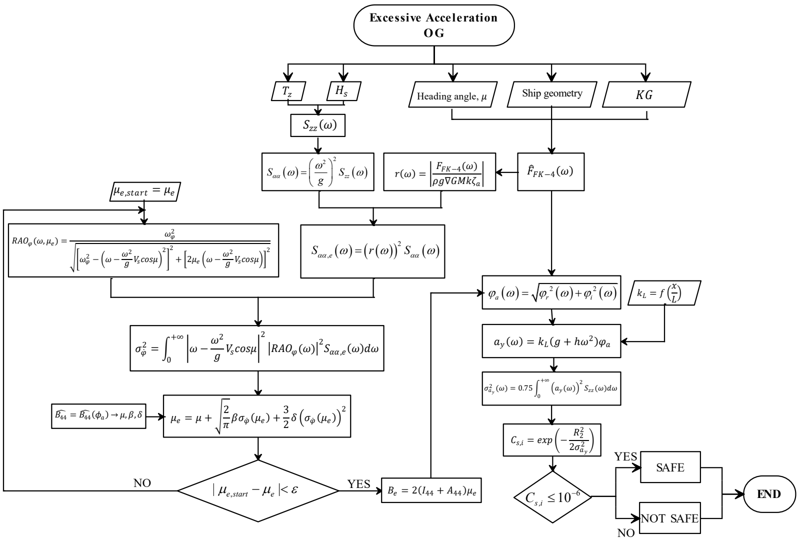

Figure 7.11: Solution algorithm for Operational Guidance application.

step of $2kn$. The standard wave scatter table for the North Atlantic has been assumed to represent the environmental conditions. Safe combinations of speed and heading have been identified for each sea state, defined as combination of significant wave height (H_s from 0.5 to $16.5m$) and mean zero-crossing period (T_z from 3.5 to $18.5m$), for a total of 272 sea states, 197 of which have non-zero probability of occurrence.

The OG for the Excessive acceleration identifies the critical speed in correspondence of which the ship is vulnerable. An example of simplified Operational Guidance which allows a quick identification of safe (green) and unsafe (red) sailing conditions, for the sea state $T_Z = 8.5s$ and $H_S = 5.5m$, is given in Figure 7.12.

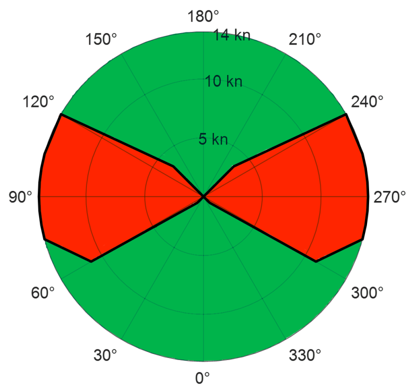

Figure 7.12: Polar plots reporting safe (green) and unsafe (red) sailing conditions, for the sea state $T_Z = 8.5s$, $H_S = 5.5m$.

A black and white representation has been used in Figure 7.13 to analyse the influence of different heading angles and ship speed. Four zero mean zero-crossing periods, 8.5, 9.5, 10.5 and 11.5s, have been considered. Each polar plot represents sea states with the same zero-crossing period and three significant wave heights, 3.5, 5.5 and 7.5m. An expected reduction of the operational domain with the increase of the significant wave height is shown.

As concerns the mean zero-crossing period, the most severe results are for $T_Z = 8.5s$, for given heading and significant wave height. The magnitude of the lateral acceleration reduces for higher periods to which corresponds a higher operability domain.

The transfer functions of lateral accelerations and the corresponding response spectra are shown in Figure 7.14, to investigate the effect of the mean zero-crossing period. The significant wave height 5.5m and the periods 8.5, 9.5, 10.5 and 11.5s have been considered, for the beam seas case. The transfer function, which shows its peak at the natural roll frequency $\omega_r = 0.64 rad/s$, depends on the sea state considered, since the equivalent linear roll damping on which it depends is a function of the sea state as well. The obtained equivalent linear damping coefficients for the significant wave height 5.5m and the periods 8.5, 9.5, 10.5 and 11.5s have been, 0.0219, 0.0211, 0.0202 and 0.0193 $1/s$, respectively, showing a reduction with the zero-crossing period. This affects, the amplitude of the transfer function peak which increases with the zero-crossing period, Figure 7.14. In Figure 7.14, the wave energy spectrum are reported for the considered sea states, showing that the one with the zero-crossing period 8.5s is the one with the highest amount of energy around the peak of the transfer function, leading to the largest response in terms of lateral accelerations.

The minimum speed, in knots, below which the short-term stability failure index is greater than the limit value 10^{-6}, is shown in tabular form for the headings of 90° and 120°, in Tables 7.4 and 7.5, respectively. Cells coloured in green identify safe sailing condition, for which the ship is not vulnerable to the exces-

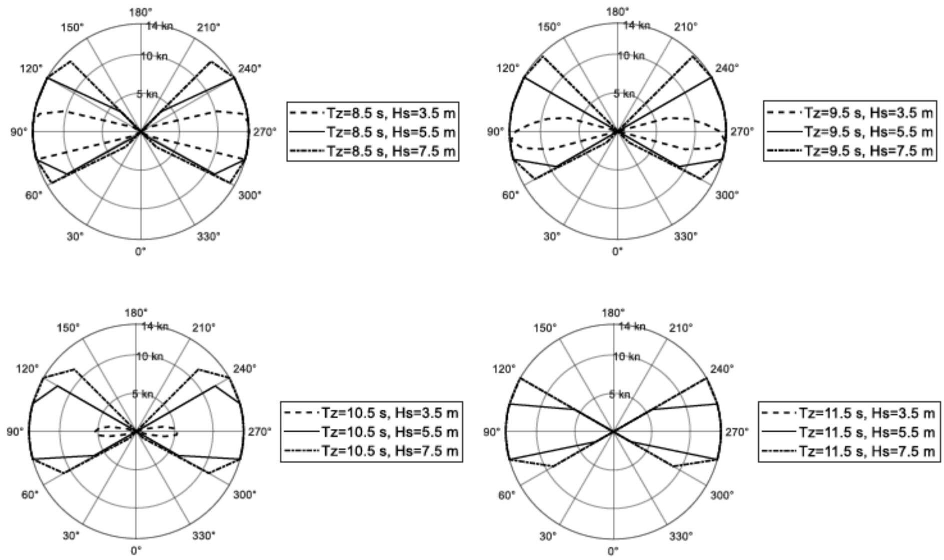

Figure 7.13: Polar plots reporting the minimum ship speed to avoid excessive accelerations, for different sea states.

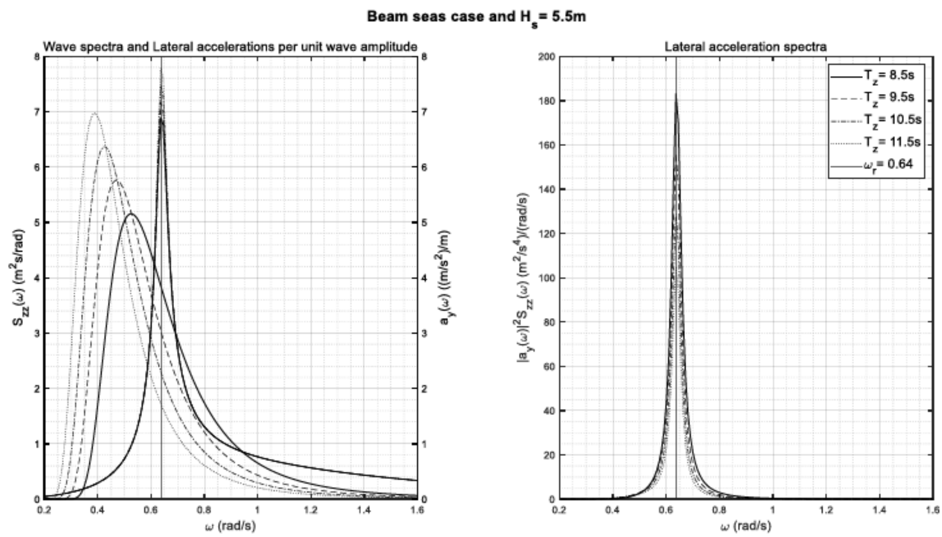

Figure 7.14: Wave spectra, transfer functions of lateral acceleration and lateral acceleration spectra. Beam seas case, significant wave height $5.5m$ and four zero-up crossing period.

sive accelerations at any speed. Cells coloured in red, reporting the ship service speed, identify critical sea states for the given heading, showing that a ship speed to avoid excessive accelerations does not exist. For such sea states a different heading should be chosen to avoid dangerous accelerations. The tables show a reduction in the number of dangerous sea states when moving far from the beam seas condition since transverse waves are the most critical conditions. In the beam seas case, the proposed procedure reduces to the Level 2 with the only difference that roll damping has to account for the lift damping component.

In Table 7.6, the minimum ship speed identified calculating the Froude-Krylov roll moment by the potential theory software HydroStar® is given, for 120° heading. The comparison between the results obtained by the modified IMO's procedure, Table 7.5, and by HydroStar®, Table 7.6, shows a moderate greater conservatism of the modified IMO's procedure. Indeed, even if the modified IMO's procedure underestimates the Froude-Krylov roll moment at higher frequencies, it is slightly overestimated at the ship natural roll frequency, around which most of the energy is concentrated in the considered phenomenon, as shown in Figure 5.4.

Similar table could be derived for any wave heading angle, identifying for each sea state the corresponding critical speed.

Finally, it has been verified that the ratio between the total duration of all situations which should be avoided and the total operational time is lower than 20%. The ratio is calculated as the sum of the products of the probability of encountering each sea state and a speed-heading factor which identifies the combinations of speed and heading to be avoided on the total sailing conditions. The North Atlantic wave scatter diagram has been considered for the verification; the weighted sum, equal to 0.017, does not exceed 0.2 therefore, the loading condition is in compliance with the regulation and OG can be considered acceptable for operation using onboard OG.

Excessive Acceleration Simplified Operational Guidance: Modified IMO's procedure (μ=90°)

Minimum speed		Tz (s)															
		3.5	4.5	5.5	6.5	7.5	8.5	9.5	10.5	11.5	12.5	13.5	14.5	15.5	16.5	17.5	18.5
	0.5	0.0	0.0	0.0	0.0	0.0	0.0	0.0	0.0	0.0	0.0	0.0	0.0	0.0	0.0	0.0	0.0
	1.5	0.0	0.0	0.0	0.0	0.0	0.0	0.0	0.0	0.0	0.0	0.0	0.0	0.0	0.0	0.0	0.0
	2.5	0.0	0.0	0.0	1.2	4.3	1.4	0.0	0.0	0.0	0.0	0.0	0.0	0.0	0.0	0.0	0.0
	3.5	0.0	0.0	0.0	14.0	14.0	14.0	13.2	5.4	0.0	0.0	0.0	0.0	0.0	0.0	0.0	0.0
	4.5	0.0	0.0	13.5	14.0	14.0	14.0	14.0	14.0	11.6	3.9	0.0	0.0	0.0	0.0	0.0	0.0
	5.5	0.0	0.0	14.0	14.0	14.0	14.0	14.0	14.0	14.0	14.0	7.3	0.9	0.0	0.0	0.0	0.0
	6.5	0.0	0.0	14.0	14.0	14.0	14.0	14.0	14.0	14.0	14.0	14.0	9.5	2.8	0.0	0.0	0.0
	7.5	0.0	0.0	14.0	14.0	14.0	14.0	14.0	14.0	14.0	14.0	14.0	14.0	10.7	4.1	0.0	0.0
Hs (m)	8.5	0.0	0.0	14.0	14.0	14.0	14.0	14.0	14.0	14.0	14.0	14.0	14.0	14.0	11.1	4.8	0.0
	9.5	0.0	0.0	14.0	14.0	14.0	14.0	14.0	14.0	14.0	14.0	14.0	14.0	14.0	14.0	11.1	5.0
	10.5	0.0	14.0	14.0	14.0	14.0	14.0	14.0	14.0	14.0	14.0	14.0	14.0	14.0	14.0	14.0	10.7
	11.5	0.0	14.0	14.0	14.0	14.0	14.0	14.0	14.0	14.0	14.0	14.0	14.0	14.0	14.0	14.0	14.0
	12.5	0.0	14.0	14.0	14.0	14.0	14.0	14.0	14.0	14.0	14.0	14.0	14.0	14.0	14.0	14.0	14.0
	13.5	0.0	14.0	14.0	14.0	14.0	14.0	14.0	14.0	14.0	14.0	14.0	14.0	14.0	14.0	14.0	14.0
	14.5	0.0	14.0	14.0	14.0	14.0	14.0	14.0	14.0	14.0	14.0	14.0	14.0	14.0	14.0	14.0	14.0
	15.5	0.0	14.0	14.0	14.0	14.0	14.0	14.0	14.0	14.0	14.0	14.0	14.0	14.0	14.0	14.0	14.0
	16.5	0.0	14.0	14.0	14.0	14.0	14.0	14.0	14.0	14.0	14.0	14.0	14.0	14.0	14.0	14.0	14.0

Table 7.4: Minimum ship speed - Heading 90° - Modified IMO's procedure.

Excessive Acceleration Simplified Operational Guidance: Modified IMO's procedure (μ=120°)

Minimum speed		Tz (s)															
		3.5	4.5	5.5	6.5	7.5	8.5	9.5	10.5	11.5	12.5	13.5	14.5	15.5	16.5	17.5	18.5
	0.5	0.0	0.0	0.0	0.0	0.0	0.0	0.0	0.0	0.0	0.0	0.0	0.0	0.0	0.0	0.0	0.0
	1.5	0.0	0.0	0.0	0.0	0.0	0.0	0.0	0.0	0.0	0.0	0.0	0.0	0.0	0.0	0.0	0.0
	2.5	0.0	0.0	0.0	0.0	0.0	0.0	0.0	0.0	0.0	0.0	0.0	0.0	0.0	0.0	0.0	0.0
	3.5	0.0	0.0	0.0	0.2	2.4	1.1	0.0	0.0	0.0	0.0	0.0	0.0	0.0	0.0	0.0	0.0
	4.5	0.0	0.0	0.0	4.1	8.1	9.2	7.1	2.0	0.0	0.0	0.0	0.0	0.0	0.0	0.0	0.0
	5.5	0.0	0.0	0.7	7.1	12.4	14.0	14.0	11.9	5.8	0.0	0.0	0.0	0.0	0.0	0.0	0.0
	6.5	0.0	0.0	2.4	9.7	14.0	14.0	14.0	14.0	14.0	8.1	0.0	0.0	0.0	0.0	0.0	0.0
	7.5	0.0	0.0	3.7	12.0	14.0	14.0	14.0	14.0	14.0	14.0	9.5	0.0	0.0	0.0	0.0	0.0
Hs (m)	8.5	0.0	0.0	4.6	13.8	14.0	14.0	14.0	14.0	14.0	14.0	14.0	9.8	0.0	0.0	0.0	0.0
	9.5	0.0	0.0	5.6	14.0	14.0	14.0	14.0	14.0	14.0	14.0	14.0	14.0	9.3	0.0	0.0	0.0
	10.5	0.0	0.0	6.8	14.0	14.0	14.0	14.0	14.0	14.0	14.0	14.0	14.0	14.0	8.1	0.0	0.0
	11.5	0.0	0.0	7.7	14.0	14.0	14.0	14.0	14.0	14.0	14.0	14.0	14.0	14.0	14.0	6.7	0.0
	12.5	0.0	0.0	8.3	14.0	14.0	14.0	14.0	14.0	14.0	14.0	14.0	14.0	14.0	14.0	13.8	4.4
	13.5	0.0	0.0	9.4	14.0	14.0	14.0	14.0	14.0	14.0	14.0	14.0	14.0	14.0	14.0	14.0	11.3
	14.5	0.0	0.0	9.8	14.0	14.0	14.0	14.0	14.0	14.0	14.0	14.0	14.0	14.0	14.0	14.0	14.0
	15.5	0.0	0.0	10.8	14.0	14.0	14.0	14.0	14.0	14.0	14.0	14.0	14.0	14.0	14.0	14.0	14.0
	16.5	0.0	0.0	11.2	14.0	14.0	14.0	14.0	14.0	14.0	14.0	14.0	14.0	14.0	14.0	14.0	14.0

Table 7.5: Minimum ship speed - Heading 120° - Modified IMO's procedure.

Excessive Acceleration Simplified Operational Guidance: F-K roll moment calculated by HydroStar® software (μ=120°)

Minimum speed		Tz (s)															
		3.5	4.5	5.5	6.5	7.5	8.5	9.5	10.5	11.5	12.5	13.5	14.5	15.5	16.5	17.5	18.5
	0.5	0.0	0.0	0.0	0.0	0.0	0.0	0.0	0.0	0.0	0.0	0.0	0.0	0.0	0.0	0.0	0.0
	1.5	0.0	0.0	0.0	0.0	0.0	0.0	0.0	0.0	0.0	0.0	0.0	0.0	0.0	0.0	0.0	0.0
	2.5	0.0	0.0	0.0	0.0	0.0	0.0	0.0	0.0	0.0	0.0	0.0	0.0	0.0	0.0	0.0	0.0
	3.5	0.0	0.0	0.0	0.0	2.0	0.5	0.0	0.0	0.0	0.0	0.0	0.0	0.0	0.0	0.0	0.0
	4.5	0.0	0.0	0.0	4.0	7.5	8.2	6.2	0.8	0.0	0.0	0.0	0.0	0.0	0.0	0.0	0.0
	5.5	0.0	0.0	0.5	6.9	11.8	14.0	13.8	10.3	4.1	0.0	0.0	0.0	0.0	0.0	0.0	0.0
	6.5	0.0	0.0	2.3	9.5	14.0	14.0	14.0	14.0	13.2	6.4	0.0	0.0	0.0	0.0	0.0	0.0
	7.5	0.0	0.0	3.5	11.3	14.0	14.0	14.0	14.0	14.0	14.0	7.3	0.0	0.0	0.0	0.0	0.0
Hs (m)	8.5	0.0	0.0	4.2	13.4	14.0	14.0	14.0	14.0	14.0	14.0	14.0	7.5	0.0	0.0	0.0	0.0
	9.5	0.0	0.0	5.5	14.0	14.0	14.0	14.0	14.0	14.0	14.0	14.0	14.0	6.9	0.0	0.0	0.0
	10.5	0.0	0.0	6.7	14.0	14.0	14.0	14.0	14.0	14.0	14.0	14.0	14.0	14.0	6.0	0.0	0.0
	11.5	0.0	0.0	7.3	14.0	14.0	14.0	14.0	14.0	14.0	14.0	14.0	14.0	14.0	12.6	4.1	0.0
	12.5	0.0	0.0	8.3	14.0	14.0	14.0	14.0	14.0	14.0	14.0	14.0	14.0	14.0	14.0	10.7	3.0
	13.5	0.0	0.0	9.2	14.0	14.0	14.0	14.0	14.0	14.0	14.0	14.0	14.0	14.0	14.0	14.0	8.5
	14.5	0.0	0.0	9.7	14.0	14.0	14.0	14.0	14.0	14.0	14.0	14.0	14.0	14.0	14.0	14.0	14.0
	15.5	0.0	0.0	10.6	14.0	14.0	14.0	14.0	14.0	14.0	14.0	14.0	14.0	14.0	14.0	14.0	14.0
	16.5	0.0	0.0	11.1	14.0	14.0	14.0	14.0	14.0	14.0	14.0	14.0	14.0	14.0	14.0	14.0	14.0

Table 7.6: Minimum ship speed - Heading 120° - Froude-Krylov roll moment calculated by HydroStar®.

7.4 Discussion and conclusions

In this Chapter, a bulk carrier has been considered as test case for the application of vulnerability criteria, Operational Limitations and simplified Operational Guidance.

It has been preliminary verified that the ship does not satisfy Level 1 and Level 2 of the criterion, in the considered loading condition. Initially, OL related to maximum significant wave height have been applied considering the standard wave scatter table for the North Atlantic showing that the considered loading condition may be accepted for unrestricted operation with specific limitations on the maximum significant wave height.

Two commercial routes have been considered to investigate how the vulnerability of the ship changes with the environmental conditions. Results show that the most dangerous crossed area, taken as representative of the route, may lead to results even more conservative than Level 2. This can be explained noting that the sea states for which the ship is potentially vulnerable may have higher probabilities of occurrence compared with the standard scatter table. This outcome is strictly related to the specific route and sometimes leads to too conservative results which give no significant improvement in ship operability, in terms of maximum significant wave height. Indeed, the sea states having period around the ship natural roll period can have high or low probability of occurrence affecting the long-term stability failure index, leading to more conservative results in the first case or less conservative in the second one.

An improvement in operability is obtained by weighting the tables associated to the crossed areas. This technique requires the knowledge of the length of each segment covered by the ship on crossed areas on the considered route. Results related to combinations of scatter tables are more conservative when the mean scatter table is used, with respect to the weighted one. These findings are ship-specific and cannot be generalized since the long-term stability failure index is related to the weight of each sea state. The probability of sea states in which the ship is more exposed to the phenomenon could be magnified or not by the technique used in deriving the scatter table.

OL satisfy the condition of less than 20% of cases to avoid, in all the examined cases, except for the most dangerous area on Route 2. For the cases for which condition is respected the loading conditions can be accepted for limited operations on the route.

It is worth to underline that the maximum significant wave height, obtained applying OL, cannot be considered as an intrinsic operability limit of the ship. The different obtained values of the significant wave height can be explained recalling the probabilistic character of the SGISC that assumes a certain level of risk for the stability failure. Potentially dangerous sea states have different probabilities of occurrence if different environmental conditions are considered, affecting the long-term probability associated to the stability failure.

Definitely, the application of OL allows the identification of the environmental conditions for which a sufficient level of safety is attained. However, it would be important to provide univocal guidelines on how to derive the scatter tables associated to routes crossing more than one area in order to avoid a non-uniform application of OL and different limitations in terms of maximum significant wave height.

In the performed case study, particular attention has been paid to the evaluation of roll damping since it was demonstrated in Rudaković and Bačkalov (2017) that the Simplified Ikeda's Method does not properly evaluate the eddy damping component for ships having large block coefficients as the subject ship has. For the bulk carrier the modified formulation returns a lower roll damping due to the particular value of the block coefficient, leading to a larger value of the long-term stability failure index, compared to the results obtained applying the Simplified Ikeda's Method without any modification. In particular, it has been shown that the Operational Limitations developed on Route 1, referring to the mean and weighted tables, identify the vulnerability of the ship for the full table if the modified formulation of the damping is adopted while no vulnerability is identified when the Simplified Ikeda's Method is adopted without any modification. This confirms the necessity of proper roll damping estimation in the assessment.

A procedure for the development of simplified OG has been presented. The procedure has been obtained as generalization, to any wave heading angle and ship speed, of the Level 2 procedure for the Excessive acceleration criterion, that was developed by the IMO working group for the ship at zero speed in beam waves. In particular, the formulation for the calculation of the Froude-Krylov exciting roll moment for any heading angle developed in Chapter 5 has been used to describe the wave excitation.

Polar diagrams have been provided to identify safe combinations of ship speed and heading for relevant sea states. A tabular representation is proposed for given headings to identify the minimum ship speed to avoid large lateral accelerations, for the sea states reported in standard wave scatter table. The results showed that, with the proposed method, the application of OG allows an increase of the operability domain, comparable to the one obtained by a commercial software.

It should be verified that the identified safe sailing condition are actually feasible for the ship, since in heavy weather an increase in ship speed or a change in heading could be not practical due to speed loss in waves, reduced steering capabilities or occurrence of other dangerous phenomena.

Operability could be further improved applying deterministic or probabilistic OG, accounting for an appropriate number degrees of freedom, a more precise modelling of exciting forces and moments and non-linearities.

Chapter 8

Case study 2 - UDC Fishing vessel

A fishing vessel is considered as second case study for the Excessive acceleration criterion and for the application of the on-board system developed in Chapter 6.

The vessel has been selected due to the potential vulnerability of this ship typology with respect to dynamic phenomena in waves, caused by the peculiar hull forms, size, loading conditions and type of operations (Mata-Álvarez-Santullano and Souto-Iglesias (2014)). The recent accident of the 50-meters long Galician vessel Villa de Pitanxo can be mentioned. The vessel sunk in February 2022, while sailing in heavy seas and wind off the Canadian east coast, with the survival of 3 crew members on a total of 24.

Stability related accidents, although not the most common ones, are the ones which cause the largest number of victims in the fishing sector, Krata (2008). Many operations on fishing vessels are carried out at very low or even zero speed, often in beam waves exposing the vessel to synchronous rolling and eventually large accelerations.

Even if the SGISC are not intended to be applied to fishing vessels, extensive research has been conducted on them, due to their vulnerability in waves. At IMO level, the 34.5-meters long fishing vessel studied in Spyrou (1996), is reported in the Explanatory Notes, IMO SDC 8/WP.4/Add.2 (2022), as an example of application of Level 2 of Surf-riding/broaching. Fishing vessels were tested against Parametric roll, Pure loss of stability and Surf-riding/broaching criteria in IMO SLF 55/INF.15 (2012), IMO SDC 1/INF.8 (2013) and IMO SDC 2/INF.10 (2014). The dynamic behaviour of fishing vessels in waves was studied by Mata-Álvarez-Santullano and Souto-Iglesias (2014) that conducted an analysis on a set of five fishing vessels built between 1999 and 2001 which sank between 2004 and 2007 which were compared with the ones they replaced. The analysis focused on intact stability criteria currently into force at the time of their construction (IMO Res. A.749(18)) and in terms of operability, assumed to be an indicator of ship safety. It was concluded that operability calculations based on linear theory cannot be enough to assess ship safety and it was emphasized the importance of the training of the crew with respect to stability. Míguez González et al. (2015) examined seven fishing vessels of various size against the vulnerability criteria for Parametric roll, Pure loss of stability and Dead ship condition, showing that the criteria are a valuable tool to evaluate the overall safety level of the ship. Matsuda et al. (2017) conducted capsizing model experiments in following and quartering seas for a large sample of fishing vessels, showing their high vulnerability to dynamic phenomena in waves. A Polish fishing vessel, capsized in the North Sea due to Surf-riding/broaching, was taken as test case in Szozda and Krata (2022), to check if she would be recognized as vulnerable to Surf-riding by the application of the SGISC, confirming that both Level 1 and Level 2 were able to recognize the vulnerability of the vessel.

Fishing vessels can suffer lateral accelerations in beam or nearly beam seas, Mata-Álvarez-Santullano and Souto-Iglesias (2014). Yu et al. (2022) examined a fishing vessel with respect to the Level 1 and Level 2 of Excessive acceleration analysing the vulnerability of the vessel with and without a suspended load. DSA was conducted as well although the vessel was found not vulnerable to Level 2. Experimental and numerical investigations were performed demonstrating that the presence of the suspended load determined an increase of acceleration.

8.1 Galician mid-sized stern trawler

A mid-sized stern trawler typical of the fleet of Galicia (Spain) has been considered for application and testing of the proposed system. The vessel was a subject of extensive research in recent years which identified the potential vulnerability of the vessel to dangerous phenomena in waves, Míguez González and Bulian (2018), Santiago Caamaño et al. (2019).

The vessel main characteristics are reported in Table 8.1 while the body plan is shown in Figure 8.1, a 3D view is given in Figure 8.1 . The wheelhouse has been considered as calculation point for lateral accelerations. Six different loading conditions were examined in Santiago Caamaño et al. (2019), used here as main reference for input data. The loading condition *"Departure from the fishing ground with full catch and fishing gear, 35% of fuel oil and stores and no ice"* has been chosen because is the most susceptible to lateral accelerations, having the highest initial transverse stability. Hydrostatic properties have been calculated by MAXSURF®. The righting arm curve in calm water for considered loading condition is given in Figure 8.3.

The verification of the vulnerability of the vessel to the Excessive acceleration criterion has been conducted as preliminary calculation. The metacentric height and the height of the location above the waterline exceed the 8% and 70% of the ship breadth prescribing the verification of the criterion for the considered loading condition and location, as explained in Chapter 3. Once the vessel vulnerability has been identified, Operational Limitations related to area and maximum significant wave height have been applied.

Main characteristics	**Units**	
Length overall, L_{OA}	*(m)*	34.5
Length between perpendiculars, L_{BP}	*(m)*	29.0
Breadth, B	*(m)*	8.00
Draught, d	*(m)*	3.48
Displacement, Δ	*(t)*	489
Trim, θ	$^\circ$	0
Longitudinal location of centre of gravity, LCG	*(m)*	14.015
Height of the centre of gravity, KG	*(m)*	3.43
Metacentric height, GM	*(m)*	0.659
Natural roll frequency, ω_r	*(rad/s)*	0.804
Natural roll period, T_r	*(s)*	7.81
Longitudinal distance of the bridge deck from AP, x_{AP}	*(m)*	23.5
Height of the bridge deck from BL, H_{BL}	*(m)*	10.20

Table 8.1: Fishing vessel main parameters.

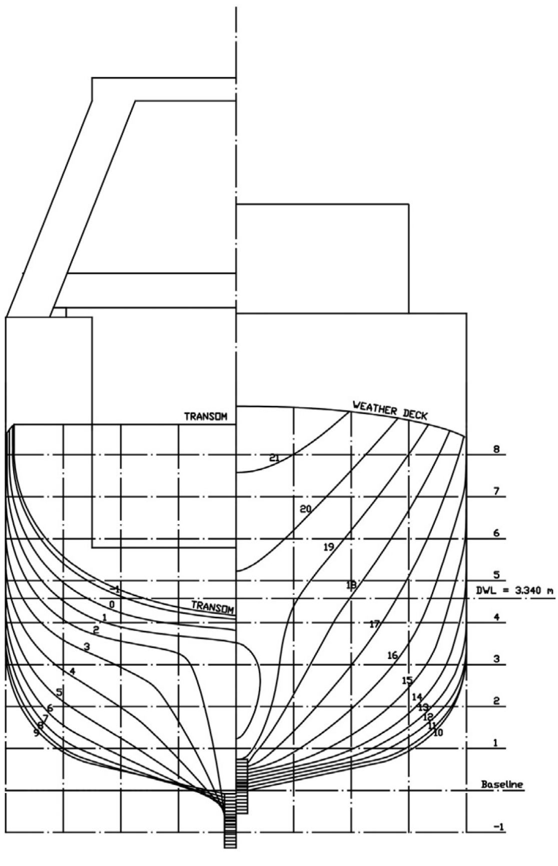

Figure 8.1: Fishing vessel body plan.

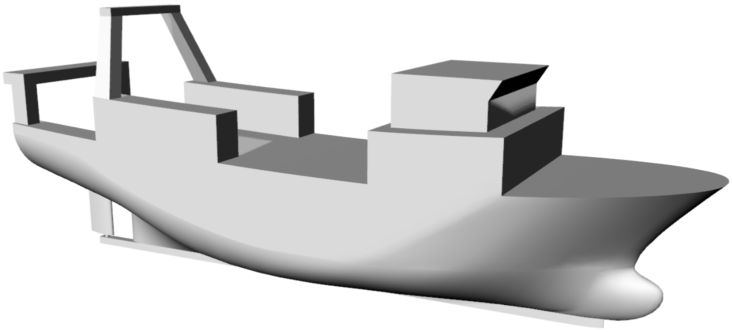

Figure 8.2: Fishing vessel 3D view.

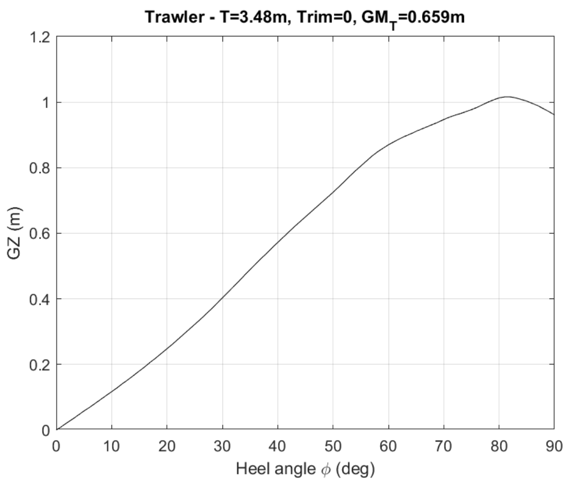

Figure 8.3: Righting arm curve in calm water.

8.1.1 Vulnerability criteria

For the loading condition and location under analysis, Level 1, given by equation 3.1, is not satisfied since the computed acceleration is higher than the limit value:

$$\varphi k_L \left(g + 4\pi^2 \frac{h}{T_r^2} \right) = 10.7 m/s^2 > R_{EA1} = 4.64 m/s^2$$

where:

$$\varphi = 0.68\ rad$$

$$k_L = 1.11$$

and h is the height of the considered location above the roll axis, assumed to be located at the midpoint between the centre of gravity and the waterline:

$$h = H_{BL} - 0.5(d + KG) = 6.745 m$$

Level 2 confirmed the vulnerability of the vessel, since the long-term stability failure index, equation 3.14, is higher than the limit value:

$$C = 8.24 \cdot 10^{-4} > R_{EA2} = 3.9 \cdot 10^{-4}$$

The standard deviation of lateral acceleration, obtained by the application of Level 2, is reported in Table 8.2 as a fraction of the gravity acceleration, for each sea state in the standard wave scatter table for the North Atlantic. A pale red is used to identify the sea states for which the standard deviation is higher than $0.1g$, typically used as limit value for operability calculations concerning lateral acceleration at bridge (Lewis (1989), Faltinsen (1990)), showing a higher vulnerability in sea states having mean zero-crossing close to the natural roll period.

Excessive Acceleration Level 2: standard deviation of lateral acceleration σ_{LAi} as a fraction of the gravity acceleration g																	
		Tz (s)															
		3.5	4.5	5.5	6.5	7.5	8.5	9.5	10.5	11.5	12.5	13.5	14.5	15.5	16.5	17.5	18.5
Hs (m)	0.5	0.02	0.05	0.07	0.07	0.06	0.05	0.05	0.04	0.04	0.03	0.03	0.02	0.02	0.02	0.02	0.02
	1.5	0.05	0.12	0.15	0.15	0.13	0.12	0.11	0.09	0.08	0.07	0.07	0.06	0.05	0.05	0.04	0.04
	2.5	0.08	0.17	0.21	0.21	0.19	0.17	0.15	0.13	0.12	0.11	0.10	0.09	0.08	0.07	0.07	0.06
	3.5	0.10	0.22	0.27	0.26	0.24	0.22	0.19	0.17	0.15	0.14	0.12	0.11	0.10	0.09	0.08	0.08
	4.5	0.13	0.26	0.32	0.31	0.29	0.26	0.23	0.20	0.18	0.16	0.15	0.13	0.12	0.11	0.10	0.09
	5.5	0.16	0.30	0.36	0.36	0.33	0.29	0.26	0.23	0.21	0.19	0.17	0.15	0.14	0.13	0.12	0.11
	6.5	0.18	0.34	0.40	0.40	0.37	0.33	0.29	0.26	0.23	0.21	0.19	0.17	0.16	0.15	0.13	0.12
	7.5	0.21	0.38	0.44	0.44	0.40	0.36	0.32	0.29	0.26	0.23	0.21	0.19	0.17	0.16	0.15	0.14
	8.5	0.24	0.41	0.48	0.47	0.44	0.39	0.35	0.31	0.28	0.25	0.23	0.21	0.19	0.18	0.16	0.15
	9.5	0.26	0.45	0.52	0.51	0.47	0.42	0.38	0.34	0.30	0.27	0.25	0.23	0.21	0.19	0.18	0.16
	10.5	0.29	0.48	0.55	0.54	0.50	0.45	0.40	0.36	0.33	0.29	0.27	0.24	0.22	0.20	0.19	0.17
	11.5	0.32	0.51	0.58	0.57	0.53	0.48	0.43	0.38	0.35	0.31	0.28	0.26	0.24	0.22	0.20	0.19
	12.5	0.34	0.54	0.62	0.60	0.56	0.51	0.45	0.41	0.37	0.33	0.30	0.27	0.25	0.23	0.21	0.20
	13.5	0.37	0.57	0.65	0.63	0.59	0.53	0.48	0.43	0.39	0.35	0.32	0.29	0.26	0.24	0.22	0.21
	14.5	0.39	0.60	0.68	0.66	0.61	0.56	0.50	0.45	0.40	0.37	0.33	0.30	0.28	0.26	0.24	0.22
	15.5	0.42	0.63	0.71	0.69	0.64	0.58	0.52	0.47	0.42	0.38	0.35	0.32	0.29	0.27	0.25	0.23
	16.5	0.44	0.66	0.73	0.72	0.67	0.61	0.55	0.49	0.44	0.40	0.36	0.33	0.30	0.28	0.26	0.24

Table 8.2: Standard deviation of lateral acceleration as a fraction of the gravity acceleration.

Table 8.3 reports the short-term stability failure indexes, which represent the probability that lateral acceleration will exceed the value of $9.81 m/s^2$, for the sea states in the standard wave scatter table. The value 10^{-6} has been chosen to distinguish between potentially safe and unsafe sea states, coloured in green and orange, respectively. The chosen values is used in the Interim guidelines on

Excessive Acceleration Level 2: short-term stability failure indexes $C_{s,i}$																	
		Tz (s)															
		3.5	4.5	5.5	6.5	7.5	8.5	9.5	10.5	11.5	12.5	13.5	14.5	15.5	16.5	17.5	18.5
Hs (m)	0.5	0.0E+00	8.7E-81	1.3E-47	4.6E-49	3.7E-60	5.0E-78	1.4E-102	1.8E-134	1.2E-174	2.8E-224	1.2E-284	0.0E+00	0.0E+00	0.0E+00	0.0E+00	0.0E+00
	1.5	7.9E-101	5.8E-16	2.4E-10	1.2E-10	1.0E-12	5.6E-16	2.2E-20	5.4E-26	6.7E-33	3.1E-41	3.7E-51	7.9E-63	2.0E-76	4.1E-92	4.0E-110	1.2E-130
	2.5	4.6E-39	5.8E-08	1.8E-05	1.2E-05	1.3E-06	3.8E-08	3.3E-10	8.3E-13	5.4E-16	8.4E-20	2.6E-24	1.5E-29	1.2E-35	1.3E-42	1.6E-50	1.6E-59
	3.5	4.4E-21	3.5E-05	9.6E-04	7.7E-04	1.9E-04	2.2E-05	1.2E-06	3.1E-08	3.6E-10	1.8E-12	3.5E-15	2.5E-18	5.8E-22	4.2E-26	8.4E-31	4.3E-36
	4.5	2.1E-13	7.8E-04	7.0E-03	5.9E-03	2.2E-03	4.9E-04	6.6E-05	5.2E-06	2.4E-07	6.1E-09	8.3E-11	5.7E-13	1.9E-15	2.8E-18	1.7E-21	4.4E-25
	5.5	2.0E-09	4.6E-03	2.2E-02	1.9E-02	9.4E-03	3.0E-03	6.6E-04	1.0E-04	1.0E-05	6.5E-07	2.6E-08	6.5E-10	9.3E-12	7.4E-14	3.2E-16	7.2E-19
	6.5	4.5E-07	1.4E-02	4.7E-02	4.2E-02	2.4E-02	9.7E-03	2.9E-03	6.6E-04	1.1E-04	1.3E-05	1.0E-06	5.6E-08	2.0E-09	4.7E-11	6.8E-13	5.9E-15
	7.5	1.4E-05	3.1E-02	7.9E-02	7.2E-02	4.5E-02	2.2E-02	8.2E-03	2.4E-03	5.6E-04	9.7E-05	1.3E-05	1.2E-06	8.1E-08	3.9E-09	1.2E-10	2.7E-12
	8.5	1.5E-04	5.5E-02	1.2E-01	1.1E-01	7.2E-02	3.9E-02	1.7E-02	6.2E-03	1.8E-03	4.2E-04	7.7E-05	1.1E-05	1.1E-06	9.1E-08	5.2E-09	2.2E-10
	9.5	7.7E-04	8.3E-02	1.5E-01	1.4E-01	1.0E-01	6.1E-02	3.0E-02	1.3E-02	4.4E-03	1.3E-03	3.0E-04	5.6E-05	8.3E-06	9.6E-07	8.5E-08	5.7E-09
	10.5	2.6E-03	1.2E-01	1.9E-01	1.8E-01	1.4E-01	8.6E-02	4.7E-02	2.2E-02	8.9E-03	3.0E-03	8.6E-04	2.0E-04	3.9E-05	6.0E-06	7.4E-07	7.1E-08
	11.5	6.6E-03	1.5E-01	2.3E-01	2.2E-01	1.7E-01	1.1E-01	6.7E-02	3.4E-02	1.5E-02	6.0E-03	2.0E-03	5.5E-04	1.3E-04	2.5E-05	4.1E-06	5.2E-07
	12.5	1.4E-02	1.8E-01	2.7E-01	2.5E-01	2.0E-01	1.4E-01	8.8E-02	4.9E-02	2.4E-02	1.0E-02	3.9E-03	1.3E-03	3.5E-04	8.2E-05	1.6E-05	2.6E-06
	13.5	2.4E-02	2.2E-01	3.0E-01	2.9E-01	2.3E-01	1.7E-01	1.1E-01	6.6E-02	3.5E-02	1.6E-02	6.8E-03	2.5E-03	7.8E-04	2.1E-04	5.0E-05	9.9E-06
	14.5	3.8E-02	2.5E-01	3.4E-01	3.2E-01	2.7E-01	2.0E-01	1.4E-01	8.4E-02	4.7E-02	2.4E-02	1.1E-02	4.3E-03	1.5E-03	4.8E-04	1.3E-04	3.0E-05
	15.5	5.5E-02	2.8E-01	3.7E-01	3.5E-01	3.0E-01	2.3E-01	1.6E-01	1.0E-01	6.2E-02	3.3E-02	1.6E-02	7.0E-03	2.7E-03	9.4E-04	2.9E-04	7.6E-05
	16.5	7.6E-02	3.2E-01	4.0E-01	3.8E-01	3.3E-01	2.6E-01	1.9E-01	1.2E-01	7.7E-02	4.4E-02	2.3E-02	1.1E-02	4.5E-03	1.7E-03	5.7E-04	1.7E-04

Table 8.3: Short-term stability failure indexes.

SGISC to identify the sea states for which simplified Operational Guidance can be developed, equation 3.46.

The long-term index C, equation 3.14, has been calculated using damping coefficients by roll decay tests conducted at the University of A Coruña (Spain) towing tank, explained in detail in Subsection 8.3.2. The coefficients have been calculated experimentally since the ratio between ship breadth and mean draught ratio B/d and the midship section coefficient C_m are outside the range of applicability of the Simplified Ikeda's Method. Table 8.4 reports the damping coefficients obtained from the analysis of the roll decay tests, for which a quadratic fitting of the decay curve was adopted. In order to get an insight into the effect of the damping coefficients on the estimation of the long-term stability failure index, the calculation has been repeated again by using the Simplified Ikeda's method, obtaining a long-term index C equal to $2.26 \cdot 10^{-2}$.

The effect of roll damping is shown in Figure 8.4 through the lateral acceleration transfer function, for the sea state having significant wave height $H_s = 1.5m$ and mean zero-crossing period $T_z = 5.5s$. For the considered sea state the equivalent linear damping coefficient μ_e is equal to 0.0108 $1/s$ if calculated using the damping coefficients obtained by the Simplified Ikeda's Method and 0.0259 $1/s$ if calculated by the coefficients used by roll decay tests. An overestimation of the transfer function around the natural roll frequency $0.804 rad/s$ can be noticed in the case of the coefficients calculated by means of the Simplified Ikeda's Method.

μ	$(1/s)$	0.0025
β	$(1/rad)$	0.344
δ	(s/rad^2)	0

Table 8.4: Roll damping coefficients.

8.1.2 Operational Limitations

Once the ship was found vulnerable to Level 2, Operational Limitations have been developed using environmental conditions alternative to the North Atlantic. The subject ship is intended to operate off the North-West Spain coast, which fall into Area 16 and Area 17 of the Global Wave Statistics (Hogben et al. (1986)).

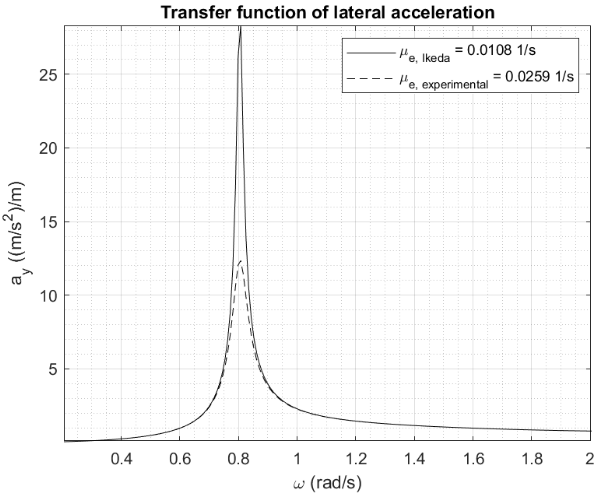

Figure 8.4: Lateral acceleration transfer function calculated using the linear damping coefficient μ_e from the application of the Simplified Ikeda's Method and by roll decay tests.

Parameter	$C(-)$ (full table)	$H_{s,max}(m)$
North Atlantic	$8.24 \cdot 10^{-4}$	6.5
Area 16	$1.20 \cdot 10^{-3}$	5.5
Area 17	$1.15 \cdot 10^{-3}$	5.5

Table 8.5: Summary results of Level 2 assessment and OL related to area and maximum significant wave height.

Operational Limitations related to these areas have not been able to solve the vulnerability of the vessel. Hence, Operational Limitations related to maximum significant wave height have been applied by limiting the standard scatter table up to the maximum allowable significant wave height. No normalization has been performed since the ship stay in port when the wave height is expected to exceed the expected maximum one. The maximum significant wave height was found equal to $5.5m$ for Area 16 and $6.5m$ for Area 17. The results of the application of OL are summarized in Table 8.5, where the identified maximum significant wave height is reported for the North Atlantic and Areas 16 and 17, while the trend lines of the long-term stability failure index for the three considered scatter tables are given in Figure 8.5.

It is worth to underline that Operational Limitations are based on the calculation of a long-term probability index, therefore the probability of occurrence of excessive lateral accelerations in the long-term is lowered to an acceptable level by imposing an upper limitations to the wave height, but the ship could still experience the phenomenon for sea states having wave height below the identified maximum one. Therefore, the crew must always operate with prudent seamanship and it can be assisted by on-board systems as the one introduced in Chapter 6.

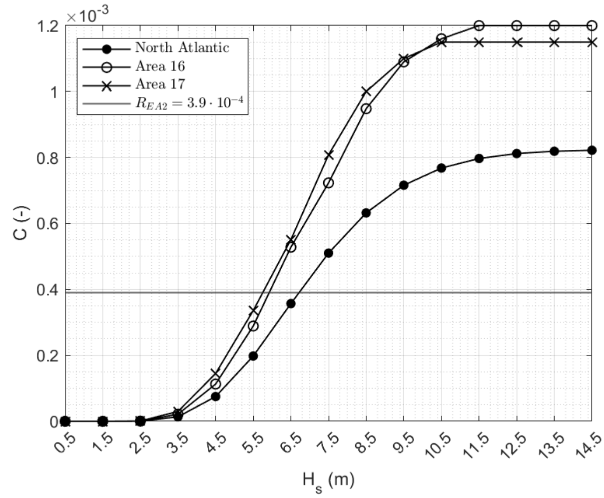

Figure 8.5: Long-term index as a function of the significant wave height.

8.2 Feasibility of the Direct Stability Assessment

In Chapter 2, the verification using deterministic criteria was mentioned as one of the possible alternatives to perform a DSA. Table 2.2 reports the design sea states to be considered in the assessment. The criteria to be verified in the assessment are the greatest mean 3-hour lateral acceleration and the mean 3-hour roll angle calculated with respect to all design situations.

For each design situation, at least five simulations of three hours should be performed. For each simulation, the maximum roll amplitude and lateral accelerations are taken, obtaining five values for the roll amplitude and five for lateral accelerations. The mean value of these fives value represents the mean 3-hour maximum amplitude.

The assessment is verified if:

1. the mean 3-hour maximum roll angle does not exceed half of the minimum among: 40°; the angle of vanishing stability in calm water, φ_v; the angle of submergence of unprotected openings in calm water $\varphi_{unprotected}$;

2. the mean 3-hour maximum lateral acceleration does not exceed $\frac{9.81}{2} m/s^2$.

For the stern trawler under analysis, unprotected openings have not been considered and then the reference value for the assessment has been assumed equal to 40°. Five simulations of three hours were performed in ShipX® software by SINTEF Ocean, through the VERES (VEssel RESponses) package, with weakly non-linear modelling of the Froude-Krylov excitation and restoring forces. Details of the numerical model can be found in Subsection 8.3.1.

The sea state having mean zero-crossing period $T_z = 6.5s$ and significant wave height $H_s = 2.5m$, has been selected for the simulations. Figure 8.6 provides the five lateral acceleration time series. The chosen significant wave height for the selected period is smaller than the prescribed one, Table 2.2. This particular choice has been made to show that for this particular case the DSA fails even for situations less extreme than the design ones. Indeed, the mean 3-hour roll amplitude is 33.6 while the mean 3-hour lateral acceleration for the considered sea state is $8.31 m/s^2$, which are significantly higher than the limit values. The maximum values of the lateral acceleration in the considered sea states and mean 3-hour maximum lateral acceleration are reported in Table 8.6.

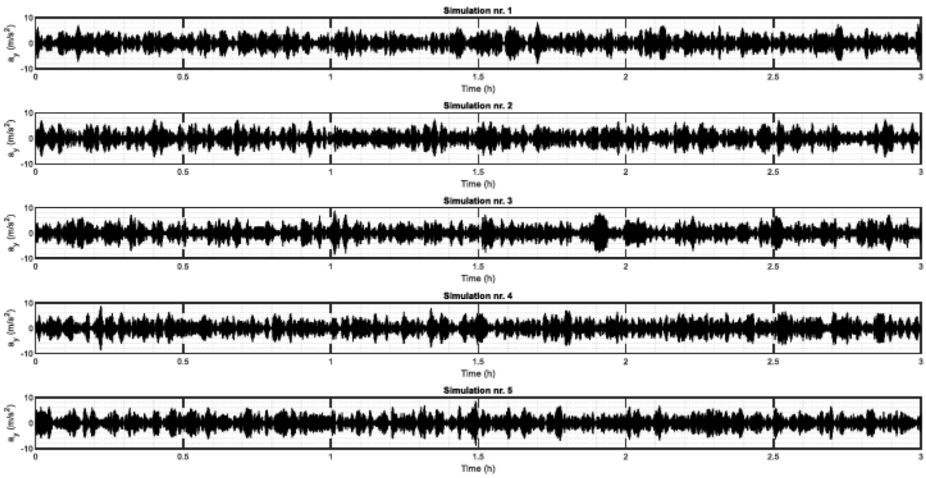

Figure 8.6: Lateral acceleration time series. Five simulations of 3 hours duration.

Simulation	$a_{y,max}(m/s^2)$	φ_{max}(deg)
1	8.03	32.3
2	7.31	30.3
3	8.73	36.8
4	8.66	32.3
5	8.80	36.3
Mean 3-hour	$a_{y,3h} = 8.31$	$\varphi_{3h} = 33.6$

Table 8.6: Maximum values of the lateral acceleration and roll angle in the tested sea states and mean 3-hour maximum amplitudes.

8.3 Application of the on-board system

The short-term indexes reported in Table 8.3 show that large accelerations can be experienced also for sea states having the significant wave height lower than the maximum one identified by the application of Operational Limitations. For this reason, the system presented in Chapter 6 has been considered to inform the crew on the actual state of the vessel in terms of accelerations.

The application of the proposed system has been conducted on numerical and experimental time series in irregular beam waves, for relevant combinations of sea states.

Time series of almost $1h$ have been merged to simulate changes in the sea states, keeping constant the loading condition. Different variations could be made, keeping constant the sea state and varying the loading conditions, simulating the changes in the loading condition during a fishing campaign. Variations in both the sea state and the loading condition could be also performed, without affecting the characteristics of the proposed systems.

In the Thesis, only sea states variations have been considered, referring to two type of situations:

1. the mean zero-crossing period is kept constant and the significant wave height is increased almost every hour;

2. the significant wave height is kept constant and the mean zero-crossing period is increased almost every hour.

In the first scenario, it is expected that the system initially identifies a safe condition that becomes potentially dangerous in time. In the second scenario the system can always identify safe (or unsafe) conditions or can start identifying an unsafe condition and later a safe conditions.

It is worth to underline that the considered variations of significant wave height and mean zero-crossing period are for testing purposes, and more complex situations are expected in real conditions where deviations from the assumed theoretical environmental conditions may occur. For the selected fishing vessel, important variations in the loading conditions are expected, which may affect the response in terms of roll motion and lateral accelerations, for given environmental conditions.

Time windows having length of $20min$ have been assumed, during which the process is assumed to be stationary. An overlapping of 87.5% has been adopted among two consecutive time windows, allowing the system to return a value of the RMS and of the extreme value each $2.5min$, providing a frequent update of the awareness of the actual condition of the vessel.

As concerns the limiting values for the RMS, $0.10g$ (probable risk) and $0.2g$ (extreme safety level) have been chosen as thresholds for the monitoring of the actual condition. If the RMS is in between the two limiting values an alert is provided while if the RMS exceeds the greatest value an alarm is given. The limit values could be lowered for wet decks, for example the fishing deck.

The values $g/3$ and $g/2$ have been selected as thresholds for the most probable extreme values of acceleration $\overline{a}_{y,T}$ in the exposure time T.

A summary of the standards used for the monitoring and estimation stages of the on-board system is provided in Table 8.7.

	MONITORING	ESTIMATION
	RMS (m/s^2)	$\overline{a}_{y,T}(m/s^2)$
ALERT	$0.1g$	$g/3$
ALARM	$0.2g$	$g/2$

Table 8.7: Summary of the standards used for the monitoring and estimation stages of the on-board system.

The numerical time series have been obtained by means of ShipX® software and an experimental campaign has been conducted to test the system on a different source of data.

The examined situations have been selected following the guidelines for the DSA conducted with deterministic criteria, IMO MSC.1/Circ.1627 (2020). Beam waves, zero forward speed and sea states having mean zero-crossing periods in the range $0.70 \div 1.3$ of the natural roll period T_r have been assumed as test conditions.

Therefore, sea states having the mean zero-crossing periods from $5.5s$ to $9.5s$ and significant wave heights from $0.5m$ to $3.5m$ have been considered. The number of considered sea states has been partly reduced in the experimental tests due to the wave generator limits. The Bretschneider wave energy spectrum has been assumed to describe the environmental conditions.

In the following subsections, a description of the numerical roll motion model and of the experimental tests is given. Finally, the application of the proposed system is shown.

8.3.1 Numerical simulations

Simulated time series have been generated by means of ShipX®, based on the strip theory as developed by Salvesen et al. (1970). The software can perform time-domain simulations, with weakly non-linear modelling of the Froude-Krylov excitation and restoring forces. The program allows the user to introduce the matrices for the hydrodynamic coefficients to account for viscous effects.

An equivalent linear damping has been calculated for each of the simulated sea states by the knowledge of the linear roll damping coefficient μ_e calculated by Level 2 of the Excessive acceleration criterion via stochastic linearization, IMO SDC 8/WP.4/Add.2 (2022):

$$\mu_e = \mu + \sqrt{\frac{2}{\pi}}\beta\sigma_{\dot{\varphi}}\left(\mu_e\right) \tag{8.1}$$

where μ and β are the linear and quadratic damping coefficients calculated by the roll decay tests, Table 8.4, and $\sigma_{\dot{\varphi}}$ the standard deviation of roll velocity. This kind of representation of roll damping allows to account for the influence of the sea state on the roll damping. A graphical representation of the obtained equivalent linear damping coefficients for all the sea states reported in the standard wave scatter table, is given in Figure 8.7, showing an expected increase of damping with the significant wave height and maximum values for zero-crossing periods around the natural roll period. The equivalent roll damping coefficients used in the simulations are given in Table 8.8.

The software returns ship motion responses which have been used to calculate lateral accelerations:

$$a_y = \ddot{\eta}_G - \ddot{\varphi}(H - KG) + \ddot{\psi}(x_{AP} - LCG) + g\varphi \tag{8.2}$$

where $\ddot{\eta}_G$ is the sway acceleration, $\ddot{\psi}$ is the yaw acceleration and LCG is the longitudinal distance from the aft perpendicular of the centre of gravity.

Due to the particular considered scenario, i.e. beam waves and zero speed, the effect of sway and yaw motions on the calculated lateral accelerations has been analysed. To this aim, a comparison between lateral accelerations calculated by the 3-DOF and 1-DOF approaches has been performed.

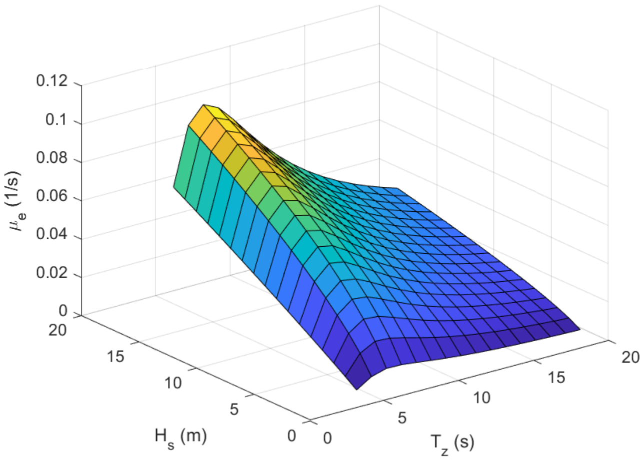

Figure 8.7: Equivalent linear roll damping coefficient as a function of the sea state.

H_s(m)	T_z(s)	$\mu_e(1/s)$
1.5	5.5	0.0259
1.5	6.5	0.0255
1.5	7.5	0.0236
1.5	8.5	0.0214
2.5	5.5	0.0347
2.5	6.5	0.0341
2.5	7.5	0.0315
2.5	8.5	0.0285
3.5	6.5	0.0415
3.5	7.5	0.0383

Table 8.8: Summary of the equivalent linear roll damping coefficients in the tested sea states.

Simulations have been performed considering a total simulation time of $70min$ with $0.05s$ of time step, for each sea state. A summary of the comparison is given in Table 8.9, showing negligible differences in terms of RMS of the times series and up to $15-20\%$ for maximum values. Two simulations performed considering only roll motion and considering the simultaneous effect of roll, sway and yaw are reported in Figure 8.8.

Due to the obtained differences in the obtained maxima, accelerations have been calculated by equation 8.2 in the application of the on-board monitoring system.

8.3.2 Experimental tests

Non-linearities can play an important role in ship roll response, especially for wave periods around the natural roll period. Coupling with other ship motions could

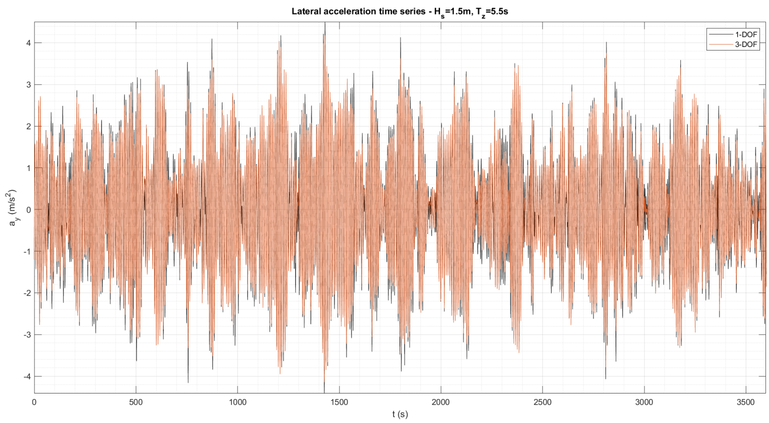

Figure 8.8: Lateral acceleration time series derived from the simulation conducted by ShipX® software, for the sea state $H_s = 1.5m$ and $T_z = 5.5s$.

		3-DOF		1-DOF	
H_s(m)	T_z(s)	$a_{y,max}(m/s^2)$	RMS (m/s^2)	$a_{y,max}(m/s^2)$	RMS (m/s^2)
1.5	5.5	4.18	1.30	4.51	1.34
1.5	6.5	5.90	1.52	5.87	1.49
1.5	7.5	4.94	1.37	4.95	1.32
1.5	8.5	4.61	1.25	3.89	1.17
2.5	5.5	5.99	1.92	6.56	2.00
2.5	6.5	8.35	2.15	8.40	2.11
2.5	7.5	7.66	2.14	6.72	2.05
2.5	8.5	8.07	1.96	6.90	1.8
3.5	6.5	10.25	2.74	8.99	2.67
3.5	7.5	8.21	2.54	7.91	2.35

Table 8.9: Summary of the comparison between 3-DOF and 1-DOF approaches.

be not properly described by simplified numerical models and the hydrodynamic coefficients values could deviate from the real values. Such effects may be not captured by simplified mathematical models and could affect the performance of the proposed system.

For this reason, an experimental campaign has been conducted in the towing tank of the Center for Marine and Industrial Technological Investigations (CITENI) of the University of A Coruña (Spain), Figure 8.9. The towing tank is $56m$ long, $4.20m$ wide and $1.80m$ deep and it is equipped with a unidirectional wave-maker.

The 1/30 geosim fiberglass model of the fishing vessel is shown in Figure 8.9. The ship displacement in model scale was obtained by ballasting the model. The metacentric height was calculated through inclining experiments and the weights were adjusted to obtain the required metacentric height. The weights were positioned to obtain a zero trim and zero heel condition, measured by an inclinometer.

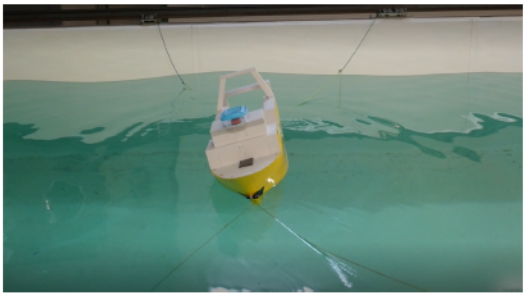

Figure 8.9: Towing tank of the University of A Coruña and scaled model of the fishing vessel.

Roll decay tests were performed according to the MSC.1/Circ.1200 guidelines (2006), that prescribe a minimum number of four tests. For each test, the model was heeled to an angle larger than 25° and the roll time history was recorded until the model reached rolling angles smaller than 0.5°. An Inertial Motion Unit (IMU) with a sampling frequency of $100Hz$ was used to record the time history.

In the present analysis, a quadratic representation of the non-linear damping was adopted to properly model roll damping both at large roll angles, where the non-linearities are predominant, and at small angles. The linear and quadratic damping coefficients were calculated considering the linear decrement of roll decay, fitting the decay curve through a second-degree polynomial, as summarized in Table 8.4 and Figure 8.10, obtaining linear and quadratic coefficients respectively equal to 0.0207 and 0.0161.

Then, the linear damping coefficient calculated for the model is:

$$\mu_{model} = 0.0207\frac{\omega_r}{2\pi} \tag{8.3}$$

while the quadratic damping coefficient calculated for the model is:

$$\beta_{model} = 0.0161\frac{3}{8}\frac{180}{\pi} \tag{8.4}$$

The obtained coefficients are scaled to ship scale through the followings:

$$\mu_{ship} = \mu_{model}\sqrt{\lambda} \tag{8.5}$$

while the quadratic damping coefficient calculated for the model is:

$$\beta_{ship} = \beta_{model} \tag{8.6}$$

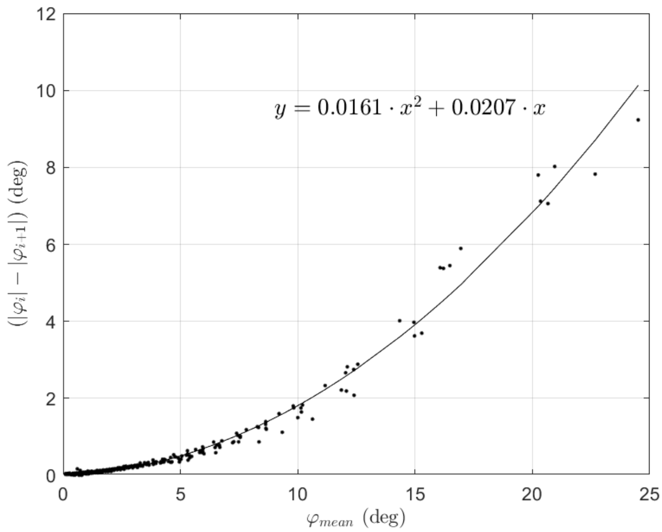

Figure 8.10: Linear decrement of roll decay.

The obtained damping coefficients have been verified comparing the time histories of the roll decay tests with simulations performed using the calculated coefficients. Figure 8.11 shows the comparison for one of the performed tests.

After the preliminary set-up of the model and the roll decay test, the experiments progressed to testing the ship behaviour in irregular beam waves.

A calibration of the wave maker was performed by measuring the waves without the model in the towing tank. The wave elevation was measured by two wave gauges located on the paddles of the wave maker and checks were performed by comparing the theoretical wave energy spectra with the obtained ones.

Roll motion and lateral accelerations at the wheelhouse were measured by an IMU. An example of measured roll motion and lateral acceleration time series for the sea states having significant wave height $H_S = 1.5m$ and mean zero-crossing period $T_z = 5.5s$, is given in Figure 8.12, with the time in full scale.

Maximum lateral accelerations have been plotted as a function of the mean zero-crossing period for the selected significant wave height, Figure 8.13. It can be noticed that, for a given significant wave height, the largest accelerations occur for the zero-crossing period of $T_z = 5.5s$. Accelerations larger than the gravity accelerations are experienced for the significant wave height of $3.5m$, for which the zero-crossing periods $6.5s$ and $7.5s$ were tested.

8.3.3 Results and discussion

Before applying the proposed system, the results obtained by ShipX® software have been compared with the experimental results. The results are summarized in Table 8.10 in terms of RMS and maximum values of the lateral accelerations, showing a general good agreement although the differences are not negligible for some sea states.

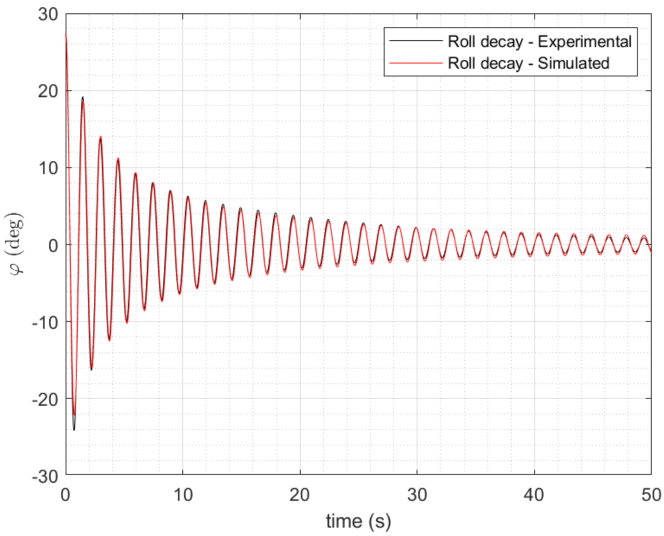

Figure 8.11: Roll decay test - Comparison of experimental and simulated data.

The amplitudes of the lateral accelerations follow a Rayleigh distribution, as shown in Figure 8.14 for four sea states, although formulas 6.1 and 6.2 may be applied also for non-narrow band processes. It can be seen that the Rayleigh distribution fits well the peaks of the lateral accelerations, although the largest peaks start to deviate from this distribution.

As concerns the assumption that consecutive peaks are statistically independent, it cannot be necessarily true but it was shown, Lewis (1989), that the violation of such assumption leads to more conservative estimations, which is a benefit in terms of safety.

As a preliminary verification of the estimation of extreme values, formulas 6.1 and 6.2 have been applied considering different time series. The results are summarized in Table 8.11, where results from simulations and experiments are reported. The exception are the sea states with significant wave height $0.5m$, for which only results from simulations are given, since it was not possible to test them in the towing tank due to the wave generator limits.

For each time series, the RMS and the mean zero-crossing period have been calculated for the first time window of $20min$ in order to estimate:

- the most probable extreme lateral accelerations $\overline{a}_{y,T}$;
- the extreme lateral acceleration $\hat{a}_{y,T}$ exceeded with probability $\alpha = 0.10$.

The above mentioned extremes are the ones that could be experienced in the next $20min$. Therefore, the maximum value of lateral acceleration in such time window has been taken and compared with the expected extremes $\overline{a}_{y,T}$ and $\hat{a}_{y,T}$. The results show that the maximum values in the considered time windows are often close to the most probable extreme value. Such value is often exceeded, especially for the simulated data. The extreme value to be exceeded with probability

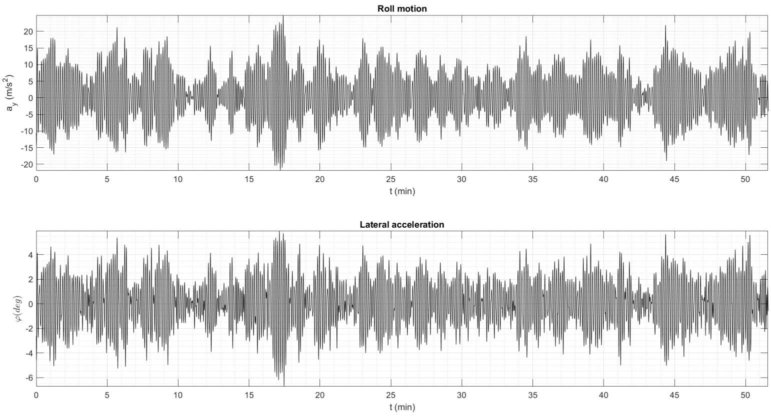

Figure 8.12: Experimental roll motion and lateral acceleration time series.

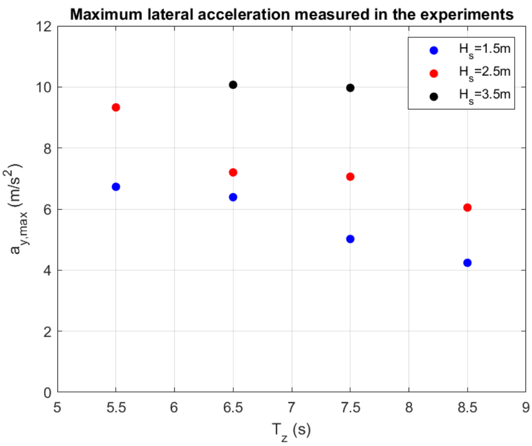

Figure 8.13: Maximum lateral accelerations measured in the experiments.

$\alpha = 0.10$ is exceeded one time for the experimental and two times for the simulated data. Due to the fact that the expected value $\overline{a}_{y,T}$ may be easily exceeded, it is taken as reference parameter for the prediction system, since it satisfies one of the requirements that a on-board system should have to let the crew rely on it. As pointed in Bačkalov et al. (2016), the crew tends to rely on an on-board system only if it provides results that can be easily understood and coherent with what they are actually experiencing, which is the case of the above mentioned metric.

In Figure 8.15, one of the combinations of sea states is shown, referring to simulated data, characterized by a sequence of three sea states of $70min$ duration. The sea states have the same mean zero-crossing period, equal to $6.5s$, and three significant wave heights, respectively equal to $0.5m$, $1.5m$ and $2.5m$. The figure shows three graphs as a functions of time, in hours. In each graph, the vertical dotted lines represent the time instant when a change in the sea state has been

		Experimental		Simulated	
H_s(m)	T_z(s)	$a_{y,max}(m/s^2)$	RMS (m/s^2)	$a_{y,max}(m/s^2)$	RMS (m/s^2)
1.5	5.5	6.73	1.85	4.18	1.30
1.5	6.5	6.39	1.79	5.90	1.52
1.5	7.5	5.02	1.64	4.94	1.37
1.5	8.5	4.24	1.56	4.61	1.25
2.5	5.5	9.33	2.61	5.99	1.92
2.5	6.5	7.20	2.33	8.35	2.15
2.5	7.5	7.06	2.22	7.66	2.14
2.5	8.5	6.05	2.18	8.07	1.96
3.5	6.5	10.07	3.12	10.25	2.74
3.5	7.5	9.97	2.63	8.21	2.54

Table 8.10: Comparison among the experimental and the simulated data.

introduced.

In the upper graph, the lateral acceleration time series is given.

In the second one, the values of the RMS in each time window are given and used to monitor the actual condition of the vessel. The limits corresponding to $0.1g$ and $0.2g$ are given as horizontal continuous orange and red lines, respectively. Three different colours are adopted to represent the markers for the calculated RMS: green if the value is less than the smallest limit value; orange if it is in between the two limit values; red if above the largest limit value. The choice of the colours has been made to clearly identify the safe conditions (green) and to emphasize the entity of the critical conditions (orange and red).

In the lowest graph, the most probable extreme value and the extreme values exceeded with probability $\alpha = 0.10$ are represented together, to show what could occur in the next twenty minutes, and to give an insight in the potential dangerous situations in the short-term and eventually to allow the crew to take corrective actions.

From the reported results, it can be seen that the RMS increases with the significant wave height, exceeding the threshold $0.1g$ after the first hour and the threshold $0.2g$ after the second hour. As concerns the estimated extreme values, the most probable extreme $\overline{a}_{y,T}$ remains lower than the first limit value $g/3$ for the first hour. During the second hour, it is very close to the second threshold $g/2$ and trespasses it many times, while during the third hour it is always higher than $g/2$, raising an alarm all the time. The extreme value $\hat{a}_{y,T}$ is reported for informative purposes, to provide an indication on what it could be experienced in the worst scenario.

The same representation is shown in Figure 8.16 for the combination of simulated data with mean zero-crossing period equal to $7.5s$ and significant wave heights equal to $0.5m$, $1.5m$ and $2.5m$, respectively, with similar outcomes.

The combination of simulated data with mean zero-crossing equal to $T_z = 5.5s$, $6.5s$, $7.5s$ and $8.5s$ and significant wave height $H_s = 1.5m$ is provided in Figure 8.17. From the second graph, it can be seen that the RMS is almost constant for the four considered sea states, with a slight reduction in its magnitude with the increase of the mean-zero crossing period of the waves since it is moving far from the resonant condition of the vessel. The RMS is always in the orange zone

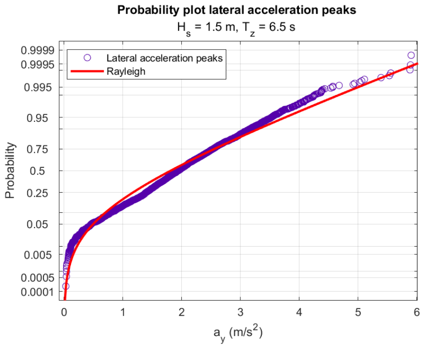

(a) Sea state $H_s = 1.5m$ and $T_z = 6.5s$

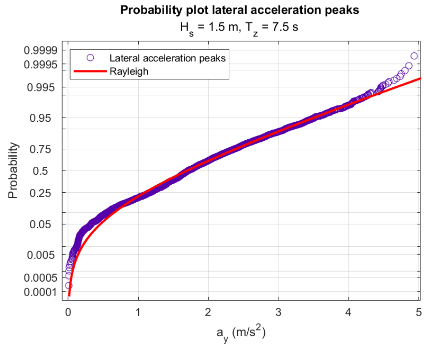

(b) Sea state $H_s = 1.5m$ and $T_z = 7.5s$

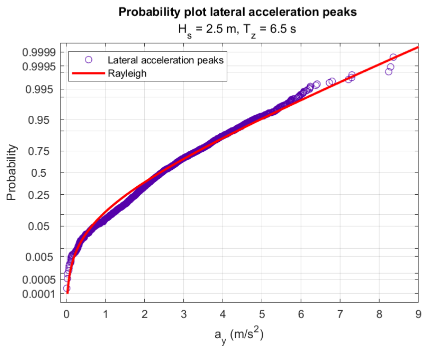

(c) Sea state $H_s = 2.5m$ and $T_z = 6.5s$

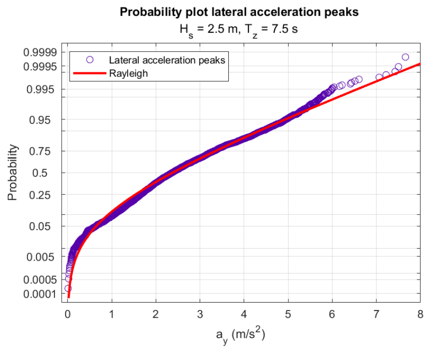

(d) Sea state $H_s = 2.5m$ and $T_z = 7.5s$

Figure 8.14: Probability plots of the lateral accelerations obtained by ShipX® software - Rayleigh distribution.

between the two limit values $0.1g$ and $0.2g$. The most probable extreme $\overline{a}_{y,T}$ remains lower than the second limit value $g/2$ almost all the time, exceeding it few times during the second and third hours, while the extreme $\hat{a}_{y,T}$ exceeds many times the threshold of $g/2$.

The same variations of mean zero-crossing period for the significant wave height $1.5m$ is considered referring to experimental data, Figure 8.18. Results analogous to the ones obtained with simulated data are shown, with the main difference that the most probable extreme is most of the times higher than the limit value $g/2$. For the considered scenario the ship is experiencing all the time dangerous conditions, and based on the provided alarm the crew is expected to take corrective actions, as an increase of ship speed, to introduce additional roll damping, or a change in the wave heading, to reduce the excitation forces due to the waves.

In order to have a better insight on how many times the most probable extreme value is actually exceeded, the same combinations of sea states reported in Figure 8.17 is given in Figure 8.19. In the Figure, an additional blue line is added in the lower graph, that represents the maximum value recorded in the $20min$ subsequent to each prediction. The results show that the most probable extreme value is often exceeded. It must be underlined that in order to perform the comparison

		Experimental			Simulated		
H_s (m)	T_z (s)	$a_{y,max}$ (m/s^2)	$\overline{a}_{y,T}$ (m/s^2)	$\hat{a}_{y,T}$ (m/s^2)	$a_{y,max}$ (m/s^2)	$\overline{a}_{y,T}$ (m/s^2)	$\hat{a}_{y,T}$ (m/s^2)
0.5	5.5	-	-	-	2.38	2.02	2.44
0.5	6.5	-	-	-	1.83	1.75	2.13
0.5	7.5	-	-	-	2.06	2.26	2.74
0.5	8.5	-	-	-	1.83	1.71	2.06
1.5	5.5	4.90	6.34	7.65	4.18	4.16	5.03
1.5	6.5	6.39	5.79	6.99	5.90	4.69	5.67
1.5	7.5	4.53	4.90	5.91	4.69	4.41	5.34
1.5	8.5	4.24	4.95	5.98	4.06	3.37	4.09
2.5	5.5	7.56	8.13	9.79	5.42	5.73	6.92
2.5	6.5	7.20	7.44	8.96	5.93	7.72	9.34
2.5	7.5	6.28	7.52	9.08	5.95	7.07	8.57
2.5	8.5	6.02	6.91	8.34	8.07	5.73	6.95
3.5	6.5	10.07	9.61	11.6	8.90	8.41	10.17
3.5	7.5	9.97	7.72	9.31	7.80	8.46	10.24

Table 8.11: Observed maxima of lateral acceleration, and estimations of the expected and extreme values exceeded with probability $\alpha = 0.10$, for the experimental and simulated data.

the observed maximum values are not represented at their exact time but they are anticipated by $20min$. Indeed, each prediction is given at the end of the corresponding window and refers to the following time window. The maximum value then should be plotted $20min$ later than the corresponding prediction. In addition, due to the overlapping among consecutive windows, the same maximum value may repeat on several windows, as evident in the Figure.

As a final remark, it can be observed that the RMS of lateral accelerations time series is the governing parameter for both tasks performed by the proposed systems, i.e. the monitoring of the actual loading condition and the estimation of the extreme values. Therefore, it may be expected that one of systems raises an alarm before the other in all situations. In order to verify it, it can be useful to briefly recall the assumed limit values for the two tasks:

- in the monitoring stage, the RMS of lateral accelerations is compared with $0.1g$ and $0.2g$;
- in the estimation stage, the most probable extreme value $\overline{a}_{y,T}$, equation 6.1, is compared with $g/3$ and $g/2$.

The most probable extreme value $\overline{a}_{y,T}$ becomes a function of only the RMS and of the mean zero-crossing period T_z of the process once the exposure time T is fixed. Equation 6.1 can be rewritten defining the limits in terms of RMS:

$$\sqrt{m_0} < \frac{a_{lim}}{\sqrt{2\ln\frac{T}{T_z}}} \tag{8.7}$$

The mean zero-crossing period is assumed to vary in the range between $3.5s$ and $18.5s$ although it will generally assume intermediate values.

Referring to the exposure time of $20min$ and considering the lowest limit value $g/3$, the limiting RMS is $0.96m/s^2$, for the mean zero-crossing period $3.5s$; the limiting RMS is $1.13m/s^2$ for the mean zero-crossing period $18.5s$. In practice, the RMS will fall in the middle of these two limiting values, i.e. very close to the lower limiting value for the monitoring stage, i.e. $0.1g = 0.981m/s^2$. Therefore, the system will identify at the same time the exceeding of the lowest limits corresponding to both stages of the system.

As concerns the highest thresholds of both parts of the system, something different happens. Indeed, considering the limit value $g/2$, the limiting RMS is $1.44m/s^2$ for the mean zero-crossing period $3.5s$ and $1.70m/s^2$ for the mean zero-crossing period $18.5s$. Both values are lower than $0.2g = 1.96m/s^2$ associated to the monitoring stage. Therefore, the part of the system based on the estimation of the most probable extreme value will be dominant with respect to the part relative to the monitoring of the actual condition of the vessel. This can be graphically seen, for instance, in Figure 8.18, where the most probable extreme is always above the second threshold, and all the markers are red, while the RMS is always in between $0.1g$ and $0.2g$, and all the markers are orange.

Apart from this theoretical consideration, it can be observed that the two systems consider two different aspects of the same phenomenon, since one provides information on what is happening on-board and the other provides information on what could happen in the short-time. Providing both information will allow to have a better understanding of the scenario under which the ship is sailing, helping the crew to take the best decision to guarantee safety.

8.4 Conclusions

In this Chapter, a mid-sized stern trawler has been studied. The vessel was already a subject of previous studies that identified her vulnerability to dangerous dynamic phenomena in waves.

A loading condition has been identified as particularly prone to suffer excessive acceleration and used as test case to investigate the applicability of the criterion. Indeed, due to the typical operations she has to deal with and the harsh conditions she has to face, the vessel can experience dangerous lateral accelerations.

As a preliminary assessment, it has been verified the vulnerability of the vessel to Level 1 and Level 2, in the selected loading condition. Operational Limitations related to route and maximum significant wave height have been developed to impose limitations to the environmental conditions under which the ship can sail. Due to the particular operational area, which falls into Area 16 and Area 17 of the Global Wave Statistics (Hogben et al. (1986)) it has been shown that OL related to area return results more severe than those obtained by assuming the standard wave scatter table for the North Atlantic.

An investigation on the applicability of the DSA using deterministic criteria has been conducted. To this aim, five 3-hours simulations have been performed by ShipX® software for the sea state having mean zero-crossing period $T_z = 6.5s$ and significant wave height $H_s = 2.5m$. For each simulation, the largest roll amplitude and the greatest acceleration have been measured and used to judge the ship vulnerability. The obtained values confirmed the vulnerability of the vessel since they are higher than the corresponding thresholds. The selected sea state has significant wave height lower than the design sea state for that zero-crossing period and DSA would confirm the ship vulnerability.

The standard deviation of lateral acceleration for the sea states in the standard scatter table, shows that the operability criterion for lateral acceleration is exceeded in many sea states. For this reason, it has been proposed to equip the vessel with the on-board system for the monitoring and estimation of the lateral acceleration at the wheelhouse proposed in Chapter 6.

The proposed system is composed by two parts that use the recorded lateral acceleration time series in the last $20min$ to perform their tasks. The first part monitors the actual condition of the vessel by calculating the RMS of lateral acceleration in the last recorded time window and compares it with the limit values from operability criteria. The second one, estimates the extreme values that could be experienced in the following $20min$. Two extreme values are calculated based on the theory from Ochi (1973): the most probable one $\overline{a}_{y,T}$ and the extreme value $\hat{a}_{y,T}$ exceeded with probability $\alpha = 0.1$. The most probable extreme value is assumed as reference value for the estimation part of the proposed system since it is frequently exceeded, while the one exceeded with probability $\alpha = 0.1$ is given as an indication of what could be experienced in the worst scenario. The used formulation is specific for a given exposure time T and offers the advantage of being independent of the bandwidth parameter ϵ. Therefore it is applicable also in real conditions, where it is expected a certain broadness of the sea state and of the associated responses. The estimated extreme values are compared with two limit values, one equal to half of the gravity acceleration derived from the deterministic Operational Guidance for the Excessive acceleration failure mode, IMO MSC.1/Circ.1627 (2020), and the other taken as one-third of the gravity acceleration.

The analysis has been conducted on simulated and experimental data, for sea states having mean zero-crossing period close to the ship natural roll frequency. The simulated data were obtained by ShipX$^{®}$ software. The experimental tests were conducted in the towing tank of the University of A Coruña (Spain) on a 1/30 model of the fishing vessel.

The application of the system confirmed that the most probable extreme value is exceeded many times, making it as a suitable metric for the system.

The application of the system should be verified on real voyage data, due to the expected increased variability of the recordings, which can challenge some of the assumptions at the basis of the system.

Due to its general character, the system could be also integrated by the monitoring and estimations of other ship responses. Referring to the particular phenomenon under analysis in the Thesis, which is mainly generated by synchronous rolling, attention should be paid on rolling motion, whose RMS could be compared to a limit value, as one of those associated to operability criteria (4.0° or others), or the estimated extreme value could be compared with half of the limit value for roll angle defined in the Interim guidelines.

The analysis performed on the fishing vessel, has not included the effects of fishing nets, water on deck, significant variations in the loading condition during operations. These aspects should be carefully addressed in future studies, since they may affect the magnitude and the characteristics of ship responses, also in a non-linear way, affecting the performance of the system.

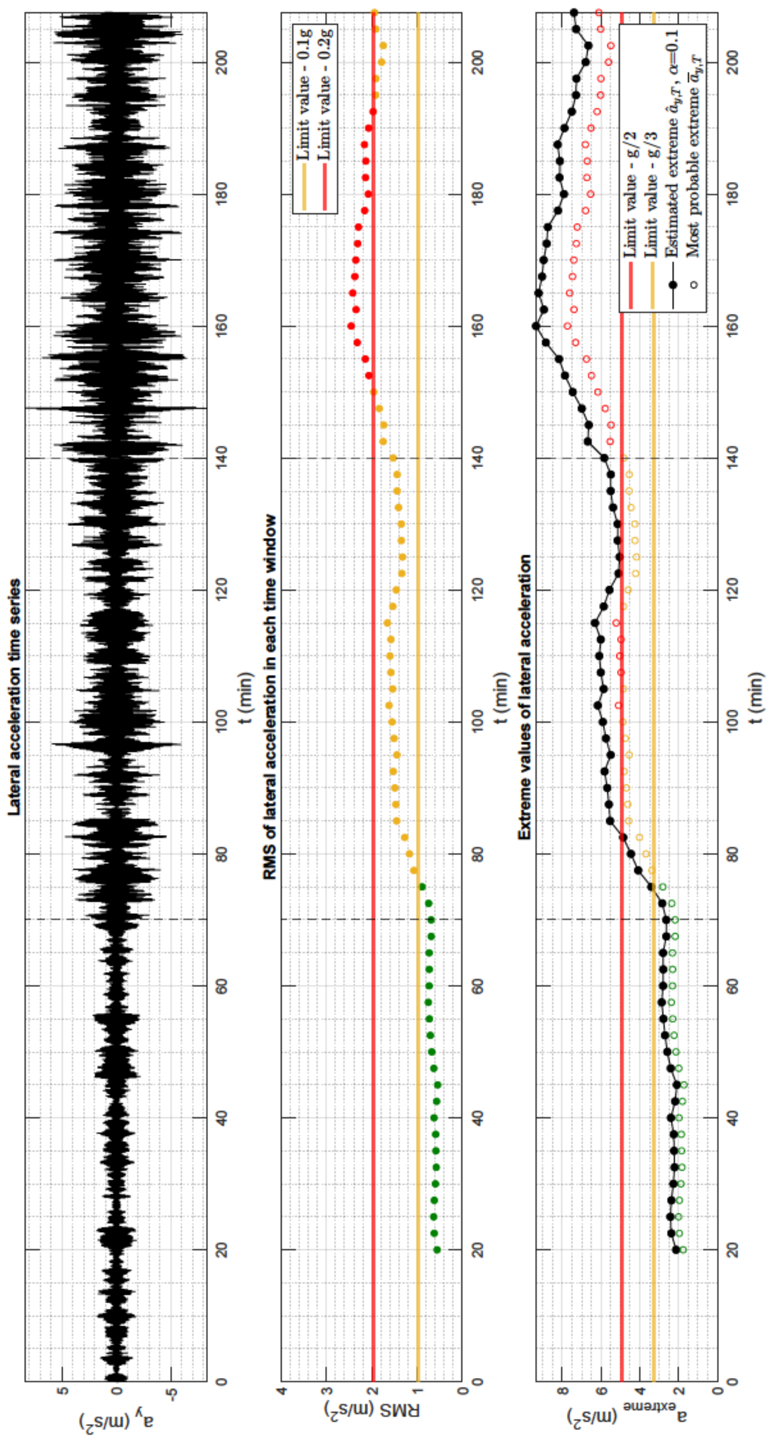

Figure 8.15: From top to bottom. Simulated lateral acceleration time series for $T_z = 6.5s$ and $H_s = 0.5m$, $1.5m$ and $2.5m$, RMS values, and extreme values.

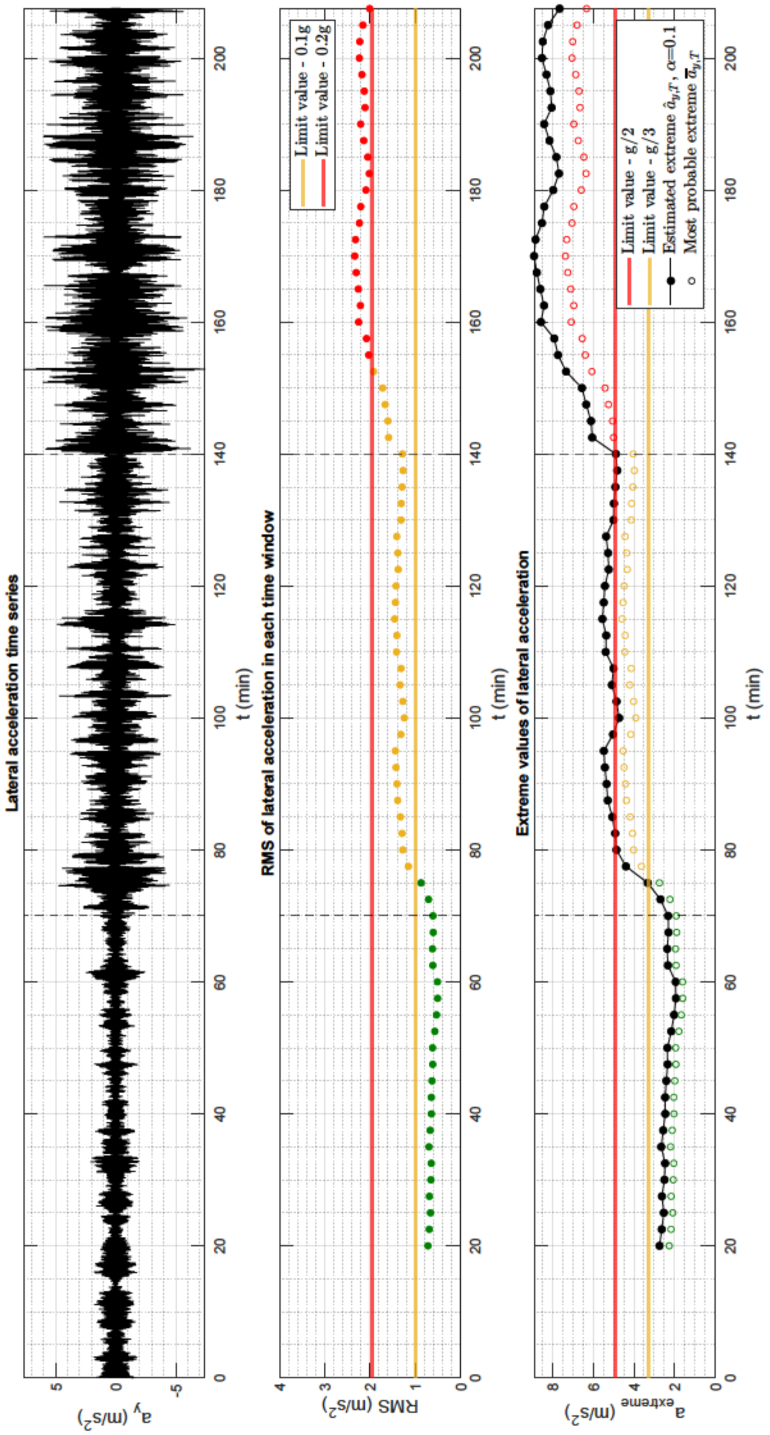

Figure 8.16: From top to bottom. Simulated lateral acceleration time series for $T_z = 7.5s$ and $H_s = 0.5m$, $1.5m$ and $2.5m$, RMS values, and extreme values.

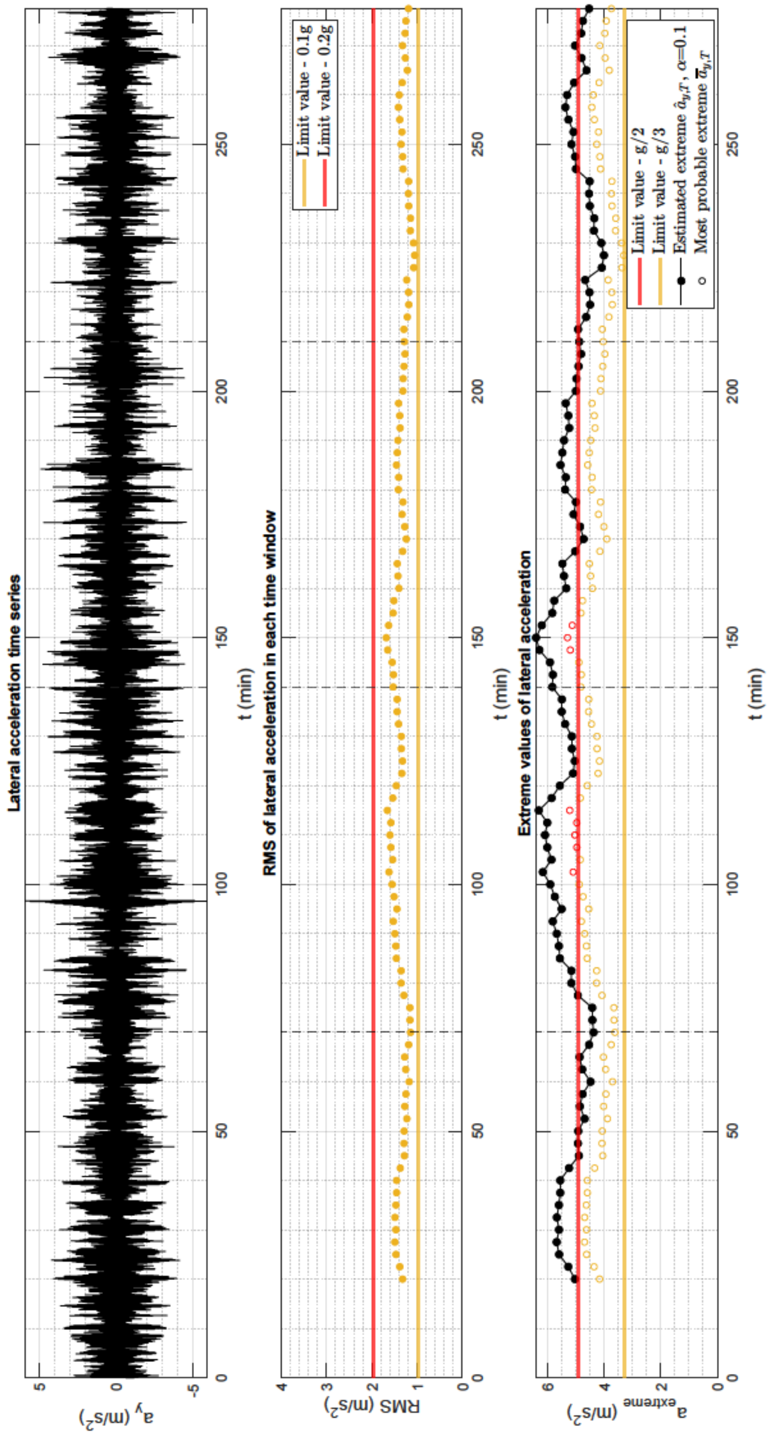

Figure 8.17: From top to bottom. Simulated lateral acceleration time series for $T_z = 5.5s$, $6.5s$, 7.8 and $8.5s$ and $H_s = 1.5m$, RMS values, and extreme values.

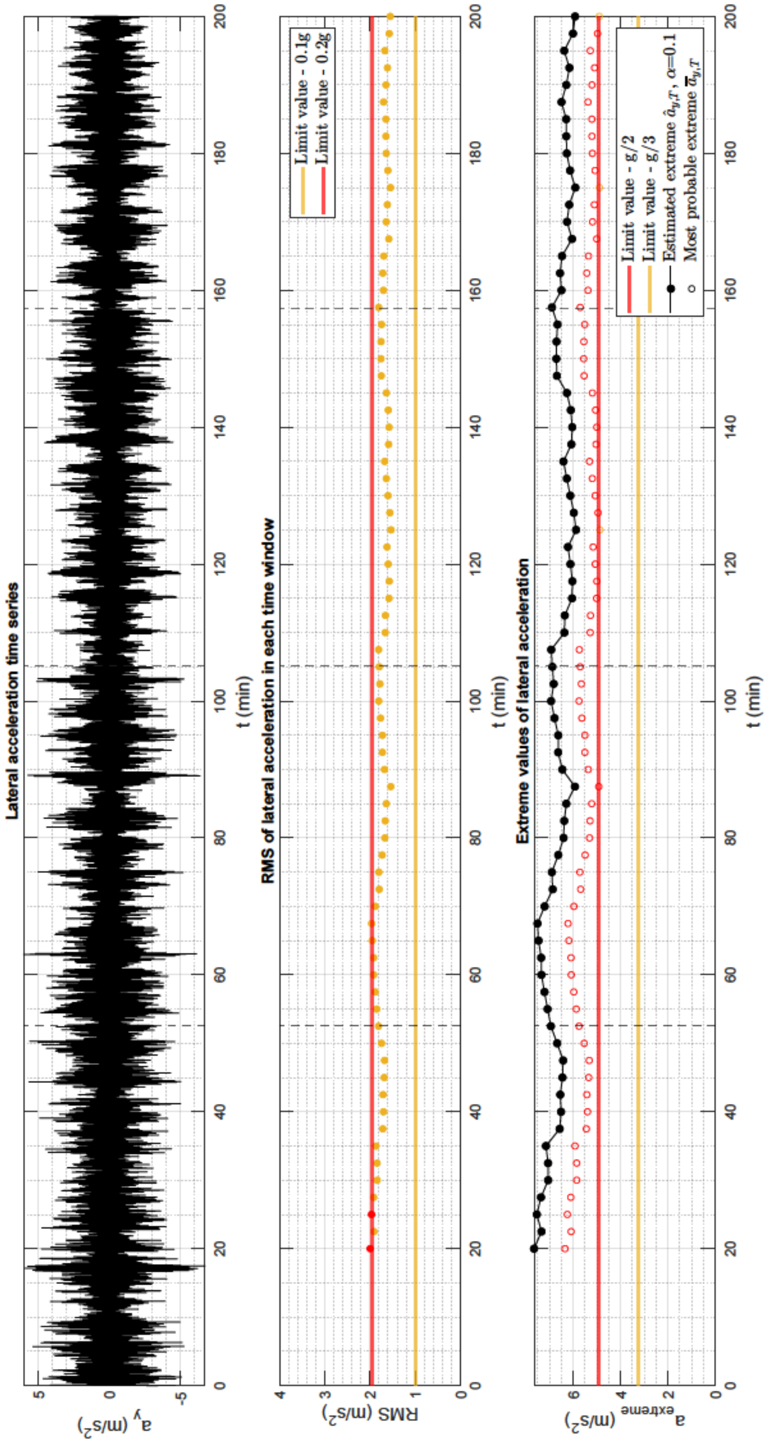

Figure 8.18: From top to bottom. Experimental lateral acceleration time series for $T_z = 5.5s$, $6.5s$, 7.8 and $8.5s$ and $H_s = 1.5m$, RMS values, and extreme values.

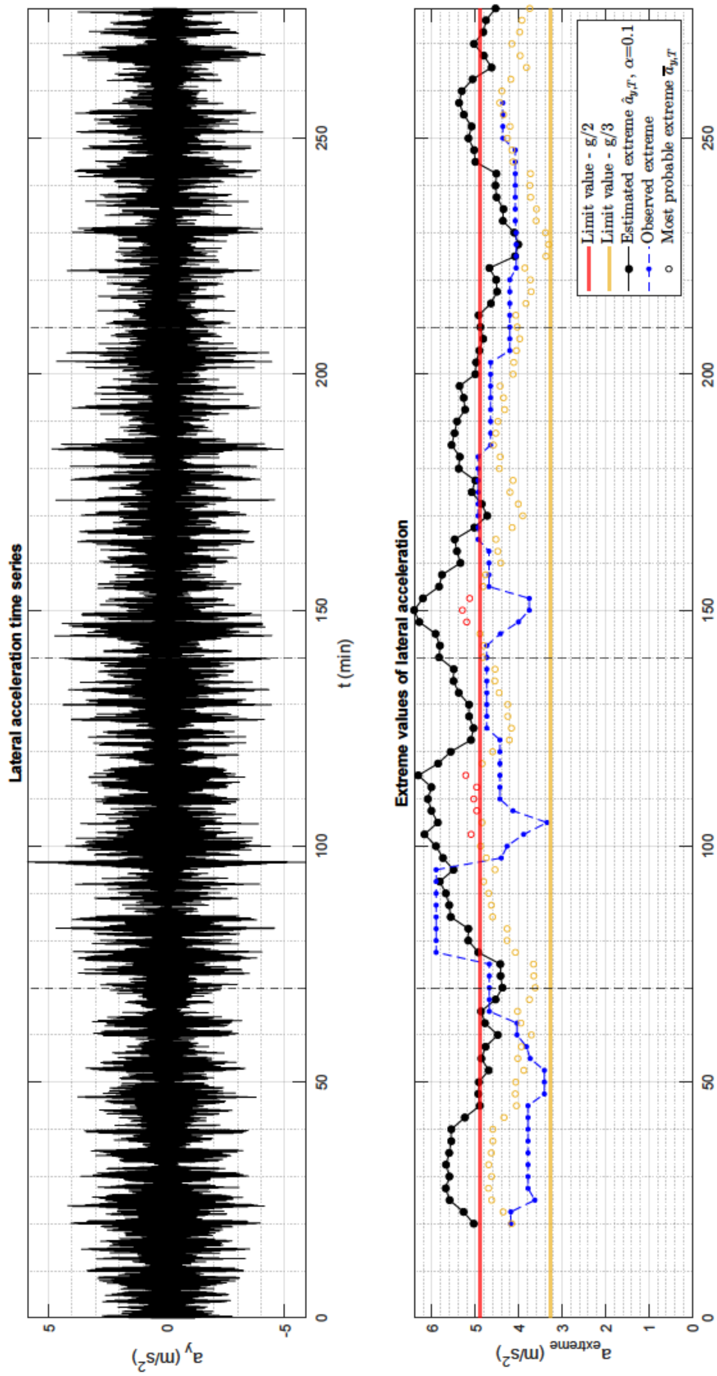

Figure 8.19: From top to bottom. Simulated lateral acceleration time series for $T_z = 5.5s$, $6.5s$, 7.8 and $8.5s$ and $H_s = 1.5m$ and estimated and observed extreme values.

This page was intentionally left blank.

Chapter 9

Conclusions and future works

The present Thesis is placed in the trial period of the Second Generation Intact Stability Criteria (SGISC), finalized in 2020 by the International Maritime Organization, which will be included in Part A of the 2008 IS Code after an extensive testing phase. During their trial stage feedback is expected based on the gained experience.

In the Thesis, the Excessive acceleration failure mode has been deeply investigated, referring to both design and operational aspects, from physical, regulatory and practical point of views.

Accidents which occurred in recent years, clearly demonstrated the inadequacy of the current intact stability regulation in preventing dynamic stability accidents that some ship typologies may suffer. Modern ships significantly deviate from the original set of ships used for the development of the first generation of intact stability rules, due to the evolution of hull forms, size, loading conditions and type of operations. In addition, the phenomena addressed by the SGISC are characterized by the presence of waves. The only criterion in the current regulations that includes the effect of the environmental conditions is the Weather Criterion, which is partly based on a physical model but with the introduction of many empirical assumptions, which - strictly speaking - would make it adequate for ships similar to the ones used in its development only.

The Excessive acceleration criterion refers to dangerous lateral accelerations that could be experienced on board in beam waves, especially in loading conditions characterized by large initial stability, such as ballast condition and partly loaded ship. Synchronous resonance and low roll damping may significantly increase the magnitude of lateral accelerations which could be a source of risk for people on board. In fact, the introduction of the criterion in the SGISC framework is a consequence of some accidents which occurred in the recent years, reviewed in the introductory part of the Thesis.

All the aspects that play a role in the occurrence of the phenomenon should be considered in a rigorous mathematical model, such as the number of degrees of freedom, the external forces and moments (Froude-Krylov and diffraction), the instantaneous wetted surface of the vessel, the body exact formulation of the hydrodynamic coefficients and the effect of viscosity. However, such an accurate model would be extremely complex, making its application unfeasible and numerically challenging. For this reason, the IMO working groups adopted the multi-layered structure, conceiving the vulnerability criteria as simple tools to be applied to most of the designs and aiming at justifying the application of the DSA only if strictly necessary.

In Chapter 1 the phenomenon is introduced jointly with a state of the art. The structure of the Thesis is presented and the main accidents that led to the introduction of the criterion in the regulatory framework are introduced.

Chapter 2 is dedicated to an overview of the structure of the SGISC and of the different levels of assessment. Chapter 3 is specifically dedicated to Excessive acceleration criterion, with particular attention to the theoretical background of Level 1 and Level 2. The vulnerability criteria rely on a 1-DOF roll motion model, non-linear in the damping term. Level 1 is obtained by simplification of the model noticing that accelerations may be calculated at the natural roll frequency, since most of the energy in the considered phenomenon is concentrated around it. In Level 2, accelerations are calculated on a finite range of wave frequencies but still keeping some simplifying assumptions. One of them is related to the evaluation of the external roll moment, reduced to the Froude-Krylov component only, calculated for an equivalent ship whose transversal sections are rectangles having the same breadth at the waterline and the same underwater area of the original sections.

The numerical code for the verification of the vulnerability criteria, implemented in Matlab® programming language has been described and validated in Chapter 4 according to the example reported in the Explanatory notes IMO SDC 8/WP.4/Add.2 (2022).

Chapter 5 presents a mathematical formulation of the exciting Froude-Krylov roll moment, whose novelty is the generalization to any wave heading of the standard methodology for the estimation of the effective wave slope function implemented in Level 2. It has been validated showing that the mathematical formulation coincides with the standard methodology when beam waves are considered. Moreover, the Froude-Krylov roll moment calculated by the proposed formulation has been compared with the one obtained by a 3-D potential flow commercial software, for a barge and a bulk carrier. The presented formulation has been proposed for implementation in the rules, thanks to its accuracy and simplicity. Its adoption would allow a uniform and univocal application of the rules, without the need of validation of commercial software by the Administration.

Chapter 6 presents an on-board decision-making systems intended to integrate Operational Measures developed at the design stage. The system monitors the actual operational condition of the vessel comparing the root mean square of lateral acceleration from measured data with thresholds from the operability criteria for lateral acceleration ($0.1g$ and $0.2g$). Lateral accelerations that could occur in the short term are calculated based on the extreme value theory and compared with thresholds values ($g/3$ and $g/2$), raising an alarm if dangerous conditions are met.

Finally, two test cases have been presented in Chapter 7 and Chapter 8, respectively. The first case is a bulk carrier found vulnerable to Level 1 and 2. Operational Limitations related to maximum significant wave height have been developed for the standard wave scatter table. Then, two long routes have been considered to analyse how the equivalent scatter table should be defined when many geographical areas are crossed. The results showed a certain variability demonstrating that a clear and univocal way to develop OL on long routes should be given for uniform application of the rules. OG have been developed based on the generalization to any ship speed and wave heading of Level 2 procedure. Particular attention has been paid to roll damping, since it has been shown that the modification of the formulation for its estimation can cause significantly different results.

In Chapter 8 a fishing vessel available at the University of A Coruña has been considered. The vessel has been extensively studied in recent years, demonstrating her vulnerability to dynamical phenomena in waves. A loading condition characterized by large initial stability has been selected among the available ones since it is expected to be the most vulnerable to Excessive acceleration. After the verification of the vulnerability criteria and the development of Operational Limitations, a study has been conducted on the feasibility of the Direct Stability Assessment using deterministic criteria, confirming the vulnerability of the ship. Once identified the vulnerability of the ship, it has been noticed that the ship could still experience dangerous accelerations in sea states having significant wave heights lower than the maximum one identified by the application of Operational Limitations. The results is not surprising, since it has been seen that the RMS of lateral acceleration calculated from the application of Level 2 exceeds the operability criterion $0.1g$ in most of the sea states, especially around the natural roll frequency. For this reason, the system presented in Chapter 6 based on the monitoring of accelerations and estimation of the extreme values that could be experienced in the short-term has been applied. The monitoring system does not require any calibration, returns estimates that are really close to the observed values and is easy to understand. The system has been tested on simulated and experimental data. The experimental tests have been conducted in the towing tank of the University of A Coruña (Spain) in irregular beam waves. The obtained results are promising showing that the most probable extreme calculated at the estimation stage is often exceeded, making it a very good metric to inform the crew and to allow it to take corrective actions if dangerous conditions are met.

It has been shown for both the test cases that the proper estimation of roll damping is of paramount importance for the final outcomes of the assessment. In this respect, CFD simulations may be performed to accurately estimate roll damping or even to create databases from which the coefficients for a given ship in several loading conditions could be extracted. Such a database could be possibly used to estimate roll damping in for similar ships as well.

Several operational aspects can be addressed in future research. As concerns Operational Guidance developed at design stage, the application of deterministic and probabilistic Operational Guidance should be carried out to identify potential issues or potential improvements in procedures and adopted methodologies. The consistency with the less accurate simplified Operational Guidance should be investigated as well. Due to the large number of sailing and loading conditions to be tested, an extensive use of experimental tests or CFD simulations is not feasible. Their use is expected for calibration of hydrodynamic coefficients, as roll damping, or to simulate certain wave conditions for validation of numerical codes as done in the present Thesis. The assessment conducted by hybrid multi-DOF motion models represents a fruitful way, but further efforts are needed to improve the underlying methods due to the important role of non-linearities in heavy seas.

The integration of safe sailing conditions identified for different dynamic phenomena should be carefully addressed, keeping in mind the inherent uncertainties of the involved parameters, as the actual metacentric height, the inertial properties of the ship and the characteristics of wind and waves that may be significantly different from the theoretical ones and it could be difficult for the crew to select the most representative guidance among the developed ones. As concerns on-board monitoring and guidance systems, additional effort is required due to the necessity of providing systems offering a good compromise between accuracy, computational effort and time cost. In the Thesis, the estimation of extreme values has been performed but particular attention should be paid, especially in particularly severe sea states, in the adopted peak extraction technique, that could be based on the extraction of all the peaks in a given time series or only peaks above a certain threshold. According to the adopted technique and the severity of the sea states, different distributions may be assumed to fit the data and describe the extreme values, which could affect the performance of the system. Addressing these issues is of paramount importance in order to avoid an underestimation of the extreme values or, conversely, an overestimation that could lead to unnecessary actions by the crew.

Finally, an integration among the Operational Measures derived from the application of the SGISC and the consolidate Seakeeping operability criteria should be considered. Although they focus on different aspects, safety for the SGISC and operability for Seakeeping criteria, it is also true that operability criteria provide useful information that, with a proper calibration of the thresholds, could integrate the main findings from the application of the SGISC. This has been demonstrated for the stern trawler test case. The operability criterion for lateral acceleration at bridge, presented in tabular form, has anticipated the main findings from the application of the monitoring system, identifying in a simple and immediate way the sea states for which a potential danger could occur.

Bibliography

Australian Transport Safety Bureau (2009). *Marine Occurence Investigation No.263 MO-2009-002 Final. Independent investigation into the loss of containers from the Hong Kong registered container ship Pacific Adventurer off Cape Moreton, Queensland*. Tech. rep. URL: www.atsb.gov.au.

Bačkalov, I (2019). "A Probabilistic Analysis of Stability Regulations for River-Sea Ships". In: *Contemporary Ideas on Ship Stability: Risk of Capsizing*. Ed. by V L Belenky et al. Cham: Springer International Publishing, pp. 707–723. ISBN: 978-3-030-00516-0. DOI: 10.1007/978-3-030-00516-0{_}41. URL: https://doi.org/10.1007/978-3-030-00516-0_41.

Bačkalov, I et al. (July 2016). "Improvement of ship stability and safety in intact condition through operational measures: Challenges and opportunities". In: *Ocean Engineering* 120, pp. 353–361. ISSN: 00298018. DOI: 10.1016/j.oceaneng.2016.02.011.

Begovic, E, C Bertorello, G Boccadamo, et al. (Dec. 2018). "Application of surf-riding and broaching criteria for the systematic series D models". In: *Ocean Engineering* 170, pp. 246–265. ISSN: 00298018. DOI: 10.1016/j.oceaneng.2018.08.062.

Begovic, E, C Bertorello, B Rinauro, et al. (Feb. 2023). "Simplified operational guidance for second generation intact stability criteria". In: *Ocean Engineering* 270, p. 113583. ISSN: 0029-8018. DOI: 10.1016/J.OCEANENG.2022.113583.

Begovic, E, B Rinauro, and F Cakici (2019). "Application of the 2nd Generation Intact Stability Criteria for fast semi displacement ships". In: *International Maritime Association of the Mediterranean (IMAM)*. Varna, Bulgaria.

Begović, E et al. (June 2021). "Case studies of SGISC Operational Limitations for pure loss of stability and excessive acceleration". In: *Proceedings of the 1st International Conference on the Stability and Safety of Ships and Ocean Vehicles*. Glasgow, Scotland, UK.

— (Jan. 2022). "Excessive acceleration simplified Operational Guidance". In: *International Journal of Naval Architecture and Ocean Engineering* 14. ISSN: 20926790. DOI: 10.1016/j.ijnaoe.2022.100473.

Belenky, V (2020). *Continued development of second generation intact stability criteria*. Tech. rep. West Bethesda, MD, USA: Naval Surface Warfare Center.

Belenky, V, C C Bassler, and K J Spyrou (2011). *Development of Second Generation Intact Stability Criteria*. Tech. rep. West Bethesda, MD, USA: Naval Surface Warfare Center.

Boccadamo, G and G Rosano (Dec. 2019). “Excessive acceleration criterion: Application to naval ships”. In: *Journal of Marine Science and Engineering* 7.12. ISSN: 20771312. DOI: 10.3390/JMSE7120431.

BSU (2008). *Investigation Report 45/07. Loss overboard of 10 containers from JRS CANIS at estuary of Elbe river on 12 January 2007 at 02.40*. Tech. rep. URL: www.bsu-bund.de.

— (2009). *Investigation Report 510/08 Fatal accident on board the CMV CHICAGO EXPRESS during Typhoon "HAGUPIT" on 24 September 2008 off the coast of Hong Kong*. Tech. rep. URL: www.bsu-bund.de.

— (2011). *Investigation Report 391/09. Fatal accident on board the CMV CCNI GUAYAS during Typhoon 'KOPPU' on 15 September 2009 in the sea area off Hong Kong (Including analysis of Serious Marine Casualty 520/09. Pilot injured on board the CMV FRISIA LISSABON on 16 October 2009 west of Borkum on the Westerems)*. Tech. rep. URL: www.bsu-bund.de.

Bulian, G and A Orlandi (2022). “Effect of environmental data uncertainty in the framework of second generation intact stability criteria”. In: *Ocean Engineering* 253, p. 111253. ISSN: 0029-8018. DOI: https://doi.org/10.1016/j.oceaneng.2022.111253.

Duan, F et al. (Oct. 2022). “A fast time domain method for predicting of motion and excessive acceleration of a shallow draft ship in beam waves”. In: *Ocean Engineering* 262. ISSN: 00298018. DOI: 10.1016/j.oceaneng.2022.112096.

Faltinsen, O M (1990). *Sea loads on ships and offshore structures*. Cambridge, UK: Cambridge University Press.

France, W N et al. (2001). “An Investigation of Head-Sea Parametric Rolling and its Influence on Container Lashing Systems”. In: *SNAME Annual Meeting 2001 Presentation*.

Galeazzi, R, M Blanke, T Falkenberg, et al. (Nov. 2015). “Parametric roll resonance monitoring using signal-based detection”. In: *Ocean Engineering* 109, pp. 355–371. ISSN: 00298018. DOI: 10.1016/j.oceaneng.2015.08.037.

Galeazzi, R, M Blanke, and N K Poulsen (2013). “Early detection of parametric roll resonance on container ships”. In: *IEEE Transactions on Control Systems Technology* 21.2, pp. 489–503. ISSN: 10636536. DOI: 10.1109/TCST.2012.2189399.

Graham, R (1990). “Motion-Induced Interruptions as Ship Operability Criteria”. In: *Naval Engineers Journal* 102.2, pp. 65–71. DOI: https://doi.org/10.1111/j.1559-3584.1990.tb02556.x.

Hogben, N, N M C Dacunha, and G F Olliver (1986). *Global Wave Statistics*. Feltham (UK): British Maritime Technology.

IACS Rec. No.34 (2001). *Standard Wave Data*. Tech. rep.

Ikeda, Y, Y Himeno, and N Tanaka (1978a). *A prediction method for ship roll damping*. Tech. rep. Report of Department of Naval Architecture, University of Osaka Prefecture.

— (1978b). *Components of roll damping of ship at forward speed*. Tech. rep. Report of Department of Naval Architecture, University of Osaka Prefecture.

IMCO Res. A.167 (ES.IV) (1968). *Recommendation on intact stability for passenger and cargo ships under 100 metres in length. Resolution A.167(ES.IV)*. Tech. rep.

IMCO Res. A.168 (ES.IV) (1968). *Recommendation on intact stability of fishing vessels. Resolution A.168 (ES.IV).* Tech. rep.
IMO MSC 105/20 (2022). *Report of the Maritime Safety Committee on its 105th session*. Tech. rep.
IMO MSC.1/Circ.1200 (2006). *Interim guidelines for alternative assessment of the Weather Criterion*. Tech. rep.
IMO MSC.1/Circ.1228 (2007). *Revised guidance to the master for avoiding dangerous situations in adverse weather and sea conditions*. Tech. rep.
IMO MSC.1/Circ.1281 (2008). *Explanatory Notes to the International Code on Intact Stability, 2008*. Tech. rep.
IMO MSC.1/Circ.1627 (2020). *Interim Guidelines on the Second Generation Intact Stability Criteria*. Tech. rep.
IMO MSC.1/Circ.1652 (2022). *Explanatory notes to the Interim Guidelines on second generation intact stability criteria*. Tech. rep.
IMO Res. A.562(14) (1985). *Recommendation on a severe wind and rolling criterion (Weather Criterion) fot the intact stability of passenger and cargo ships of 24 metres in length and over*. Tech. rep.
IMO Res. A749(18) (1993). *Code on Intact Stability for types of ships covered by IMO instruments*. Tech. rep.
IMO Res. MSC.267(85) (2008). *Adoption of the International Code on Intact Stability 2008 (2008 IS CODE)*. Tech. rep.
IMO Res. MSC.75(69) (1998). *Adoption of amendments to the Code on Intact Stability for all types of ships covered by IMO instruments (Resolution A.749(18))*. Tech. rep.
IMO SDC 1/INF.8 (2013). *Information collected by the Correspondence Group on Intact Stability regarding the second generation intact stability criteria development*. Tech. rep.
IMO SDC 2/INF.10 (2014). *Information collected by the Correspondence Group on Intact Stability*. Tech. rep.
IMO SDC 3/INF.10 (2015). *Information collected by the Correspondence Group on Intact Stability regarding second generation intact stability criteria*. Tech. rep.
IMO SDC 4/5/1/Add.4 (2016). *Report of the correspondence group (part 5)*. Tech. rep.
IMO SDC 4/5/13 (2016). *Comments on documents SDC 4/5/1 and SDC 4/INF.4*. Tech. rep.
IMO SDC 6/INF.3 (2018). *Information collected by the Correspondence Group on Intact Stability*. Tech. rep.
IMO SDC 8/WP.4/Add.1 (2022). *Development of explanatory notes to the interim guidelines on second generation intact stability criteria*. Tech. rep.
IMO SDC 8/WP.4/Add.2 (2022). *Development of explanatory notes to the interim guidelines on second generation intact stability criteria*. Tech. rep.
IMO SDC 8/WP.4/Add.5 (2022). *Development of explanatory notes to the interim guidelines on second generation intact stability criteria*. Tech. rep.
IMO SLF 44/INF.6 (2001). *Weather criterion for large passenger ships*. Tech. rep.
IMO SLF 52/3/2 (2009). *Stability hazards imposed by extremely steep quartering waves*. Tech. rep.

IMO SLF 52/3/5 (2009). *Proposal with regard to the scope of new generation criteria*. Tech. rep.

IMO SLF 52/WP.1 (2010). *Report of the working group (part 1)*. Tech. rep.

IMO SLF 53/5/5 (2010). *Comments on the structure of new generation intact stability criteria (report of the correspondence group)*. Tech. rep.

IMO SLF 54/INF.12 (2011). *Information collected by the intersessional Correspondence Group on Intact Stability*. Tech. rep.

IMO SLF 54/INF.6 (2011). *Theoretical investigation into the loss of containers of the Pacific Adventurer off Cape Morton Queensland*. Tech. rep.

IMO SLF 55/INF.15 (2012). *Information collected by the Correspondence Group on Intact Stability*. Tech. rep.

Journee, J M J and W W Massie (2001). *Offshore Hydromechanics*. 1st. Delft (Netherland): Delft University of Technology.

Kawahara, Y, K Maekawa, and Y Ikeda (June 2009). "A Simple Prediction Formula of Roll Damping of Conventional Cargo Ships on the Basis of Ikeda's Method and Its Limitation". In: *Proceedings of the 10th International Conference on Stability of Ships and Ocean Vehicles*. St. Petersburg, Russia.

Kobylinski, L (1975). "Rational stability criteria and probability of capsizing". In: *1st International Conference on the Stability of Ships and Ocean Vehicles*. Glasgow, UK.

Kobylinski, L K and S Kastner (2003). *Stability and Safety of ships. Volume I: Regulation and Operation*. Amsterdam: Elsevier. ISBN: 0080441483.

Kracht, A M and A Jacobsen (1992). "D Series Systematic Experiments with Models of Fast Twin-Screw Displacement Ships". In: *The Society of Naval Architects and Marine Engineers*.

Krata, P (Sept. 2008). "Total Losses of Fishing Vessels Due to the Insufficient Stability". In: *Article in TransNav the International Journal on Marine Navigation and Safety of Sea Transportation* 2.3.

Krüger, S, F Kluwe, and H Vorhölter (2008). *Decision Support for Large Amplitude Roll Motions based on Nonlinear Time-Domain Simulations*. Tech. rep. Liege, Belgium.

Kuroda, T et al. (Sept. 2019). "Direct Stability Assessment for excessive acceleration failure mode and validation by model test". In: *Ocean Engineering* 187. ISSN: 00298018. DOI: 10.1016/j.oceaneng.2019.106137.

Lewis, E L (1989). *Principle of Naval Architecture*. Vol. III. Jersey City, NJ United States: Society of Naval Architects and Marine Engineers.

Lloyd, A R J M (1989). *SEAKEEPING: Ship Behaviour in Rough Weather*. Chichester, West Sussex, England: John Wiley & Sons.

Maki, A, L Dostal, Y Maruyama, M Sakai, et al. (Sept. 2021). "Theoretical estimation of roll acceleration in beam seas using PDF line integral method". In: *Journal of Marine Science and Technology (Japan)* 26.3, pp. 828–834. ISSN: 09484280. DOI: 10.1007/s00773-020-00770-1.

Maki, A, L Dostal, Y Maruyama, K Sasa, et al. (Nov. 2022). "Enhanced estimation method and approximation method of the PDF of roll angular acceleration and jerk in beam seas". In: *Ocean Engineering* 264. ISSN: 00298018. DOI: 10.1016/j.oceaneng.2022.112159.

Mata-Álvarez-Santullano, F and A Souto-Iglesias (Mar. 2014). “Stability, safety and operability of small fishing vessels”. In: *Ocean Engineering* 79, pp. 81–91. ISSN: 0029-8018. DOI: 10.1016/J.OCEANENG.2014.01.011.
Matsuda, A, D Terada, and H Hashimoto (June 2017). “The characteristics of capsizing phenomena of Japanese fishing vessels”. In: *Proceedings of the 16th International Ship Stability Workshop*. Belgrade, Serbia.
Míguez González, M and G Bulian (Jan. 2018). “Influence of ship dynamics modelling on the prediction of fishing vessels roll response in beam and longitudinal waves”. In: *Ocean Engineering* 148, pp. 312–330. ISSN: 00298018. DOI: 10.1016/j.oceaneng.2017.11.032.
Míguez González, M, V Díaz Casás, et al. (2015). “Investigation of the Applicability of the IMO Second Generation Intact Stability Criteria to Fishing Vessels”. In: *12th International Conference on the Stability of Ships and Ocean Vehicles*, pp. 349–359.
Míguez González, M, F López Peña, et al. (June 2011). “Roll Large Amplitude Roll Motion Forecasting through an Artificial Neural Network System”. In: *Proceedings of the 12th International Ship Stability Workshop*. Washington D.C (USA).
Newman, J N (1977). *Marine Hydrodynamics*. Cambridge: The MIT Press.
Nielsen, U D, P Friis-Hansen, and J J Jensen (Apr. 2009). “A step towards risk-based decision support for ships - Evaluation of limit states using parallel system analysis”. In: *Marine Structures* 22.2, pp. 209–224. ISSN: 09518339. DOI: 10.1016/j.marstruc.2008.08.002.
Ochi, M. K. (1989). *Applied Probability and Stochastic Processes in Engineering and Physical Sciences*. John Wiley & Sons.
Ochi, Michel K (1973). “On prediction of extreme values”. In: *Journal of Ship Research* 17.1, pp. 29–37.
Papanikolaou, A, E Alfred Mohammed, and S E Hirdaris (Aug. 2014). “Stochastic uncertainty modelling for ship design loads and operational guidance”. In: *Ocean Engineering* 86, pp. 47–57. ISSN: 00298018. DOI: 10.1016/j.oceaneng.2014.01.014.
Petacco, N (2019). “Second Generation Intact Stabilitycriteria: Analysis, Implementation and Applications tosignificant ship typologies”. PhD thesis. Genova, Italy: University of Genova.
— (Dec. 2022). “An alternative methodology for the simplified operational guidance in the framework of second generation intact stability criteria”. In: *Ocean Engineering* 266. ISSN: 00298018. DOI: 10.1016/j.oceaneng.2022.112665.
Petacco, N and P Gualeni (July 2020). “IMO second generation intact stability criteria: General overview and focus on operational measures”. In: *Journal of Marine Science and Engineering* 8.8. ISSN: 20771312. DOI: 10.3390/JMSE8070494.
— (Sept. 2022). “A SGISC-Based Study about operational Profiles of Navy Vessels”. In: *Proceedings of the 18th International Ship Stability Workshop*. Gdansk, Poland, pp. 13–15.
Petacco, N, P Gualeni, JY Billard, et al. (June 2017). “An integration of present navy ships intact stability criteria in the perspective of ship performance assessment in a seaway”. In: *Proceedings of the 16th International Ship Stability Workshop*. Belgrade, Serbia, pp. 5–7.

Petacco, N, P Gualeni, and G Stio (2020). "Second Generation Intact Stability criteria: Application of operational limitations & guidance to a megayacht unit". In: *Proceedings of 5th International Conference on Maritime Technology and Engineering, MARTECH 2020*. Lisbon, Portugal.

Rahola, J. (1939). "The judging of the stability of ships and the determination of the minimum amount of stability". PhD thesis. Helsinki.

Rinauro, B et al. (2020). "Surf-Riding Operational Measures for Fast Semidisplacement Naval Hull Form". In: *Proceedings of the 12th Symposium on High Speed Marine Vehicles*. Naples, Italy: IOS Press.

Rosano, G, E Begović, et al. (Oct. 2020). "Second Generation Intact Stability Criteria fallout on naval ships limiting KG curves". In: *Proceedings of the 12th Symposium on High Speed Marine Vehicles*. Naples, Italy.

Rosano, G and B Rinauro (2020). "Vulnerability assessment to dead ship condition and excessive acceleration criteria for semi-displacement hulls". In: *International Conference on Post Graduate Research*. Gdansk, Poland.

Rossell, H E and L B Chapman (1939). *Principles of Naval Architecture – Written by a Group of Authorities*. Ed. by H. E. Rossell and Chapman L. B. SNAME. Vol. I. New York: SNAME, pp. 99–137.

Rudaković, S and I Bačkalov (June 2017). "On application of standard methods for roll damping prediction to inland vessels". In: *Proceedings of the 16th International Ship Stability Workshop*. Belgrade, Serbia, pp. 5–7.

— (July 2019). "Operational limitations of a river-sea container vessel in the framework of the Second Generation Intact Stability Criteria". In: *Ocean Engineering* 183, pp. 409–418. ISSN: 00298018. DOI: 10.1016/j.oceaneng.2019.05.013.

Rudaković, S, G Bulian, and I Bačkalov (Nov. 2019). "Effective wave slope coefficient of river-sea ships". In: *Ocean Engineering* 192. ISSN: 00298018. DOI: 10.1016/j.oceaneng.2019.106427.

— (2021). "Natural Roll Period of River-sea Ships". In: *Proceedings of the 1st International Conference on the Stability and Safety of Ships and Ocean Vehicles*. Glasgow, Scotland, UK, pp. 7–11.

Salvesen, N, E O Tuck, and O Faltinsen (1970). "Ship Motions and Sea Loads". In: *Transactions of the Society of Naval Architects and Marine Engineers* 78, pp. 250–287.

Santiago Caamaño, L, R Galeazzi, M Miguez González, et al. (2019). "Experimental Validation of Transverse Stability Monitoring System for Fishing Vessels". In: *IFAC*. Vol. 52. 21. Elsevier B.V., pp. 57–63. DOI: 10.1016/j.ifacol.2019.12.283.

Santiago Caamaño, L, R Galeazzi, U D Nielsen, et al. (Oct. 2019). "Real-time detection of transverse stability changes in fishing vessels". In: *Ocean Engineering* 189. ISSN: 00298018. DOI: 10.1016/j.oceaneng.2019.106369.

Schrøter, C et al. (June 2017). "Sample Applications of the Second Generation Intact Stability Criteria – Robustness and Consistency Analysis". In: *Proceedings of the 16th International Ship Stability Workshop*. Belgrade, Serbia, pp. 5–7.

Shigunov, V, O El Moctar, et al. (2011). "On the Consideration of Lateral Accelerations in Ship Design Rules". In: *Proceedings of the 12th International Ship Stability Workshop*. Washington D.C., USA. DOI: 10.13140/2.1.3460.2886.

Shigunov, V, H Rathje, and O El Moctar (2013). “Towards safer container shipping”. In: *Ship Technology Research* 60.1, pp. 34–40. ISSN: 09377255. DOI: 10.1179/str.2013.60.1.003.

Shigunov, Vladimir et al. (June 2021). “Operational measures for intact ship stability”. In: *Proceedings of the 1st International Conference on the Stability and Safety of Ships and Ocean Vehicles*. Glasgow, Scotland, UK.

Spyrou, K J (Mar. 1996). “Dynamic Instability in Quartering Seas: The Behavior of a Ship During Broaching”. In: *Journal of Ship Research* 40.01, pp. 46–59. ISSN: 0022-4502. DOI: 10.5957/jsr.1996.40.1.46.

St. Denis, M and W J Pierson (1953). “On the Motions of Ships in Confused Seas”. In: *The Society of Naval Architects and Marine Engineers (annual meeting)*. New York, USA.

Szozda, Z and P Krata (Mar. 2022). “Towards evaluation of the second generation intact stability criteria - Examination of a fishing vessel vulnerability to surf-riding, based on historical capsizing”. In: *Ocean Engineering* 248, p. 110796. ISSN: 0029-8018. DOI: 10.1016/J.OCEANENG.2022.110796.

Terada, D et al. (Sept. 2018). “Direct estimation of natural roll frequency using onboard data based on a Bayesian modeling procedure”. In: *Proceedings of the 13th International Conference on the Stability of Ships and Ocean Vehicles*. Kobe, Japan.

Tompuri, M, P Ruponen, and D Lindroth (2016). “Second generation intact stability criteria and operational limitations in initial ship design”. In: *Proceedings of PRADS2016*. Copenhagen (Denmark).

Umeda, N and A Francescutto (June 2016). “Current state of the second generation intact stability criteria - achievements and remaining issues”. In: *Proceedings of the 15th International Ship Stability Workshop*. Stockholm, Sweden.

Yu, Y et al. (Sept. 2022). “URANS prediction of excessive acceleration during lifting operation”. In: *Ocean Engineering* 259. ISSN: 00298018. DOI: 10.1016/j.oceaneng.2022.111877.